WAVELET METHODS FOR SOLVING A CLASS OF NONLINEAR DIFFERENTIAL EQUATIONS

Ph.D. Thesis

By
Kotapally Harish Kumar

DISCIPLINE OF MATHEMATICS
INDIAN INSTITUTE OF TECHNOLOGY INDORE

January 2018

WAVELET METHODS FOR SOLVING A CLASS OF NONLINEAR DIFFERENTIAL EQUATIONS

A THESIS

Submitted in partial fulfillment of the
requirements for the award of the degree

of
DOCTOR OF PHILOSOPHY

by
Kotapally Harish Kumar

DISCIPLINE OF MATHEMATICS
INDIAN INSTITUTE OF TECHNOLOGY INDORE

January 2018

INDIAN INSTITUTE OF TECHNOLOGY INDORE

CANDIDATE'S DECLARATION

I hereby certify that the work which is being presented in the thesis entitled **WAVELET METHODS FOR SOLVING A CLASS OF NONLINEAR DIFFERENTIAL EQUATIONS** in the partial fulfillment of the requirements for the award of the degree of **DOCTOR OF PHILOSOPHY** and submitted in the **DISCIPLINE OF MATHEMATICS, Indian Institute of Technology Indore**, is an authentic record of my own work carried out during the time period from July 2013 to July 2017 under the supervision of Dr. V. Antony Vijesh, Associate Professor, IIT Indore.

The matter presented in this thesis has not been submitted by me for the award of any other degree of this or any other institute.

Signature of the student with date

(**KOTAPALLY HARISH KUMAR**)

This is to certify that the above statement made by the candidate is correct to the best of my knowledge.

Signature of Thesis Supervisor with date

(**DR. V. ANTONY VIJESH**)

KOTAPALLY HARISH KUMAR has successfully given his Ph.D. Oral Examination held on 5th January 2018.

Sign of Chairperson (OEB)　　Sign of External Examiner　　Sign of Thesis Supervisor

Sign of PSPC Member1　　Sign of PSPC Member2　　Sign of Convener, DPGC

Sign of Head of Discipline

ACKNOWLEDGEMENTS

I take great pleasure in expressing my sincere gratitude to my supervisor Dr. V. Antony Vijesh for his support and valuable guidance in the successful completion of this work. It is my pleasure to thank my PSPC members Dr. Niraj Kumar Shukla and Dr. Ram Bilas Pachori for reviewing my research progress and giving their valuable suggestions and comments.

I am highly thankful to Professor Pradeep Mathur, Director for the excellent facilities provided to carry out the research work at IIT Indore.

I express my gratitude to Professor Neelesh Kumar Jain, Dean of Academic Affairs, Dr. Swadesh Kumar Sahoo, Head, School of Basic Sciences and Dr. Sk. Safique Ahmad, Head, Discipline of Mathematics for their academic support. I would also like to offer my sincere thanks to all the faculty and staff members at IIT Indore for their support and cooperation.

I wish to specially thank Dr. G. Chandhini, Assistant Professor, NIT Surathkal for carefully reading all my research works and for the valuable suggestions.

I feel elated to extend my gratitude to my fellow mates Hareesh, Mansi, Roopali and Saurabh for their cooperation during my work. Their annotations and criticisms are the key to the successful completion of this work. Special thanks to my colleagues K.D. Shukla, Robin Singh, Ram Bharat and Sunil Pathak for their moral support and words of encouragement and Rangeet Mitra for the initial guidance for coding in Matlab. I am ever thankful to all my friends for being empathetic and encouraging me during moments of crisis.

Words can not express of how grateful I am to Linia Anie Sunny, Nitin Bisht and Rupsha Roy for the stimulating discussions, sleepless nights of working together before deadlines. It was due to their support I could traverse this journey with least hurdles. I am indebted to Linia Anie Sunny for her encouragement and moral support throughout this journey. She was kind enough to undertake the editing work and I acknowledge for the meticulous work she has done.

Last but not the least, I would like to thank my family: my parents and to my brothers and sister for supporting me spiritually throughout the writing of thesis and my life in general.

This thesis is only a beginning of my journey. Above all, I owe it all to Almighty God for granting me the wisdom, health and strength to undertake this research task and enabling me to its completion. Finally, I would like to leave the remaining space in memory of Gouri Shanker (1993-2010), my cousin.

DEDICATION

I dedicate my dissertation work to my family. A special feeling of gratitude to my loving parents, Jogappa and Padma whose words of encouragement and push for tenacity ring in my ears. My sister Harika and her husband Bhanu have never left my side and are very special.

I also dedicate this dissertation to my friends who have supported me throughout the process. I dedicate this work and give special thanks to my best friends Bala Gangadhar, Lakshmi and Bharath for being there for me throughout the entire doctorate program.

LIST OF PUBLICATIONS

1. Vijesh V.A., Kumar K.H. (2015), *Wavelet based quasilinearization method for semi-linear parabolic initial boundary value problems*, Appl. Math. Comput., 266, 1163–1176.
2. Vijesh V.A., Kumar K.H. (2015), *Wavelet based numerical simulation of non linear Kilen/Sine gordon equation*, J. Combinatorics, Information and System Sciences, 40 (1), 225–244.
3. Vijesh V.A., Sunny L.A., Kumar K.H. (2016), *Legendre wavelet–quasilinearization technique for solving q-difference equations*, J. Difference Equ. Appl., 22 (4), 594–606.
4. Kumar K.H., Vijesh V.A. (2016), *Chebyshev wavelet quasilinearization scheme for coupled nonlinear Sine-Gordon equations*, J. Comput. Nonlinear Dynam., 12(1), 011018 (Nov 22, 2016), 05 pages.
5. Vijesh V.A., Kumar K.H. (2017), *Erratum on wavelet based quasilinearization method for semi-linear parabolic initial boundary value problems [Appl. Math. Comput. 266 (2015) 1163-1176]*, Appl. Math. Comput., 314, Page number 484.
6. Kumar K.H., Vijesh V.A., *Wavelet based iterative methods for a class of 2D-partial integro differential equations*, Comput. Math. Appl., article in press.
7. Kumar K.H., Vijesh V.A., *Legendre wavelet based iterative schemes for fourth order elliptic equations with nonlocal boundary conditions*, under review.

ABSTRACT

This thesis in six chapters develops an efficient wavelet operational matrix approach for solving various types of nonlinear partial differential equations and partial integro differential equations. While operational matrix wavelet methods have been studied earlier by Celik, Hariharan, Lepik, Mittal, Ray, Razzaghi, Rehman, Siraj, Yin, Yousefi and many others, our work majorly concentrates on discretizations exclusively based on wavelet methods associated with quasilinearization including differential and integral equations with more than two variables. This thesis also contributes theoretically an interesting unification of quasilineariztaion and independent existence and uniqueness theorems for q-initial and q-boundary value problems.

To make the thesis self-contained, **Chapter 1** gives a brief introduction to the basic concepts of wavelets and its development as a powerful tool in the area of numerical analysis. A short literature survey is also done to demonstrate its demand and effectiveness.

Chapter 2 deals with numerical methods based on quasilinearization Haar wavelets and Legendre wavelets to solve a class of semi-linear parabolic initial boundary value problem. Through an appropriate illustration of the numerical scheme, it is shown that the proposed scheme is robust and easy to apply. This chapter also provides an interesting unification of quasilinearization in the abstract space setting.

Two different approaches based on Haar and Legendre wavelets are studied in **Chapter 3** to solve a class of two dimensional parabolic integro-differential equations that arises in nuclear reactor models and population models. A comparative numerical study is done to show the efficiency of the proposed schemes.

In the first part of **Chapter 4**, new numerical techniques are proposed for solving nonlinear Klien/ Sine Gordon equation with initial and boundary conditions. The quasi-linearization technique is carefully combined with Chebyshev and Legendre wavelet based collocation methods and numerical results obtained suggests that the proposed scheme is better than the methods available in the recent literature. The last and second part of this chapter, extends the previous section to a coupled sine-Gordon equation with initial and boundary conditions.

Chapter 5 is a new attempt to solve a fourth order elliptic equations with nonlocal boundary conditions by coupling with two iterative procedures including quasilinearization and Legendre wavelets. The efficiency of the proposed scheme is illustrated through a comparative numerical study with the literature.

The existence and uniqueness theorems for a $q-$initial and $q-$boundary value problem is obtained in **Chapter 6** using classical Newton's method. A Legendre wavelet technique is proposed to solve the equations numerically that produces higher accuracy and is straightforward to apply.

KEYWORDS: Chebyshev wavelet, Collocation method, Coupled sine-Gordon equation, Fisher equation, Haar wavelet, Huxley equation, Initial boundary value problem, Klein-Gordon equation, Legendre Wavelet, Monotone iterative technique, Newell - Whitehead - Segal equation, Parabolic partial differential equation, Partial integro-differential equation, q-boundary value problem, q-initial value problem, Quasilinearization, Sine-Gordon equation.

TABLE OF CONTENTS

LIST OF FIGURES

LIST OF TABLES

CHAPTER 1

INTRODUCTION

1.1. Literature on wavelets

In the field of applied mathematics, wavelets turned out to be a recent revolutionary advancement. It was initially found in the areas of digital signal processing and geophysics and was considered to be an efficient alternative to the classical Fourier analysis on a later stage. Arens, Daubechies, Fourgeau, Giard, Grossmann, Mallat, Meyer and Morlet are some who contributed during its initial developments. Wavelets appeared in diverse fields such as signal processing, image processing, quantum mechanics, fractals and numerical analysis [**102**]. Referring to its wide applicability in computer imaging, animation and encoding fingerprint databases, its future in the areas like breast cancer diagnosis, weather prediction and internet traffic description can be highly anticipated [**43**].

It was in 1990s that wavelets gained its attention in the area of numerical analysis [**88**]. One of the major areas in numerical analysis is developing numerical techniques to solve nonlinear differential equations. Nonlinear differential equations frequently appear in mathematical modeling to resolve problems that commonly arise in the field of business, engineering, science and technology. Even after giving consideration to the qualitative and quantitative properties like existence and uniqueness, it is rarely possible to derive the explicit solutions for these nonlinear differential equations. Developing numerical schemes to find approximate solutions of nonlinear equations is one of the most important research area in mathematics. Numerical methods can be broadly classified into two groups; say methods that

- approximate corresponding governing equations. Example: Finite difference type schemes.

- approximate solution and then substitute it into the equations. Example: Spectral methods.

In recent years, developing efficient numerical techniques for various types of differential equations using wavelets have attracted several researchers. This is due to the following reasons:

- The favorable properties such as orthogonality, multiresolution analysis, vanishing moment and compact support.
- Accuracy in approximations of functions and operators.
- Development of operational matrices of integration and differentiation associated to each wavelets. This simplifies implementation of numerical (wavelet) schemes considerably.

In contrast to the spectral methods, basis elements of wavelet based methods combine the advantages of being infinitely differentiable yet having small compact support. Consequently, wavelet based methods not only have spectral accuracy but also have good localization. Thus the differentiation and integration matrices of the spectral collocation are dense, while they are sparse in the case of wavelet approximation. Developing numerical solution of differential equations via wavelet is based on one of the following three approaches [**100**]. Approximating the unknown solution of the differential equation

- by suitable known function and its translation called scaling function [**79**].
- by suitable known function and its dilation as well as translation known as "wavelets" [**87**].
- by wavelet transform instead of scaling function or wavelets [**60**].

The following subsections provide a short literature review on the recent developments of differential equations based on various types of wavelets. [**43, 44, 88**] and [**100**] provide reviews on wavelet based schemes that are available in the literature. Though there are many aspects of wavelets like Wavelet-Galerkin method that are used to solve differential equations, the following subsections concentrate only on methods based on operational matrices.

1.1.1. Haar Wavelet

One of the simplest wavelets ever introduced is Haar wavelet which was used by Alfred Haar in 1910 [**43**]. The Haar wavelet family on the interval $[0, 1)$ is a collection of functions $\{h_i(x) : i \in \mathbb{N}\}$ defined by

$$h_1(x) = \begin{cases} 1 & \text{if } x \in [0,1) \\ 0 & \text{otherwise} \end{cases} \tag{1.1}$$

and

$$h_2(x) = \begin{cases} 1 & \text{if } x \in [0,\frac{1}{2}) \\ -1 & \text{if } x \in [\frac{1}{2},1) \\ 0 & \text{otherwise.} \end{cases} \tag{1.2}$$

Rest of the members in Haar wavelet family are defined on subintervals of $[0, 1)$ by

$$h_i(x) = \begin{cases} 1 & \text{if } x \in [\alpha,\beta) \\ -1 & \text{if } x \in [\beta,\gamma) \\ 0 & \text{otherwise,} \end{cases} \tag{1.3}$$

where $\alpha = \frac{k}{m}, \beta = \frac{k+0.5}{m}, \gamma = \frac{k+1}{m}, i = 2, 3, ..., 2M,\ m = 2^j,\ j = 0, 1, ..., J,$ is the dilation parameter and $k = 0, 1, ..., m-1$, is the translation parameter. The relation between i, m and k can expressed as $i = m + k + 1$. J denotes the maximal level of resolution. It is interesting to observe that other than the scaling function h_1, all the remaining wavelets are generated from the mother wavelet $h_2(x)$ by the operations of dilation and translation. The Haar wavelet functions are orthogonal to each other, i.e.,

$$\int_0^1 h_i(x)h_j(x)dx = \begin{cases} 0 & \text{if } i \neq j \\ \frac{1}{2^i} & \text{if } i = j. \end{cases} \tag{1.4}$$

The Haar wavelets' operational matrix of integration was first derived by Jin-Sheng Guf and Wei-Sun Jiang [**36**] and its applicability was demonstrated by solving a linear time invarying system

$$0.25\frac{dy}{dt} + y(t) = u(t) \tag{1.5}$$

where $u(t)$ is the unit step function and $y(0) = 0$. Later the most followed Haar wavelets' operational matrix was developed by C.F. Chen and C.H. Hsiao [**24**] for systematically handling lumped and distributed-parameters dynamic systems. This technique was further extended by U. Lepik [**81**] to solve higher order ordinary differential equations with initial and boundary conditions which was also used to solve a linear heat equation. In [**82**], Haar wavelet was expanded for solving a nonlinear ordinary integro-differential equation. By discretizing space domain completely by wavelets and time domain by finite difference, various parabolic and hyperbolic partial differential equations were studied extensively by several researchers including Lepik [**81**], Mittal [**104**], Siraj [**58**], Hariharan [**48**], Celik [**23**], Esen [**111**]. It has to be noted that authors generally assumed even the terms with order greater than that of the highest derivative term [**8, 59, 85, 151, 171**] in the governing equation to be belonging in $L^2[0,1]$ space. But it is shown in [**10**], to get better accuracy it is sufficient to assume only up to highest derivative term in the governing equation need to in $L^2[0,1]$. Availing block pulse function, the operational matrix for fractional integration was obtained by J. Wu and C. Chen in [**173**] and was used for solving fractional order differential equations. Some interesting Haar wavelet methods were employed in [**8, 9, 55, 74, 83, 84, 122, 130, 137, 138, 149, 170, 171, 191**] to deal with various other types of equations. The applicability of Haar wavelet techniques was further enlarged by handling irregular domains [**191**], singular differential equations [**66**] and problems arising from stochastic calculus [**105**] also. See [**43, 44**] for the review articles on various developments of Haar wavelet based numerical techniques.

1.1.2. Legendre Wavelet

Though Haar wavelets are very simple and easy to implement, more members from its family are required to approximate smooth functions efficiently. Wavelets based on orthogonal polynomials were then utilized by researchers to overcome this drawback of

Haar wavelets. One of such wavelets that was very frequently used in the literature was Legendre wavelets.

The Legendre wavelet family on the interval $[0, 1]$ can be defined using the well known Legendre polynomial $L_m(x)$ defined on $[-1, 1]$, where m denotes the degree of the polynomial. The Legendre wavelets family is given by

$$\psi_{m,n}(x) = \begin{cases} 2^{\frac{k}{2}}\sqrt{m+\frac{1}{2}}L_m(2^k x - \hat{n}) & \text{if } x \in [\frac{\hat{n}-1}{2^k}, \frac{\hat{n}+1}{2^k}) \\ 0 & \text{otherwise,} \end{cases} \tag{1.6}$$

where $m, n, k \in \mathbb{N}$, $n = 1, 2, \ldots 2^{k-1}$ and $\hat{n} = 2n - 1$. The following well known recurrence relation is used to find the Legendre polynomials. For $m = 1, 2, 3, \ldots$

$$L_0(x) = 1, \quad L_1(x) = x \tag{1.7}$$

$$L_{m+1}(x) = \left(\frac{2m+1}{m+1}\right) x L_m(x) - \left(\frac{m}{m+1}\right) L_{m-1}(x). \tag{1.8}$$

The above (1.6) also can be written as a more simplified form

$$\psi_i(x) = \begin{cases} 2^{\frac{k}{2}}\sqrt{m+\frac{1}{2}}L_m(2^k x - \hat{n}) & \text{if } x \in [\frac{\hat{n}-1}{2^k}, \frac{\hat{n}+1}{2^k}) \\ 0 & \text{otherwise,} \end{cases} \tag{1.9}$$

where $n = 1, 2, \cdots 2^{k-1}$, $m = 0, 1, 2, \cdots$ and $i = n + 2^{k-1}m$. Using the orthogonal property of Legendre polynomial it is easy to verify that the Legendre wavelets family form an orthonormal basis for $L^2(0, 1)$. Consequently, any square integrable function $f(x)$ can be approximated as

$$f(x) \simeq \sum_{i=1}^{N} a_i \psi_i(x) = A^T \Psi(x), \tag{1.10}$$

where A and $\Psi(x)$ are $N = (2^{k-1}M)$ column vectors with $A^T = [a_1, a_2 \ldots, a_N]$ and $\Psi^T(x) = [\psi_1(x), \psi_2(x) \ldots, \psi_N(x)]$. Using the operational matrix of integration, one can approximate the indefinite integral of the vector $\Psi(x)$ as

$$\int_0^x \Psi(t)dt \approxeq P\Psi(x), \tag{1.11}$$

where P is an operational matrix of integration that can be explicitly represented as

$$\mathbf{P} = \begin{bmatrix} L & F & F & \dots & F \\ O & L & F & \ddots & F \\ \vdots & O & L & \ddots & F \\ & & & & F \\ O & O & \dots & O & L \end{bmatrix}_{N\times N}$$

with

$$\mathbf{L} = \begin{bmatrix} 1 & \frac{1}{\sqrt{3}} & 0 & \dots & 0 & 0 & 0 \\ -\frac{\sqrt{3}}{3} & 0 & \frac{\sqrt{3}}{3\sqrt{5}} & 0 & \dots & 0 & 0 \\ 0 & -\frac{\sqrt{5}}{5\sqrt{3}} & 0 & \frac{\sqrt{5}}{5\sqrt{7}} & 0 & 0 & 0 \\ 0 & 0 & -\frac{\sqrt{7}}{7\sqrt{5}} & \ddots & \ddots & 0 & \dots \\ \vdots & \ddots & \ddots & \ddots & \dots & \ddots & \dots \\ 0 & \vdots & \ddots & \ddots & -\frac{\sqrt{2M-3}}{(2M-3)\sqrt{2M-5}} & 0 & \frac{\sqrt{2M-3}}{(2M-3)\sqrt{2M-1}} \\ 0 & \vdots & \dots & \dots & 0 & -\frac{\sqrt{2M-1}}{(2M-1)\sqrt{2M-3}} & 0 \end{bmatrix}_{M\times M},$$

$$\mathbf{F} = \begin{bmatrix} 2 & 0 & 0 & \dots & 0 \\ 0 & 0 & 0 & \dots & 0 \\ \vdots & \vdots & \vdots & \vdots & \vdots \\ 0 & 0 & \dots & 0 & 0 \end{bmatrix}_{M\times M} \quad \text{and } \mathbf{O} = \begin{bmatrix} 0 & 0 & 0 & \dots & 0 \\ 0 & 0 & 0 & \dots & 0 \\ \vdots & \vdots & \vdots & \vdots & \vdots \\ 0 & 0 & \dots & 0 & 0 \end{bmatrix}_{M\times M}.$$

The pioneer work using Legendre wavelets' operational matrix for integration was led by M. Razzaghi and S. Yousefi [**133, 135**] by solving the linear time invarying system (1.5) and Bessel differential equation. Subsequently, M. Razzaghi and his collaborators handled various types of differential equations arising from radiative transfer [**131**], optical control problems [**132, 134**], variational problems [**135**] and Volterra-Fredholm integral equations [**17, 180**] using Legendre wavelets. By discretizing time domain using finite difference and approximating space domain using Legendre wavelets, various partial differential equations were solved in [**58, 95, 122, 179**]. By deriving Legendre wavelets' operational matrix for classical derivative, F. Mohammadi and M. M. Houseini [**106**] solved two point boundary value problems. Later the Legendre wavelets' operational matrix for fractional derivatives was derived by F. Mohammadi, M. M. Hosseini and S. T. Mohyud-Din [**107**] to solve Bagley-Torvik boundary value problem. Depending on the operation matrix of differentiation for Legendre wavelets, F. Yin, J. Song and F. Lu [**177**] introduced a technique to solve the Sine-Gordan equation with initial condition by approximating both space and time domains by Legendre wavelets. This was achieved by suitably coupling Legendre wavelet with Laplace transform. Later Hariharan et. al.[**42, 46, 125**] applied this approach to different types of parabolic initial value problems.

As in the case of Haar wavelets, it is interesting to note that some authors consider all the terms involved in the given governing equation to fall in $L^2[0,1]$ space [**10, 51**] whereas some assume even the higher order terms to belong in that space [**49, 53, 176**]. Usually the methods based on the first approach produce better accuracy. Different types of well known partial differential equations were successfully handled by various researchers including advection problems [**161**], Allen-Cahn equation [**42**], Burgers Poisson equation [**178**], Cauchy problem [**165**], Convective-diffusive fluid problem [**4**], diffusion equation [**58, 176**], oscillatory elliptic boundary value problem [**10**], film- Pore diffusion model [**41, 121**], Fisher's equation [**95, 125, 169**], Fitzhugh-Nagumo equation[**47**], inverse problem [**122**], Helmoltz equation [**10**], Huxley equation [**169**], Klien Gordon equation [**168, 177, 179**], Newwell-Whitehead equation [**42, 169**], Poisson's equation [**10, 176**], reaction-diffusion equation [**46, 95**], regular long wave equation [**178**] and Sine-Gordon equation[**168, 179**]. By employing different approaches using Legendre wavelets, research workers also treated various other equations like partial differential equations with complex coefficients [**52**], stochastic differential equations [**54**], Fredholm [**1, 17, 35, 64, 96, 97, 98, 101, 143, 144, 163, 180, 184, 190**] and Volterra integral equations [**7, 16, 17, 50, 97, 101, 143, 145, 152, 162, 164, 180, 182, 190**] and integro-differential equations of Fredholm [**64, 101, 143**] and Volterra [**7, 16, 50, 101, 143, 152, 162, 164**] types.

1.1.3. Chebyshev Wavelet

One of the wavelets that was studied as an effective alternative for Legendre wavelets in the literature is Chebyshev wavelets. The Chebyshev wavelet family on the interval

$[0,1]$ is defined by

$$\psi_i(x) = \begin{cases} \frac{2^{\frac{k}{2}}\alpha_m}{\sqrt{\pi}} T_m(2^k x - \hat{n}) & \text{if } x \in [\frac{\hat{n}-1}{2^k}, \frac{\hat{n}+1}{2^k}) \\ 0 & \text{otherwise,} \end{cases}$$

where

$$\alpha_m = \begin{cases} 1 & \text{for } m = 0 \\ \sqrt{2} & m > 0 \end{cases}$$

and T_m denotes the Chebyshev polynomial of degree m with $m, n, k \in \mathbb{N}$, $n = 1, 2, \ldots 2^{k-1}$, $\hat{n} = 2n-1$, $m = 0, 1, 2, \cdots$ and $i = n + 2^{k-1}m$. Clearly the orthogonal property of Chebyshev wavelets family guarantees that it forms an orthogonal set in $L^2(0,1)$. Consequently, any square integrable function $g(x)$ can be approximated as

$$g(x) \simeq \sum_{i=1}^{N_1} b_i \psi_i(x) = B^T \Psi(x) \tag{1.12}$$

where B and $\Psi(x)$ are $N_1 = (2^{k-1}M)$ column vectors with $B^T = [b_1, b_2 \ldots, b_{N_1}]$ and $\Psi^T(x) = [\psi_1(x), \psi_2(x) \ldots, \psi_{N_1}(x)]$. The indefinite integral of the vector $\Psi(x)$ can be approximated as

$$\int_0^x \Psi(t)dt \approxeq P\Psi(x) \tag{1.13}$$

using the operational matrix of integration P of Chebyshev wavelets given by

$$\mathbf{P} = \begin{bmatrix} L & F & F & \ldots & F \\ O & L & F & \ddots & F \\ \vdots & O & L & \ddots & F \\ & & & & F \\ O & O & \ldots & O & L \end{bmatrix}_{N_1 \times N_1}$$

with

$$\mathbf{L} = 2^{-k}\begin{bmatrix} 1 & \frac{1}{\sqrt{2}} & 0 & 0 & 0 & \dots & 0 \\ -\frac{\sqrt{2}}{4} & 0 & \frac{1}{4} & 0 & 0 & \dots & 0 \\ -\frac{\sqrt{2}}{3} & -\frac{1}{2} & 0 & \frac{1}{6} & 0 & \dots & 0 \\ \vdots & \vdots & \vdots & \vdots & \ddots & \vdots & \vdots \\ \frac{\sqrt{2}}{2}(\frac{(-1)^{r-1}}{r-1} - \frac{(-1)^{r+1}}{r+1}) & 0 & 0 & \dots & -\frac{1}{2(r-1)} & 0 & \frac{1}{2(r-1)} \\ \vdots & \vdots & \vdots & \vdots & \ddots & \vdots & \vdots \\ \frac{\sqrt{2}}{2}(\frac{(-1)^{M-2}}{M-2} - \frac{(-1)^{M}}{M}) & 0 & 0 & 0 & \dots & -\frac{1}{2(M-2)} & 0 \end{bmatrix}_{M\times M,}$$

,

$$\mathbf{F} = 2^{-k}\begin{bmatrix} 2 & 0 & \dots & 0 \\ 0 & 0 & \dots & 0 \\ -\frac{\sqrt{2}}{3} & 0 & \dots & 0 \\ \vdots & \vdots & \ddots & \vdots \\ \frac{\sqrt{2}}{2}(\frac{1-(-1)^{r+1}}{r+1} - \frac{1-(-1)^{r-1}}{r-1}) & 0 & \dots & 0 \\ \vdots & \vdots & \ddots & \vdots \\ \frac{\sqrt{2}}{2}(\frac{1-(-1)^{M}}{M} - \frac{1-(-1)^{M-2}}{M-2}) & 0 & \dots & 0 \end{bmatrix}_{M\times M} \quad \text{and } \mathbf{O} = \begin{bmatrix} 0 & 0 & 0 & \dots & 0 \\ 0 & 0 & 0 & \dots & 0 \\ \vdots & \vdots & \vdots & \vdots & \vdots \\ 0 & 0 & \dots & 0 & 0 \end{bmatrix}_{M\times M}$$

for $r = 2, 3, \dots M-1$.

E. Babolian and F. Fattahzadeh were the ones who proposed a new numerical method for Bessel differential equation of order zero with Chebyshev wavelets [**11, 12**]. In the literature, many researchers solved different types of differential equations with Chebyshev wavelet methods in the same way as that of Legendre wavelet methods. Fractional order delay differential equations [**139**], fractional fifth-order Sawada–Kotera equation [**38**], fractional order nonlinear integro-differential equation [**139**], fractional pantograph equation[**139**], fractional Volterra- integro differential equation [**139**], Fredholm differential equation [**2, 11**], Sine-Gordon equation [**38**], time-varying delay system [**34**] and Volterra integral equation [**11**] are a few among them. In [**34**], Ghasami et. al. derived derivative operational matrix with delay for solving linear time-varying delay system and [**139**] proposed a modified Chebyshev wavelet for different types of fractional differential equations including fractional Volterra- integro differential equations. There is no major difference between Chebyshev and Legendre wavelets in terms of accuracy while solving differential equations and the order of the error is always same [**12, 150**]. If the solution space is polynomial, then one can obtain the desired numerical solution with lesser coefficients using both Chebyshev and Legendre wavelet methods.

1.1.4. Other Wavelets

Other than the above three wavelets there are many other wavelets in the literature that are being used by researchers for solving differential equations. Some of the important wavelets like Daubechies, Lemarie-Meyers and Mallat wavelets cannot be expressed in closed form even though they are widely used in various applications. On contrary, wavelets based on trigonometric functions and orthogonal polynomials like Bernoulli, CAS, Euler and Gauss Laguerre are very handy when it comes to solving differential equations due to its explicit representations. In this direction, B. Fischer and J. Prestin proposed a unified approach for the construction of wavelets based on orthogonal polynomials [**33**].

Bernoulli wavelet [68]:

Bernoulli wavelet family on the interval $[0,1)$ is defined by

$$\psi_{m,n}(x) = \begin{cases} 2^{\frac{k-1}{2}}\bar{\beta}_m(2^{k-1}x-\hat{n}) & \text{if } x \in [\frac{\hat{n}}{2^{k-1}}, \frac{\hat{n}+1}{2^{k-1}}) \\ 0 & \text{otherwise} \end{cases} \tag{1.14}$$

with

$$\bar{\beta}_m(x) = \begin{cases} 1 & \text{for } m = 0 \\ \frac{1}{\sqrt{\frac{(-1)^{m-1}(m!)^2}{(2m)!}\alpha_{2m}}}\beta_m(x) & m > 0, \end{cases}$$

where $n = 1, 2, \ldots 2^k - 1$, $m = 0, 1 \ldots M - 1$ and $\hat{n} = n - 1$. Here $\beta_m(x)$ is the well known Bernoulli polynomial of order m

$$\beta_m(x) = \sum_{i=0}^{m} \binom{m}{i} \alpha_{m-i} x^i,$$

where α_i, $i = 0, 1 \ldots$ are the Bernoulli numbers. These numbers are a sequence of signed rational numbers which arise in the series expansion of trigonometric functions and can be defined by the identity

$$\frac{x}{e^{x-1}} = \sum_{i=0}^{\infty} \alpha_i \frac{x^i}{1!}.$$

E. Keshavarz et al. derived operational matrix for Bernoulli wavelets [**68**] from Bernoulli polynomial for solving fractional order differential equations. Further same wavelet technique is modified for solving delay fractional optimal control problems [**126**], Singular Lane-Emden equation [**15**] and Volterra integro-differential equation [**141, 142**].

Cos and Sine wavelet [**181**]**:**

S. Yousefi and A. Banifatemi [**181**] defined CAS wavelet family on the interval $[0, 1)$ as follows:

$$\psi_{m,n}(x) = \begin{cases} 2^{\frac{k}{2}} \mathrm{CAS}_m(2^k x - n) & \text{if } x \in [\frac{n}{2^k}, \frac{n+1}{2^k}) \\ 0 & \text{otherwise,} \end{cases} \tag{1.15}$$

where $\mathrm{CAS}_m(x) = \cos(2m\pi x) + \sin(2m\pi x)$, $n = 0, 1, \ldots 2^k - 1$ and $m = 0, 1 \ldots M - 1$. Based on the above definition, H. Danfu and S. Xufeng [**27**] derived operational matrix of integration for CAS wavelets. [**3, 94, 140**] are some of the works done by researchers using CAS wavelets.

Euler wavelet [**183**]**:**

Euler wavelet family on the interval $[0, 1]$ is defined by

$$\psi_{m,n}(x) = \begin{cases} 2^{\frac{k-1}{2}} \bar{E}_m(2^{k-1}x - n + 1) & \text{if } x \in [\frac{n-1}{2^{k-1}}, \frac{n+1}{2^{k-1}}) \\ 0 & \text{otherwise,} \end{cases} \tag{1.16}$$

with

$$\bar{E}_m(x) = \begin{cases} 1 & \text{for } m = 0 \\ \frac{1}{\sqrt{\frac{2(-1)^{m-1}(m!)^2}{(2m)!} E_{2m+1}(0)}} E_m(x) & m > 0. \end{cases}$$

Here $n = 1, 2, \ldots 2^k - 1$, k is assumed to be any positive integer, m is the degree of the Euler polynomials and $E_m(x)$ is the well known Euler polynomial of order m which can be defined by means of the following generating functions [**183**]:

$$\frac{2e^{xs}}{e^s+1} = \sum_{m=0}^{\infty} E_m(x)\frac{s^m}{m!} \;\; (|s| < \pi).$$

In particular, the rational numbers $E_m = 2^m E_m(\frac{1}{2})$ are called the classical Euler numbers. Also, the Euler polynomials of the first kind for $k = 0, \ldots, m$ can be constructed from the following relation:

$$\sum_{k=0}^{m} \binom{m}{k} E_k(x) + E_k(x) = 2x^m$$

where $\binom{m}{k}$ is the usual binomial coefficient. In [**183**], the Euler wavelet is first presented and an operational matrix of fractional-order integration is derived for solving nonlinear Volterra integro-differential equations.

1.2. Basic results from linear algebra

The major advantage of operational matrices is that they convert differential equations into set of algebraic equations. Consequently one require certain basic definitions and results in the matrix theory to handle the resultant algebraic equations. This subsection provides the basic results from Linear Algebra that are used in the following chapters. This section is based on the book and one can refer to [**154, 159**] for more details.

Definition 1.2.1. *A $m \times n$ matrix A is a linear operator from $\mathbb{R}^n$ to $\mathbb{R}^m$ and it is denoted $A = (a_{i,j})$ where $i = 1, 2, \ldots, m$ and $j = 1, 2, \ldots, n$.*

Definition 1.2.2. *For two matrices, X, Y of the same dimension, $m \times n$, the Hadamard product, $X \circ Y$, is a matrix, of the same dimension as the operands, with elements given by $(X \circ Y)_{i,j} = (X)_{i,j}(Y)_{i,j}$. If $X = \begin{bmatrix} x_{11} & x_{12} \\ x_{21} & x_{22} \end{bmatrix}$ and $Y = \begin{bmatrix} y_{11} & y_{12} \\ y_{21} & y_{22} \end{bmatrix}$, then $X \circ Y = \begin{bmatrix} x_{11}y_{11} & x_{12}y_{12} \\ x_{21}y_{21} & x_{22}y_{22} \end{bmatrix}$.*

Lemma 1.2.1. [**159**, P. 576] *Some of the important properties of Hadamard product are*

(*i*) $A \circ B = B \circ A$

(ii) $A \circ (B \circ C) = (A \circ B) \circ C$

(iii) $A \circ (B + C) = A \circ B + A \circ C$

(iv) $(A \circ B)^T = A^T \circ B^T = B^T \circ A^T$

for any arbitrary matrices A, B and C of same size.

Definition 1.2.3. *Let X be a matrix of size $m \times n$ and Y be a $p \times q$ matrix. Then the Kronecker product of X and Y is a matrix of size $(mp) \times (qn)$ and the matrix is defined by*

$$\mathbf{X} \otimes \mathbf{Y} == \begin{bmatrix} x_{11}Y & x_{12}Y & \cdots & x_{1n}Y \\ x_{21}Y & x_{22}Y & \cdots & x_{2n}Y \\ \ldots & \ldots & \vdots & \vdots \\ x_{n1}Y & x_{n2}Y & \cdots & x_{nn}Y \end{bmatrix}.$$

.

Remark 1.2.1. *Sometimes the Kronecker product is also called as direct product or tensor product.*

Lemma 1.2.2. [**154**, Section 2.2] *Some of the important properties of Kronecker product are*

(i) $(\alpha A) \otimes B = \alpha A \otimes B$

(ii) $(A \otimes B)^T = A^T \otimes B^T$

(iii) $(A + B) \otimes (C + D) = A \otimes C + A \otimes D + B \otimes C + B \otimes D$

(iv) $(A + B) \otimes C = A \otimes C + B \otimes C$

(v) $(A \otimes B) \times (C \otimes D) = (AC) \otimes (BD)$

for any arbitrary matrices A, B, C of same size and for any real number α.

Definition 1.2.4. *Vectorization of a matrix (X) is defined as writing all the columns of a matrix in a row form as shown below*

$$\mathbf{X} = \begin{bmatrix} x_{11} & x_{12} \\ x_{21} & x_{22} \end{bmatrix}; \ \mathbf{vec}(\mathbf{X}) = \begin{bmatrix} x_{11} \\ x_{12} \\ x_{21} \\ x_{22} \end{bmatrix}.$$

.

Lemma 1.2.3. [**159**, P.577] *Some of the important properties of Vectorization are*

(i) $vec(A+B) = vec(A) + vec(B)$

(ii) $vec(A \circ B) = vec(A) \circ vec(B)$

(iii) $vec(ABC) = (C^T \otimes A) \times vec(B)$

(iv) $vec(A \circ (B \times X \times C)) = diag(A) \times (C^T \otimes B) \times vec(X)$

for any arbitrary matrices A, B, C *and* X *of same size.*

1.3. Outline of thesis and chapter summaries

Functional equations are generally solved by assuming the unknown solution of the problem by linear combination of the basis functions which can be orthogonal or non-orthogonal. Depending upon the problems under study the orthogonal functions can be chosen according to their specific characteristics. Thus approximation by orthogonal families of basis functions was found to be useful in several science and engineering applications. Many researchers came up with different approaches to solve differential equations using wavelets. It is also observed that the operational matrix wavelet methods for the nonlinear partial differential equations in the recent literature fall into two groups; methods for initial value problems and methods for initial-boundary value problems. By assuming the existence and uniqueness of solution as well as the convergence of the quasilinearization scheme, classical quasilinearization based operational matrix wavelet method for various types of ordinary and partial differential equations are studied in the recent literature. For the time dependent nonlinear partial differential equations with initial and boundary conditions, most of the wavelet based techniques are used only for approximating derivatives with respect to space variables. The time derivatives are always approximated using finite difference approach. After **Chapter 1**, the thesis is organized as follows.

In **Chapter 2**, efficient numerical schemes based on Haar and Legendre wavelet are proposed to solve a class of semi-linear parabolic initial boundary value problems. The proposed scheme here approximates even the derivatives with respect to time using wavelet techniques. The main advantage is that the performance of the proposed approach is far more better than that of the wavelet methods that used finite difference approximation in combination with wavelet techniques. This chapter also provide convergence analysis to an interesting generalization of Quasilinearization in the abstract space setting. As an application of the main theorem an existence and uniqueness result through monotone wuasilinearization method is obtained for the following semi linear parabolic initial boundary value problem(SPIBVP):

$$\frac{\partial u}{\partial t} = \frac{\partial^2 u}{\partial x^2} + h(x,t,u) \quad \text{in } Q, \quad u|_{\partial_p Q} = \phi, \tag{1.17}$$

with initial and Dirichlet boundary conditions, where $Q = (0,1) \times (0,T)$ and $\partial_p Q = \partial Q \backslash ((0,1) \times \{T\})$ denotes the parabolic boundary of Q. Here $h : \bar{Q} \times \mathbb{R} \to \mathbb{R}$ is continuous and ϕ is the restriction of u on $\partial_p Q$ where $\Phi \in C^{2,1}(\overline{Q})$. Let α_0, β_0 be a classical lower and upper solution for (1.17). Define $m = \min\limits_{(x,t)\in\overline{Q}} \{\alpha_0, \beta_0\}$ and $M = \max\limits_{(x,t)\in\overline{Q}} \{\alpha_0, \beta_0\}$ respectively.

Theorem 1.3.1. *If $u \to f_u(x,t,u)$ and $u \to g_u(x,t,u)$ are increasing and decreasing respectively for $u \in [m, M]$, then the SPIBVP (1.17) has a unique solution in $[\alpha_0, \beta_0]$. Moreover, the sequences (α_n) and (β_n) generated by*

$$\begin{aligned} \frac{\partial \alpha_{n+1}}{\partial t} - \frac{\partial^2 \alpha_{n+1}}{\partial x^2} &= h(x,t,\alpha_n) + f_u(x,t,\alpha_n)(\alpha_{n+1} - \alpha_n) \\ &+ \quad g_u(x,t,\beta_n)(\alpha_{n+1} - \alpha_n); \quad \alpha_{n+1}|_{\partial_p Q} = \phi; \end{aligned} \tag{1.18}$$

$$\begin{aligned} \frac{\partial \beta_{n+1}}{\partial t} - \frac{\partial^2 \beta_{n+1}}{\partial x^2} &= h(x,t,\beta_n) + f_u(x,t,\alpha_n)(\beta_{n+1} - \beta_n) \\ &+ \quad g_u(x,t,\beta_n)(\beta_{n+1} - \beta_n); \quad \beta_{n+1}|_{\partial_p Q} = \phi; \end{aligned} \tag{1.19}$$

are well-defined and converge to the unique solution monotonically and quadratically.

In **Chapter 3**, iterative methods based on Haar and Legendre wavelets are presented to solve a class of two dimensional partial integro differential equations numerically of the form

$$\frac{\partial u}{\partial t} = \frac{\partial^2 u}{\partial x^2} + \frac{\partial^2 u}{\partial y^2} + au - bu^2 - cu^\gamma \int_0^t u(x,y,s)\mathrm{d}s + g(x,y,t) \tag{1.20}$$

with initial and Dirichlet boundary conditions, where a, b, c, γ are non-negative constants. This equation arises from the mathematical modeling of nuclear reactor theory and population. Two different approaches are studied to develop numerical methods based on Haar and Legendre wavelets. In the first approach, time domain is approximated with the help of forward finite difference approach. In the second approach, both time as well as space domains including integral terms are approximated by wavelets. Appropriate examples are solved using these methods and the obtained results are compared with the methods available in the recent literature. A detailed comparison study between the two approaches are also presented in this chapter.

In **Chapter 4**, wavelet techniques are modified to solve the following hyperbolic equation using Chebyshev and Legendre wavelets' operational matrix method of the form

$$u_{tt}(x,t) - u_{xx}(x,t) + g(u) = f(x,t),\ 0 \le x \le 1,\ t \ge 0, \tag{1.21}$$

with initial and Dirichlet boundary conditions. For different choice of nonlinear term $g(u)$, one can deduce important equations such as Sine-Gordon, Sinh-Gordon, Liouville, Dodd-Bullough-Mikhailov and Tzitzeica-Dodd-Bullough from Eq (1.21). In this work, numerical method based on wavelets combined with classical quasilinearization for Klein-Gordon equation is proposed. To produce better accuracy, the time derivatives of the Klein Gordon equation is also approximated using Chebyshev / Legendre wavelets. Comparison of the numerical results with various schemes shows that the results obtained are better than those in some of the recent literature and are in good agreement with the exact solution. The proposed technique is also extended for coupled nonlinear sine Gordon equation using Chebyshev wavelets of the form

$$\begin{cases} u_{tt} - u_{xx} = -\delta^2 \sin(u-w) + f(x,t) \\ w_{tt} - c^2 w_{xx} = \sin(u-w) + g(x,t) \end{cases} \tag{1.22}$$

with initial and Dirichlet boundary conditions, where c, δ are non-negative constants.

Further in **Chapter 5**, two iterative schemes are proposed to solve the following fourth order elliptic equation with nonlocal boundary conditions:

$$\begin{aligned}\Delta^2 u - b_0\Delta u + c_0 u &= f(x,u)\ x\in\Omega,\\ u(x') &= \int_\Omega \beta(x',x)u(x)\mathrm{d}x + g^{(1)}(x')\ (x'\in\partial\Omega),\\ (\Delta u)(x') &= \int_\Omega \beta(x',x)(\Delta u)(x)\mathrm{d}x - g^{(0)}(x')\ (x'\in\partial\Omega),\end{aligned}\tag{1.23}$$

where Ω is bounded domain in $\mathbb{R}^n$ with boundary $\partial\Omega$ $(n = 1, 2\ldots)$, b_0 and c_0 are constants with $b_0 \geq 0$ and $f(x,u)$, $\beta(x',x)$ and $g^{(l)}(x')(l = 0,1)$ are continuous functions in their respective domain. The function $\beta(x',x)$ is non-negative on $\partial\Omega\times\Omega$. In the first approach, classical quasilinearization is coupled with Legendre wavelet for solving fourth order elliptic differential equation (1.23) with nonlocal boundary conditions. In the second approach at each step of the iterative scheme the fourth order equation approximated by solving two linear second order equations. This approach reduce the size of the resultant matrix. A detailed comparison study is also provided.

In **Chapter 6**, by utilizing the classical Newtons method, existence and uniqueness theorems for q-initial and q- boundary value problems are studied. Another important contribution is the development of a wavelet based numerical method to solve the q-difference equations numerically. The main theorem in this chapter is given below. Consider the q-initial and q-boundary value problems:

$$D_q[x(t)] = f(t,x(t)),\ x(0)=\alpha_0,\ t\in[0,T] \tag{1.24}$$

$$D_q^2[u(t)] = g(t,u(t)),\ u(0)=0,\ u(1)=0,\ t\in[0,1]. \tag{1.25}$$

Theorem 1.3.2. *Let $u_0 \in C[0,1]$ and $B(u_0,r)\subseteq C[0,1]$. Define the constants m^* and m_* by*

$$m^* = \max\{u(t) : t\in[0,1]; u\in B(u_0,r)\}$$

and

$$m_* = \min\{u(t) : t\in[0,1]; u\in B(u_0,r)\}.$$

Assume further that

(i) *for some $\delta > 0$, g, $g_2 \in C([0,1]\times[m_*-\delta, m^*+\delta],\mathbb{R})$;*

(ii) *there exist constants* M_0, M_1 *and* M_2 *such that* $\|u_0\| = M_0$, $\|g(t, u_0(t))\| \leq M_1$ *for all* $t \in [0, 1]$ *and* $|g_2(t, s)| \leq M_2$ *for all* $(t, s) \in [0, 1] \times [m_* - \delta, m^* + \delta]$;

(iii) *for some* $L \geq 0, |g_2(t, s_1) - g_2(t, s_2)| \leq L|s_1 - s_2|$;

(iv) $K = \dfrac{L\eta}{8K_1^2(1+q)} < 1$ *and* $r > \dfrac{\eta}{K_1} + \dfrac{8LK_1(1+q)\eta^2}{64K_1^4(1+q)^2 - L^2\eta^2}$, *where* $\eta = M_0 + \frac{M_1}{4(1+q)}$, $K_1 = 1 - \frac{M_2}{4(1+q)}$ *and* $M_2 < 4(1+q)$.

Then the boundary value problem (1.25) *has a unique solution in* $\overline{B}(u_0, r)$. *Moreover, the quasilinearization scheme*

$$D_q^2 u_{n+1} = g(t, u_n) + g_2(t, u_n)(u_{n+1} - u_n), \quad u_{n+1}(0) = u_{n+1}(1) = 0$$

is well defined, $u_n \in B(u_0, r)$ *for all* n *and the* (u_n) *converges quadratically and uniformly to the unique solution of* (1.25). *For each* $n \in \mathbb{N}$, *the following error estimate holds* $\|u - u_n\| \leq \left(\frac{L}{8(1+q) - 2M_2}\right) \|u - u_{n-1}\|^2$.

The final chapter summarizes the whole work by stating various merits of the proposed methods.

CHAPTER 2

SEMI-LINEAR PARABOLIC INITIAL BOUNDARY VALUE PROBLEMS (SPIBVP)

In this chapter[1], numerical methods based on quasilinearization, Haar wavelets and Legendre wavelets are presented to solve a class of semi-linear parabolic initial boundary value problem.

2.1. Introduction

This chapter discusses the numerical method based on wavelet for semi-linear parabolic initial boundary value problem(SPIBVP)

$$\frac{\partial u}{\partial t} = \frac{\partial^2 u}{\partial x^2} + h(x,t,u) \quad \text{in } Q, \quad u|_{\partial_p Q} = \phi, \tag{2.1}$$

where $Q = (0,1) \times (0,T)$ and $\partial_p Q = \partial Q \backslash ((0,1) \times \{T\})$ denotes the parabolic boundary of Q. Here $h : \bar{Q} \times \mathbb{R} \to \mathbb{R}$ is continuous and Φ is the restriction of u on $\partial_p Q$ where $\Phi \in C^{2,1}(\overline{Q})$. Eqn (2.1) represents various mathematical models in mathematical biology, plasma physics and quantum mechanics, to name a few. Considerable attention has been directed towards the development numerical scheme for partial differential equation using operational matrix wavelet methods [**10, 23, 45, 58, 85, 93, 124, 171, 172, 177**]. This method has been systematically studied for linear partial differential equations [**10, 85, 93, 171, 172**], however very few works have been done to solve nonlinear partial differential equations [**23, 45, 58**]. It is also observed that the operational matrix wavelet methods for the nonlinear partial differential equations in the recent literature fall into two groups: methods for initial value problems [**124, 177**] and the methods for initial and boundary value problems [**23, 45, 58, 62, 130, 137**]. By assuming the existence and uniqueness of solution as well as the convergence of the quasilinearization scheme,

[1]This chapter forms the paper by V.A. Vijesh and K.H. Kumar in Journal Applied Mathematics and Computation, 266 (2015), 1163–1176.

classical quasilinearization based operational matrix wavelet method for various types of ordinary and partial differential equations are studied in [**65, 66, 67, 137, 136, 138**] and [**23, 58, 62, 74, 130**], respectively. For the time dependent nonlinear partial differential equations, with initial and boundary condition, most of the wavelet based techniques are used only for approximating derivatives with respect to space variables. The time derivatives are always approximated using finite difference approach. In the present chapter, a new numerical scheme to solve a class of SPIBVPs is proposed with systematic convergence analysis for quasilinearization. However, in contrast to the methods discussed in [**23, 58, 62, 74, 130**], the new scheme approximate even the derivatives with respect to time using wavelet techniques. Two numerical schemes have been developed by combining classical quasilinearization with two types of wavelets, namely Haar and Legendre wavelets. Numerical simulations shows that the proposed approach obtain better accuracy than the results in recent literature. The convergence analysis for quasilinearization generalises a recent result of Lakshmikantham etal [**77**] as well as simplifies the result of Buică and Precup [**22**].

The organization of this chapter is as follows. In Section 2.2, we provide a generalised version of the recent result of Lakshmikantham et al [**77**]. This section also provides the existence and uniqueness of the solution of SPIBVP and the convergence of the generalised quasilinearization method. Section 2.3 explains the extension of Haar and Legendre wavelet collocation methods in combination with quasilinearization for SPIBVP. The proposed methods have been illustrated in Section 2.4 by applying to various examples including Fisher and Newell-Whitehead-Segal type equations. The obtained numerical results are also compared with other numerical results obtained in [**130, 166, 186**] using finite difference based Haar wavelet method(FHWM), variational iterative method(VIM), uniform cubic B-spline (UCBS), extended cubic uniform B-spline (ECBS), Trigonometric cubic B-spline (TCBS) and differential quadrature method. We conclude the discussion in Section 2.5, by stating the merits of the proposed method.

2.2. Quasilinearization

In this section, we generalise the proof of an existence and uniqueness theorem as well as convergence analysis of [**77**], for the SPIBVP. Throughout this chapter we assume that $E = (E, \leq, \|\cdot\|)$ is an ordered Banach space with order cone E_+. In [**77**], Lakshmikantham et.al studied an interesting version of fixed point theorem for the operator equation $Tx = x$ where $T : E \to E$, via quasilinearization and its application to SPIBVP. The result presented in [**77**] is based on the assumption that the operator $u \to T'_u v$ is increasing in u for all $v \in E_+$. However, in the present work, quadratic convergence of the iterative procedure has been proved by relaxing the monotonicity condition assumed in [**77**]. Throughout this chapter, T is decomposed as sum of the continuous operators F and G defined on E. The generalised version of Lakshmikantham etal [**77**] result can be stated as follows.

Theorem 2.2.1. *Let E be an ordered Banach space with a normal order cone E_+. Assume that $T : E \to E$ satisfies the following hypotheses*

1. *$F, G : [v_0, w_0] \to E$ are compact; $\exists\, v_0, w_0 \in E$ such that $v_0 \leq Tv_0$, $Tw_0 \leq w_0$ and $v_0 \leq w_0$;*
2. *The Frechet derivative F'_u and G'_u exist for every $u \in [v_0, w_0]$; $u \to F'_u v$ and $u \to G'_u v$ are increasing and decreasing, respectively, on $[v_0, w_0]$ for all $v \in E_+$;*
3.

$$Fu_0 - Fu_1 \leq F'_{u_0}(u_0 - u_1) \text{ whenever } v_0 \leq u_0 \leq u_1 \leq w_0. \tag{2.2}$$

$$Gu_0 - Gu_1 \leq G'_{u_1}(u_0 - u_1) \text{ whenever } v_0 \leq u_0 \leq u_1 \leq w_0. \tag{2.3}$$

4. *$(I - F'_v - G'_w)^{-1}$ exists and it is a bounded positive operator for all $v, w \in [v_0, w_0]$. Then for $n \in \mathbb{N}$, relations*

$$\begin{aligned} v_{n+1} &= Tv_n + (F'_{v_n} + G'_{w_n})(v_{n+1} - v_n) \\ w_{n+1} &= Tw_n + (F'_{v_n} + G'_{w_n})(w_{n+1} - w_n) \end{aligned}$$

define an increasing sequence (v_n) and a decreasing sequence (w_n) which converges to the solutions of the operator equation $Tx = x$. These fixed points are equal if $Tu_1 - Tu_0 < u_1 - u_0$ for all $v_0 \leq u_0 < u_1 \leq w_0$.

Proof: We first prove that v_n, w_n exists for all $n \in \mathbb{N}$ and satisfy

$$v_0 \leq v_1 \leq \cdots \leq v_n \leq w_n \leq w_{n-1} \leq \cdots \leq w_1 \leq w_0 \tag{2.4}$$

We prove this by induction. For $n = 1$, from the definition of v_1, we have $v_1 = (I - F'_{v_0} - G'_{w_0})^{-1}(T - F'_{v_0} - G'_{w_0})v_0$. Hence v_1 exists. Similarly it is easy to verify that w_1 exists. We will show $v_1 \geq v_0$. Let $p = v_1 - v_0$.

$$\begin{aligned} p &= Tv_0 + F'_{v_0}(v_1 - v_0) + G'_{w_0}(v_1 - v_0) - v_0 \\ (I - F'_{v_0} - G'_{w_0})p &\geq 0. \end{aligned}$$

Thus $p \geq 0$. We get $v_1 \geq v_0$. Similarly it can be shown that $w_1 \leq w_0$. Let $p = v_1 - w_1$. Then

$$\begin{aligned} p &= Tv_0 - Tw_0 + F'_{v_0}(v_1 - v_0 - w_1 + w_0) \\ &\quad + G'_{w_0}(v_1 - v_0 - w_1 + w_0) \\ (I - F'v_0 - G'_{w_0})p &= Fv_0 - Fw_0 + Gv_0 - Gw_0 + F'_{v_0}(w_0 - v_0) \\ &\quad + G'_{w_0}(w_0 - v_0) \\ (I - F'v_0 - G'_{w_0})p &\leq F'_{v_0}(v_0 - w_0) + G'_{w_0}(v_0 - w_0) + F'_{v_0}(w_0 - v_0) \\ &\quad + G'_{w_0}(w_0 - v_0) \end{aligned}$$

Thus $p \leq 0$. Hence $v_1 \leq w_1$. Suppose now that v_j, w_j exist for some $j > 0$ and that

$$v_0 \leq v_1 \leq \cdots \leq v_j \leq w_j \leq w_{j-1} \leq \cdots \leq w_1 \leq w_0 \tag{2.5}$$

We have $v_{j+1} = Tv_j + (F'_{v_j} + G'_{w_j})(v_{j+1} - v_j)$. Thus $v_{j+1} = (I - F'_{v_j} - G'_{w_j})^{-1}(T - F'_{v_j} - G'_{w_j})v_j$. Consequently v_{j+1} exists. Similarly we can show that w_{j+1} exists. Let $p = v_j - v_{j+1}$.

$$\begin{aligned} p &= Tv_{j-1} - Tv_j + (F'_{v_{j-1}} + G'_{w_{j-1}})(v_j - v_{j-1}) \\ &\quad - (F'_{v_j} + G'_{w_j})(v_{j+1} - v_j) \\ (I - F'v_j - G'_{w_j})p &= Fv_{j-1} - Fv_j + F'_{v_{j-1}}(v_j - v_{j-1}) + Gv_{j-1} - Gv_j \\ &\quad + G'_{w_{j-1}}(v_j - v_{j-1}) \\ &\leq F'_{v_{j-1}}(v_{j-1} - v_j) + G'_{v_j}(v_{j-1} - v_j) + F'_{v_{j-1}}(v_j - v_{j-1}) \\ &\quad + G'_{w_{j-1}}(v_j - v_{j-1}) \\ &\leq (G'_{w_{j-1}} - G'_{v_j})(v_j - v_{j-1}) \\ (I - F'_{v_0} - G'_{w_0})p &\leq 0 \end{aligned}$$

Thus $p \leq 0$. Hence $v_j \leq v_{j+1}$. Similarly it can be shown that $w_{j+1} \leq w_j$ and $v_{j+1} \leq w_{j+1}$. Hence (2.4) is true for all $n \in \mathbb{N}$. Note that v_{n+1} can be rewritten as

$$\begin{aligned} v_{n+1} &= (I - F'_{v_0} - G'_{w_0})^{-1}(T(v_n) - (F'_{v_0} + G'_{w_0})v_n) \\ &\quad +(I - F'_{v_0} - G'_{w_0})^{-1}((F'_{v_n} + G'_{w_n}) - (F'_{v_0} + G'_{w_0}))(v_{n+1} - v_n) \end{aligned}$$

Using hypothesis (2), one can conclude that

$$0 \leq ((F'_{v_n} + G'_{w_n}) - (F'_{v_0} + G'_{w_0}))(v_{n+1} - v_n) \leq ((F'_{w_0} + G'_{v_0}) - (F'_{v_0} + G'_{w_0}))(v_{n+1} - v_n)$$

For each $n \in \mathbb{N}$, define $\gamma_n = (I - F'_{v_0} - G'_{w_0})^{-1}((F'_{w_0} + G'_{v_0}) - (F'_{v_0} + G'_{w_0}))v_n$. It is easy to see that γ_n is an increasing sequence. The compactness property of the operators $F'_{v_0}, F'_{w_0}, G'_{v_0}$ and G'_{w_0} ensures that γ_n has a convergent sub-sequence. The normality of the cone together with the monotonicity of γ_n guarantee that γ_n is a convergent sequence. Consequently $(I-F'_{v_0}-G'_{w_0})^{-1}((F'_{v_n}+G'_{w_n})-(F'_{v_0}+G'_{w_0}))(v_{n+1}-v_n) \to 0$ as $n \to \infty$. Hence v_n has a convergent sub-sequence. Once again using the normality of the cone together with the monotonicity of v_n guarantee that v_n is a convergent sequence. Similarly w_n is a convergent sequence. Let v and w be the limit of v_n and w_n respectively. From the construction of v_n and w_n, $v \leq w$. Note that

$$\begin{aligned} Tv - v_{n+1} &\geq (F'_{v_0} + G'_{w_0})(v - v_n) - (F'_{v_0} + G'_{v_0})(v_{n+1} - v_n) \\ Tv - v_{n+1} &\leq (F'_{w_0} + G'_{v_0})(v - v_n) - (F'_{v_0} + G'_{w_0})(v_{n+1} - v_n) \end{aligned}$$

Hence v and w are solutions of the operator equation $Tx = x$. If $v < w$ then $w - v = Tw - Tv < w - v$, which is a contradiction. Hence the uniqueness is proved.

Proposition 2.2.1. *Let T satisfy all the hypotheses of Theorem 2.2.1 and*

1. $\|F'_u - F'_v\| \leq L_1\|u - v\|$ *and* $\|G'_u - G'_v\| \leq L_2\|u - v\|$ *for all* $u, v \in [v_0, w_0]$ *for some* L_1 *and* $L_2 > 0$.
2. $M = \sup\{\|(I - F'_u - G'_v)^{-1}\| : u, v \in [v_0, w_0]\} < \infty$.

Then the sequences (v_n) and (w_n) converge quadratically to the same fixed point of T.

Proof: Let v be the fixed point of T. Define $r_n = v - v_n$, and $r'_n = w_n - v$, $n = 1, 2, \cdots$.

$$
\begin{aligned}
r_n &= T(v) - T(v_{n-1}) - (F'_{v_{n-1}} + G'_{w_{n-1}})(v_n - v_{n-1}) \\
(I - F'_{v_{n-1}} + G'_{w_{n-1}})r_n &\leq (F'_v - F'_{v_{n-1}})r_{n-1} + (G'_{v_{n-1}} - G'_{w_{n-1}})r_{n-1}
\end{aligned}
$$

Thus $0 \leq r_n \leq (I - F'_{v_{n-1}} - G'_{w_{n-1}})^{-1}(F'_v - F'_{v_{n-1}} + G'_{v_{n-1}} - G'_{w_{n-1}})r_{n-1}$. Since E_+ is normal, then by definition, $\exists$ a positive constant N such that $\|r_{n+1}\| \leq NM\|p_n\|\|r_{n-1}\|$, $p_n = \|F'_v - F'_{v_{n-1}} + G'_{v_{n-1}} - G'_{w_{n-1}}\|$. Simplifying further, $\|r_n\| \leq MN\left\{(L_1 + \frac{3}{2}L_2)\|\|r_{n-1}\|^2 + \frac{L_2}{2}\|r'_{n-1}\|^2\right\}$. A similar error estimate can be obtained for r'_n.

We conclude this section, by obtaining an existence and uniqueness as well as the convergence of the generalised quasilinearization for the SPIBVP (2.1) from Theorem 2.2.1, which is a key step for the proposed numerical scheme. Throughout this chapter assume that h can be decomposed as $f+g$ where f and g are convex and concave functions, respectively.

Throughout this section we made the following assumptions:

- (A_1) Let α_0 and β_0 in $C^{2,1}(\overline{Q})$ be the lower and upper solution of the SPIBVP (2.1). The constants m and M are defined by $m = \min\limits_{(x,t)\in\overline{Q}}\{\alpha_0, \beta_0\}$ and $M = \max\limits_{(x,t)\in\overline{Q}}\{\alpha_0, \beta_0\}$ respectively.
- (A_2) For some $\delta > 0$, $f, g : \overline{Q} \times [m - \delta, M + \delta] \to \mathbb{R}$ is continuous and continuously differentiable with respect to u.
- (A_3) The function $u \to f_u(x,t,u)$ and $u \to g_u(x,t,u)$ are Lipschitz continuous for $u \in [m, M]$.

Theorem 2.2.2. *If $u \to f_u(x,t,u)$ and $u \to g_u(x,t,u)$ is increasing and decreasing respectively for $u \in [m, M]$, then the SPIBVP (2.1) has a unique solution in $[\alpha_0, \beta_0]$. Moreover the sequences (α_n) and (β_n) generated by*

$$
\begin{aligned}
\frac{\partial \alpha_{n+1}}{\partial t} - \frac{\partial^2 \alpha_{n+1}}{\partial x^2} &= h(x,t,\alpha_n) + f_u(x,t,\alpha_n)(\alpha_{n+1} - \alpha_n) \\
&+ g_u(x,t,\beta_n)(\alpha_{n+1} - \alpha_n); \quad \alpha_{n+1}|_{\partial_p Q} = \phi; \qquad (2.6)
\end{aligned}
$$

$$
\begin{aligned}
\frac{\partial \beta_{n+1}}{\partial t} - \frac{\partial^2 \beta_{n+1}}{\partial x^2} &= h(x,t,\beta_n) + f_u(x,t,\alpha_n)(\beta_{n+1} - \beta_n) \\
&+ g_u(x,t,\beta_n)(\beta_{n+1} - \beta_n); \quad \beta_{n+1}|_{\partial_p Q} = \phi; \qquad (2.7)
\end{aligned}
$$

are well-defined and converge to the unique solution monotonically and quadratically.

Proof: It is enough to prove this theorem for SPIBVP with homogeneous initial condition

$$\frac{\partial u}{\partial t} = \triangle u + h(x,t,u) \quad \text{in } Q, \quad u|_{\partial_p Q} = 0. \tag{2.8}$$

From Remark 3.3 of [**77**], α_0 and β_0 are ordered that is $\alpha_0 \leq \beta_0$ in Q. Now we will convert this problem as a fixed point problem in Banach space $C(\overline{Q})$. Choose $\lambda \geq 0$ such that $f_u(x,t,\alpha) + g_u(x,t,\beta) + \lambda \geq 0$ for all $(x,t) \in \overline{Q}$ and $\alpha, \beta \in [\alpha_0, \beta_0]$. Then SPIBVP (2.8) is equivalent to

$$\frac{\partial u}{\partial t} - \triangle u + \lambda u = h(x,t,u) + \lambda u \quad \text{in } Q, \quad u|_{\partial_p Q} = 0. \tag{2.9}$$

Define an operator $T : [\alpha_0, \beta_0] \subset C(\overline{Q}) \to C(\overline{Q})$ by $T(u) = v$ where v is the solution of the linear SPIBVP

$$\frac{\partial v}{\partial t} - \triangle v + \lambda v = h(x,t,u) + \lambda u \quad \text{in } Q, \quad v|_{\partial_p Q} = 0 \tag{2.10}$$

From Theorem 9.2.5 of [**174**] the operator T is well defined. Clearly the solution of $Tx = x$ is the solution of the SPIBVP (2.8). Define an operator $F : [\alpha_0, \beta_0] \subset C(\overline{Q}) \to C(\overline{Q})$ by $F(u) = v$ where v is the solution of the linear SPIBVP

$$\frac{\partial v}{\partial t} - \triangle v + \lambda v = f(x,t,u) + \lambda u \quad \text{in } Q, \quad v|_{\partial_p Q} = 0 \tag{2.11}$$

Define another operator $G : [\alpha_0, \beta_0] \subset C(\overline{Q}) \to C(\overline{Q})$ by $G(u) = v$ where v is the solution of the linear SPIBVP

$$\frac{\partial v}{\partial t} - \triangle v + \lambda v = g(x,t,u) \quad \text{in } Q, \quad v|_{\partial_p Q} = 0 \tag{2.12}$$

Once again using Theorem 9.2.5 of [**174**] the operators F and G are well defined. It is easy to verify that $T = F + G$. Now all the hypothesis of Theorem 2.2.1 verified easily using the Remark 3.3 and Lemma 3.1 of [**77**]. From [**77**] the operators F and G are compact and the the Frechet derivative exist for all $u \in [\alpha_0, \beta_0]$. For $h \in C(\overline{Q})$, the Frechet derivative of F at u is given by $F'_u(h) = z$ where z is the solution of

$$\frac{\partial z}{\partial t} - \triangle z + \lambda z = (f_u(x,t,u) + \lambda)h \quad \text{in } Q, \quad z|_{\partial_p Q} = 0. \tag{2.13}$$

For $h \in C(\overline{Q})$, the Frechet derivative of G at u is given by $G'_u(h) = z$ where z is the solution of

$$\frac{\partial z}{\partial t} - \triangle z + \lambda z = g_u(x,t,u)h \quad \text{in } Q, \quad z|_{\partial_p Q} = 0. \tag{2.14}$$

From Lemma 3.1 of [**77**], $u \to F'_u v$ is increasing on $[\alpha_0, \beta_0]$ for all $v \in E_+$. Similarly $u \to G'_u v$ is decreasing on $[\alpha_0, \beta_0]$ for all $v \in E_+$. There exits an equivalent norm such that $\|F'_\alpha + G'_\beta\| \leq q < 1$ for all α and β in $[\alpha_0, \beta_0]$. Consequently $(I - F'_\alpha - G'_\beta)^{-1}$ exists and is a bounded positive operator for all α and β in $[\alpha_0, \beta_0]$. For the choice $\alpha_0 = u_0$ and $\beta_0 = w_0$ all the hypotheses of Theorem 2.2.1 and all the hypotheses of Proposition 2.2.1 are verified. Hence the operator equation $Tx = x$ has a unique solution. Moreover the iterative procedure

$$\alpha_{n+1} = T(\alpha_n) + F'_{\alpha_n}(\alpha_{n+1} - \alpha_n) + G'_{\beta_n}(\alpha_{n+1} - \alpha_n) \tag{2.15}$$

$$\beta_{n+1} = T(\beta_n) + F'_{\alpha_n}(\beta_{n+1} - \beta_n) + G'_{\beta_n}(\beta_{n+1} - \beta_n) \tag{2.16}$$

converges to the solution of the equation $Tx = x$ monotonically and uniformly. Equivalently the SPIBVP (2.8) has a unique solution in $[\alpha_0, \beta_0]$ and the generalised quasilinearization (2.6) and (2.7) converges monotonically and uniformly to the unique solution of the SPIBVP (2.8).

2.3. Wavelets Collocation Method

The following functions are used throughout the following sections: $p_{i,1}(x) = \int_0^x h_i(t)\mathrm{d}t$, $p_{i,2}(x) = \int_0^x p_{i,1}(t)\mathrm{d}t$ and $C_{i,1} = \int_0^1 p_{i,1}(t)\mathrm{d}t$. Using (1.1), (1.2) and (1.3) the explicit representations of $p_{i,1}$ and $p_{i,2}$ are given by

$$p_{i,1}(x) = \begin{cases} x - \alpha & \text{if } x \in [\alpha, \beta), \\ \gamma - x & \text{if } x \in [\beta, \gamma), \\ 0 & \text{otherwise.} \end{cases} \tag{2.17}$$

$$p_{i,2}(x) = \begin{cases} \frac{1}{2}(x - \alpha)^2 & \text{if } x \in [\alpha, \beta), \\ \frac{1}{4m^2} - \frac{1}{2}(\gamma - x)^2 & \text{if } x \in [\beta, \gamma), \\ 0 & \text{otherwise.} \end{cases} \tag{2.18}$$

In this section we will discuss the Haar wavelet collocation method. The approach is similar for Legendre wavelet collocation method. For further details on Legendre wavelet operational matrix method one can refer [**10, 134**]. Theorem 2.2.2 guarantees that the partial derivatives of the linear as well as nonlinear problems can be expressed as Haar wavelets series. Consequently, they can be approximated by

$$\frac{\partial^2 u}{\partial x^2} = \sum_{i=1}^{2M}\sum_{j=1}^{2M} a_{j,i} h_i(x) h_j(t) \tag{2.19}$$

$$\frac{\partial u}{\partial t} = \sum_{i=1}^{2M}\sum_{j=1}^{2M} b_{j,i} h_i(x) h_j(t) \tag{2.20}$$

Throughout this chapter, the set $\{(x_i, t_j) : x_i = t_i = \frac{i-0.5}{2M}, 1 \leq i, j \leq 2M\}$ are the set of points that are used for collocation. The following equations are obtained respectively from (2.19) and (2.20).

$$\begin{aligned} u(x,t) &= \sum_{j=1}^{2M}\sum_{i=1}^{2M} a_{j,i}(p_{i,2}(x) - xC_{i,1}) h_j(t) \\ &\quad + (u(1,t) - u(0,t))x + u(0,t) \end{aligned} \tag{2.21}$$

$$u(x,t) = \sum_{j=1}^{2M}\sum_{i=1}^{2M} b_{j,i} h_i(x) p_{i,1}(t) + u(x,0) \tag{2.22}$$

By equating (2.21) and (2.22), for each collocation point, we obtain $4M^2$ equations. Another $4M^2$ equations are obtained by substituting the expressions of $u(x,y)$ and its partial derivatives into given differential equation. These two sets of equations are solved simultaneously for the unknown Haar coefficients $a_{j,i}$'s and $b_{j,i}$'s. Then the solution can be obtained by substituting these coefficients in (2.21) or (2.22).

2.3.1. Numerical Implementation

Let α_0, β_0 be the lower and upper solutions of SPIBVP 2.1. Let the initial condition be $u(x,0) = f_1(x)$, and the boundary conditions be $u(0,t) = g_1(t)$ and $u(1,t) = g_2(t)$. Let A^T denotes transpose of the matrix A. Using the collocation points and the Eqns (2.21) and (2.22), α_{n+1} can be written as

$$\alpha_{n+1}(x,t) = \phi^T A_{n+1} P_2 - \phi^T A_{n+1} F_1 + Q_1 - Q_2 + Q_3 \tag{2.23}$$

$$\alpha_{n+1}(x,t) = P_1^T B_{n+1} \phi + Q_4 \tag{2.24}$$

where $Q_1 = x_i g_2(t_j),\ Q_2 = x_i g_1(t_j),\ Q_3 = g_1(t_j),\ Q_4 = f_1(x_i),\ A^T_{n+1} = [a_{j,i}],\ B^T_{n+1} = [b_{j,i}]$,$\phi = [h_i(t_j)],\ P_1 = [p_{i,1}(t_j)],\ P_2 = [p_{i,2}(t_j)],\ F_1 = x_i C_{i,1}$ and $\{(x_i, t_j) : x_i = t_i = \frac{i-0.5}{2M}, 1 \leq i, j \leq 2M\}$. Here A_0 and B_0 are obtained from the lower solution α_0. Again using the collocation points and the Eqns (2.21) and (2.22), β_{n+1} can be written as

$$\beta_{n+1}(x,t) = \phi^T C_{n+1} P_2 - \phi^T C_{n+1} F_1 + Q_1 - Q_2 + Q_3 \tag{2.25}$$

$$\beta_{n+1}(x,t) = P_1^T D_{n+1}\phi + Q_4 \tag{2.26}$$

Here C_0 and D_0 are obtained from β_0. Equating (2.23) and (2.24), (2.25) and (2.26) we get,

$$\phi^T A_{n+1} P_2 - \phi^T A_{n+1} F_1 - P_1^T B_{n+1}\phi = -Q_1 + Q_2 - Q_3 + Q_4 \tag{2.27}$$

$$\phi^T C_{n+1} P_2 - \phi^T C_{n+1} F_1 - P_1^T D_{n+1}\phi = -Q_1 + Q_2 - Q_3 + Q_4 \tag{2.28}$$

where $C^T_{n+1} = [c_{i,j}]$, $D^T_{n+1} = [d_{i,j}]$. From equations (2.6) and (2.7) and using the collocation points we have

$$\phi^T B_{n+1}\phi - \phi^T A_{n+1}\phi - Q_5 \circ (P_1^T B_{n+1}\phi) = Q_6 \tag{2.29}$$

$$\phi^T D_{n+1}\phi - \phi^T C_{n+1}\phi - Q_5 \circ (P_1^T D_{n+1}\phi) = Q_7 \tag{2.30}$$

where $Q_5 = (f_u(x_i, t_j, \alpha_n(x_i, t_j)) + g_u(x_i, t_j, \beta_n(x_i, t_j)))$, $Q_6 = [h(x_i, t_j, \alpha_n(x_i, t_j))] - Q_5 \circ Q_8 + Q_5 \circ Q_4$, $Q_7 = [h(x_i, t_j, \beta_n(x_i, t_j))] - Q_5 \circ Q_9 + Q_5 \circ Q_4$, $Q_8 = \alpha(x_i, t_j)$, $Q_9 = \beta(x_i, t_j)$ and $\circ$ denotes the Hadamard product. At each step, we have four unknown matrices $A_{n+1}, B_{n+1}, C_{n+1}$ and D_{n+1} and four equations (2.27), (2.28), (2.29) and (2.30). Using vectorization technique, equations can be brought into $LX = b$ and $L_1 Y = b_1$ where the elements of L are from ϕ, P_1, P_2, F, Q_1-Q_6, Q_8 and the elements of L_1 are from ϕ, P_1, P_2, F, Q_1-Q_5, Q_7, Q_9 and the elements of X are from A_{n+1}, B_{n+1} and the elements of Y are from C_{n+1}, D_{n+1} and the elements of b, b_1 are from Q_1-Q_9. This system $LX = b$ can be solved by any standard procedure to obtain A_{n+1} and B_{n+1}. Similarly solve $L_1 Y = b_1$ to obtain C_{n+1} and D_{n+1}. Then the numerical solution can be obtained by substituting these coefficients in any of these (2.23), (2.24), (2.25) and (2.26) equations. In all the numerical experiments $||\alpha_{n+1} - \alpha_n|| \leq 10^{-06}$ is used as the stopping criteria.

2.4. Numerical Examples

In this section, the wavelet based quasilinearization method is illustrated by successfully applying to different examples including Newell-Whitehead-Segel equation. Since some important partial differential equation models including Fisher equation, Allan-Cahn equation and FitzHugh-Nagumo equation are of the form $u_t = u_{xx} + au + bu^m + cu^n$, $m, n \in \mathbb{R}^+$ the present approach has been tested for various values of a, b and c with suitable initial and boundary conditions. For each example the existence and uniqueness of the solution and convergence of the proposed method has been verified using Theorem 2.2.2. To solve the examples numerically, at each iteration, the corresponding linear initial value problem has been solved using Haar and Legendre wavelets as discussed in Section 2.3. Throughout this chapter the following abbreviations have been used,

1. HWQM - Haar Wavelet Generalized Quasilinearization Method.
2. LWQM - Legendre Wavelet Generalized Quasilinearization Method.
3. J denotes the resolution of Haar wavelet and N denote the number of Legendre Wavelets.

Example 2.4.1.

The following example, known as Huxley problem, has been solved numerically using finite difference based Haar wavelet method (FHWM) in [**130**] the problem can be defined as

$$\frac{\partial u}{\partial t} = \frac{\partial^2 u}{\partial x^2} + u(1-u)(u-1) \tag{2.31}$$

with the initial and boundary conditions: $u(x,0) = \frac{1}{2} + \frac{1}{2}\tanh(\frac{x}{2\sqrt{2}})$, $0 \le x \le 1$ and $u(0,t) = \frac{1}{2} - \frac{1}{2}\tanh(\frac{t}{4})$, $u(1,t) = \frac{1}{2} + \frac{1}{2}\tanh(\frac{1}{2\sqrt{2}}(1 - \frac{t}{\sqrt{2}}))$ $t \ge 0$. For the choice $g(t,x,u) = -u^3, f(t,x,u) = 2u^2 - u$ $\alpha_0 = 0$ and $\beta_0 = 1$ all the hypotheses of Theorem 2.2.2 is satisfied. Hence the initial boundary value problem (2.4.1) has a unique solution in $[\alpha_0, \beta_0]$ and the generalised quasilinearization defined by (2.6) and (2.7) converges uniformly to the unique solution of (2.4.1). The numerical results obtained using the proposed scheme (Figure (2.1)) has been compared with the numerical schemes FHWM [**130**] and VIM [**130**]. Table 2.1 and 2.2 show that the HWQM and LWQM both performs extremely well compared to FHWM and VIM methods. Besides that, though the HWQM (Figure (2.6)) and FHWM[**130**] take same number of wavelets ($J = 3$), results obtained using HWQM is more accurate than that obtained using FHWM. This shows the advantage of wavelet method independent of finite different based time discretization.

Example 2.4.2.

In [**186**], the following Fisher's equation has been solved using various numerical based on Spline interpolation, Consider the Fisher equation with initial and boundary conditions given below.

$$\frac{\partial u}{\partial t} = \frac{\partial^2 u}{\partial x^2} + u - u^2. \tag{2.32}$$

with the initial and boundary conditions: $u(0,x) = (1 + e^{(\frac{x}{\sqrt{6}})})^{-2}$, $u(t,0) = (1 + e^{(-\frac{5t}{6})})^{-2}$ and $u(t,1) = (1 + e^{(\frac{1}{\sqrt{6}} - \frac{5t}{6})})^{-2}$. For the choice $g(t,x,u) = u - u^2, \alpha_0 = 0$ and $\beta_0 = 1$ all the hypotheses of Theorem 2.2.2 is satisfied. Hence the initial boundary value problem (2.4.2) has a unique solution in $[\alpha_0, \beta_0]$ and the generalised quasilinearization defined by (2.6) and (2.7) converges uniformly to the solution. Table 2.4 gives a comparison of various methods based on splines as well as present wavelet based HWQM and LWQM (Figure (2.2)). Though the problem has been solved on same grid for all methods, LWQM (Figure (2.7)) outperforms spline based schemes in terms of accuracy.

Example 2.4.3.

Consider the following Newell-Whitehead-Segel Equation discussed in [**186**]

$$\frac{\partial u}{\partial t} = \frac{\partial^2 u}{\partial x^2} + 2u - 3u^2. \tag{2.33}$$

with the initial and boundary conditions: $u(0,x) = \lambda$, $u(t,0) = \frac{-2\lambda e^{2t}}{(-2+3\lambda(1-e^{2t}))}$ and $u(t,1) = \frac{-2\lambda e^{2t}}{(-2+3\lambda(1-e^{2t}))}$. Numerical solution of (2.4.3), has been discussed using uniform cubic B-spline (UCBS), extended cubic uniform B-spline (ECBS) and Trigonometric cubic B-spline (TCBS) in [**186**]. For the choice $g(t,x,u) = 2u - 3u^2, \alpha_0 = 0$ and $\beta_0 = 1$ all the hypotheses of Theorem 2.2.2 is satisfied. Hence the initial boundary value problem (2.4.3) has a unique solution in $[\alpha_0, \beta_0]$ and the generalised quasilinearization defined by (2.6) and (2.7) converges uniformly to the solution. Table 2.7 gives a comparison of various methods based on splines as well as present wavelet based HWQM (Figure (2.8)) and

LWQM (Figure (2.3)). Though the problem has been solved on same grid for all methods, LWQM outperforms spline based schemes in terms of accuracy.

Example 2.4.4.

Consider the following Newell-Whitehead-Segel Equation discussed in [**186**]

$$\frac{\partial u}{\partial t} = \frac{\partial^2 u}{\partial x^2} + u - u^4 \tag{2.34}$$

with the initial and boundary conditions: $u(t,1) = (\frac{1}{2}\tanh(\frac{-3}{2\sqrt{10}}(1-\frac{7t}{\sqrt{10}})+\frac{1}{2}))^{\frac{2}{3}}$, $u(0,x) = \frac{1}{\left(1+e^{\frac{3x}{\sqrt{10}}}\right)^{2/3}}$ and $u(t,0) = (\frac{1}{2}\tanh(\frac{-3}{2\sqrt{10}}(-\frac{7t}{\sqrt{10}})+\frac{1}{2}))^{\frac{2}{3}}$. Numerical solution of (2.4.4), has been discussed using uniform cubic B-spline (UCBS), extended cubic uniform B-spline (ECBS) and Trigonometric cubic B-spline (TCBS) in [**186**]. For the choice $g(t,x,u) = u - u^4, \alpha_0 = 0$ and $\beta_0 = 1$ all the hypotheses of Theorem 2.2.2 is satisfied. Hence the initial boundary value problem (2.4.4) has a unique solution in $[\alpha_0, \beta_0]$ and the generalised quasilinearization defined by (2.6) and (2.7) converges uniformly to the solution. Table 2.8 gives a comparison of various methods based on splines as well as present wavelet based HWQM and LWQM (Figure (2.4)). Though the problem has been solved on same grid for all methods, LWQM (Figure (2.9)) outperforms spline based schemes in terms of accuracy.

Example 2.4.5.

Consider the following Fisher's type Equation discussed in [**166**] using differential quadrature method

$$\frac{\partial u}{\partial t} = \frac{\partial^2 u}{\partial x^2} + u(u-a)(1-u) \tag{2.35}$$

with the initial and boundary conditions $u(x,0) = \frac{1}{2}+\frac{1}{2}a+(\frac{1}{2}-\frac{1}{2}a)\tanh(c_3+\frac{1}{4}\sqrt{2}(-1+a)(x))$,$u(0,t) = \frac{1}{2}+\frac{1}{2}a+(\frac{1}{2}-\frac{1}{2}a)\tanh(c_3+\frac{\sqrt{2}}{4}(-1+a)(-mt))$, $u(1,t) = \frac{1}{2}+\frac{1}{2}a+(\frac{1}{2}-\frac{1}{2}a)\tanh(c_3+\frac{\sqrt{2}}{4}(-1+a)(1-mt))$ where $m = \frac{a+1}{\sqrt{2}}$ and c_3 is an arbitrary constant. Numerical solution of (2.4.5), has been discussed using differential quadrature method in [**166**] various choices of c_3 and a. For the choice $g(t,x,u) = -au - u^3, f(t,x,u) = u^2 + au^2$ $\alpha_0 = 0$ and $\beta_0 = 1$ all the hypotheses of Theorem 2.2.2 is satisfied. Hence the initial boundary value problem (2.4.5) has a unique solution in $[\alpha_0, \beta_0]$ and the generalised quasilinearization (Figure (2.5)) defined by (2.6) and (2.7) converges uniformly to the unique solution of (2.4.5). The results given in Table 2.10 show that wavelet based scheme (Figure (2.10)) perform better than the differential quadrature method discussed in [**166**].

Remark 2.4.1.

1. In all the examples considered above (Examples 2.4.1 to 2.4.5), it is interesting to note that g_x is not a non-decreasing function, which is a crucial condition in [**77**]. Hence the quasilinearization technique discussed in [**77**] cannot ensure the convergence of the iterative procedure as well as the existence and uniqueness of solutions of these example problems.
2. Another observation is that as the value of "n" is increased in the equation $u_t = u_{xx} + au + bu^n$, Haar wavelet method requires more number of wavelets to produce high accuracy. This may be due to the fact that to approximate a polynomial using step functions, large number of step functions are required.
3. It is also observed from Tables 2.3, 2.5, 2.6, 2.9 and 2.11 that though Legendre wavelet based solutions are more accurate than their Haar wavelet counterparts, computational time required by Legendre wavelets are high when compared to Haar wavelets.
4. All the numerical experiments were performed on a Intel Core i5 CPU 2.5 GHz laptop with 4 GB RAM, Windows 8 (64 bit) MATLAB R2010b.

2.5. Conclusion

In this chapter, numerical methods based on wavelets and generalised quasilinearization methods for SPIBVP are proposed. While approximating the derivatives, both time and space derivatives are discretized using wavelets techniques, unlike in any other wavelet based methods in the recent literature. To illustrate the proposed method, numerical examples are provided including Fisher equation, Huxely equation, Newell-Whitehead-Segal equation. It is seen through these examples that the performance of the new approach is far more efficient than the methods that used finite difference approximation in combination with wavelet techniques. Thus the results obtained using the quasilinearization approach along with wavelets are better than those in some of the recent literature

[**130, 166, 186**] and are in good agreement with the exact solutions as discussed in Section 2.4.

TABLE 2.1. Comparison of errors in the solution of Example 2.4.1 for $J = 3$ and $N = 8$ at $t = 0.4$ between present schemes and the scheme discussed in [**130**].

x	VIM[**130**]	Haar[**130**]	HWQM	LWQM
0.09375	$8.87e^{-07}$	$5.30e^{-04}$	$8.14e^{-08}$	$9.68e^{-11}$
0.28125	$3.27e^{-04}$	$3.78e^{-03}$	$2.84e^{-07}$	$3.83e^{-11}$
0.46875	$6.45e^{-04}$	$9.97e^{-03}$	$3.38e^{-07}$	$2.09e^{-11}$
0.65625	$9.40e^{-04}$	$1.91e^{-02}$	$3.64e^{-07}$	$1.93e^{-11}$
0.84375	$1.20e^{-03}$	$3.12e^{-02}$	$4.47e^{-07}$	$9.43e^{-11}$

TABLE 2.2. Comparison of errors in the solution of Example 2.4.1 for $J = 3$ and $N = 8$ at $t = 0.6$ between present schemes and the scheme discussed in [**130**].

x	VIM[**130**]	Haar[**130**]	HWQM	LWQM
0.15625	$5.90e^{-05}$	$2.23e^{-03}$	$1.65e^{-07}$	$6.11e^{-11}$
0.34375	$7.95e^{-04}$	$9.19e^{-03}$	$4.14e^{-07}$	$6.76e^{-12}$
0.53125	$1.50e^{-03}$	$2.08e^{-02}$	$4.90e^{-07}$	$8.91e^{-12}$
0.71875	$2.16e^{-03}$	$3.71e^{-02}$	$4.15e^{-07}$	$3.37e^{-11}$
0.90625	$2.75e^{-03}$	$6.14e^{-02}$	$4.19e^{-07}$	$1.27e^{-10}$

TABLE 2.3. Example 2.4.1 comparison between HWQM and LWQM for the number of wavelets used and required number of iterations

Method	No. of wavelets	No. of Iterations	Time(s)
HWQM	16	5	0.24
LWQM	8	7	1.61

TABLE 2.4. Comparison of errors for Example 2.4.2 for various points and time between present schemes ($J = 3$ and $N = 10$) and the schemes discussed in [**186**].

(x,t)	UCBC[**186**]	TCBC[**186**]	ECBC[**186**]	HWQM	LWQM
(0.2, 0.2)	$2.810e^{-04}$	$2.716e^{-04}$	$6.909e^{-04}$	$1.679e^{-04}$	$1.265e^{-12}$
(0.2, 0.4)	$3.030e^{-04}$	$3.249e^{-04}$	$6.760e^{-04}$	$2.917e^{-04}$	$1.291e^{-12}$
(0.2, 0.6)	$2.480e^{-04}$	$2.341e^{-04}$	$5.184e^{-04}$	$3.832e^{-04}$	$6.298e^{-13}$
(0.4, 0.2)	$4.270e^{-04}$	$4.126e^{-04}$	$1.056e^{-03}$	$6.544e^{-04}$	$2.233e^{-13}$
(0.4, 0.4)	$4.740e^{-04}$	$4.551e^{-04}$	$1.059e^{-03}$	$1.083e^{-04}$	$1.536e^{-12}$
(0.4, 0.6)	$3.970e^{-04}$	$3.764e^{-04}$	$8.328e^{-04}$	$1.462e^{-04}$	$7.052e^{-13}$
(0.6, 0.2)	$4.380e^{-04}$	$4.247e^{-04}$	$1.085e^{-03}$	$5.094e^{-05}$	$2.765e^{-12}$
(0.6, 0.4)	$4.910e^{-04}$	$4.723e^{-04}$	$1.099e^{-03}$	$1.096e^{-04}$	$8.002e^{-13}$
(0.6, 0.6)	$4.180e^{-04}$	$3.972e^{-04}$	$8.799e^{-04}$	$1.506e^{-04}$	$3.089e^{-12}$

TABLE 2.5. Example 2.4.2 comparison between HWQM and LWQM for the number of wavelets used and required number of iterations

Method	No. of wavelets	No. of Iterations	Time(s)
HWQM	16	4	0.08
LWQM	10	4	3.40

TABLE 2.6. Example 2.4.3 comparison between HWQM and LWQM for the number of wavelets used and required number of iterations

Method	No. of wavelets	No. of Iterations	Time(s)
HWQM	16	4	0.08
LWQM	10	4	3.41

Table 2.7. Comparison of errors at various points and time for Example 2.4.3 with $\lambda = 0.1$: Present methods($J = 3$ and $N = 10$) and the methods discussed in [**186**].

(x, t)	UCBC[**186**]	TCBC[**186**]	ECBC[**186**]	HWQM	LWQM
(0.2, 0.2)	$8.323e^{-04}$	$8.295e^{-04}$	$6.068e^{-04}$	$2.258e^{-05}$	$3.682e^{-10}$
(0.2, 0.4)	$1.101e^{-03}$	$1.007e^{-03}$	$6.800e^{-04}$	$7.191e^{-06}$	$2.766e^{-10}$
(0.2, 0.6)	$8.581e^{-04}$	$8.514e^{-04}$	$5.476e^{-04}$	$1.263e^{-05}$	$2.450e^{-09}$
(0.4, 0.2)	$1.226e^{-03}$	$1.222e^{-03}$	$9.013e^{-04}$	$1.713e^{-05}$	$1.843e^{-09}$
(0.4, 0.4)	$1.520e^{-03}$	$1.514e^{-03}$	$1.023e^{-03}$	$5.163e^{-06}$	$1.664e^{-09}$
(0.4, 0.6)	$1.302e^{-03}$	$1.292e^{-03}$	$8.289e^{-04}$	$1.650e^{-05}$	$2.029e^{-09}$
(0.6, 0.2)	$1.226e^{-03}$	$1.222e^{-03}$	$9.013e^{-04}$	$1.713e^{-05}$	$1.843e^{-09}$
(0.6, 0.4)	$1.520e^{-04}$	$1.514e^{-03}$	$1.023e^{-03}$	$5.163e^{-06}$	$1.664e^{-09}$
(0.6, 0.6)	$1.302e^{-03}$	$1.292e^{-03}$	$8.289e^{-04}$	$1.650e^{-06}$	$2.029e^{-09}$

Table 2.8. Comparison of errors at various points and time for Example 2.4.4: Present methods($J = 4$ and $N = 10$) and the methods discussed in [**186**].

(x, t)	UCBC[**186**]	TCBC[**186**]	ECBC[**186**]	HWQM	LWQM
(0.2, 0.2)	$3.800e^{-04}$	$3.951e^{-04}$	$9.673e^{-04}$	$4.215e^{-05}$	$2.484e^{-09}$
(0.2, 0.4)	$8.190e^{-04}$	$8.362e^{-03}$	$1.900e^{-03}$	$1.362e^{-04}$	$2.314e^{-09}$
(0.2, 0.6)	$1.112e^{-03}$	$1.130e^{-03}$	$2.446e^{-03}$	$2.367e^{-04}$	$1.707e^{-09}$
(0.4, 0.2)	$4.230e^{-04}$	$4.448e^{-04}$	$1.159e^{-03}$	$8.345e^{-05}$	$1.604e^{-10}$
(0.4, 0.4)	$1.111e^{-03}$	$1.137e^{-03}$	$2.641e^{-03}$	$2.708e^{-04}$	$1.750e^{-09}$
(0.4, 0.6)	$1.613e^{-03}$	$1.640e^{-03}$	$3.587e^{-03}$	$5.430e^{-04}$	$1.441e^{-09}$
(0.6, 0.2)	$2.890e^{-04}$	$3.111e^{-04}$	$8.863e^{-04}$	$8.107e^{-06}$	$4.167e^{-09}$
(0.6, 0.4)	$1.008e^{-03}$	$1.034e^{-03}$	$2.444e^{-03}$	$1.648e^{-04}$	$2.954e^{-10}$
(0.6, 0.6)	$1.569e^{-03}$	$1.596e^{-03}$	$3.512e^{-03}$	$4.184e^{-04}$	$5.312e^{-09}$

TABLE 2.9. Example 2.4.4 comparison between HWQM and LWQM for the number of wavelets used and required number of iterations

Method	No. of wavelets	No. of Iterations	Time(s)
HWQM	32	4	2.85
LWQM	10	4	3.41

TABLE 2.10. Comparison of L_∞ errors for Example 2.4.5 at t for $c_3 = 1$ with method discussed in [**166**]

t	$a = 0.5$ [**166**]	HWQM $J = 5$	LWQM $N = 6$	$a = 1.5$ [**166**]	HWQM $J = 5$	LWQM $N = 6$
0.2	$2.412e^{-06}$	$8.627e^{-08}$	$1.115e^{-10}$	$2.105e^{-05}$	$3.046e^{-07}$	$1.199e^{-11}$
0.5	$2.227e^{-06}$	$7.800e^{-07}$	$9.539e^{-11}$	$1.736e^{-05}$	$2.241e^{-06}$	$1.305e^{-09}$

TABLE 2.11. Example 2.4.5 comparison between HWQM and LWQM for the number of wavelets used and required number of iterations

Method	No. of wavelets	No. of Iterations	Time(s)
HWQM	32	6	10.01
LWQM	6	6	0.87

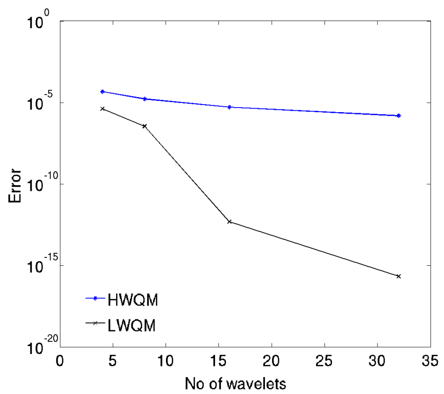

FIGURE 2.1. Comparison of errors for HWQM and LWQM for Example 2.4.1

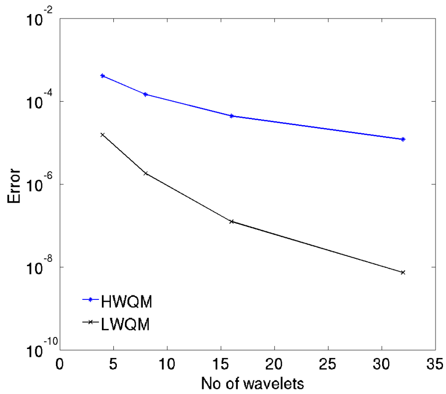

FIGURE 2.2. Comparison of errors for HWQM and LWQM for Example 2.4.2.

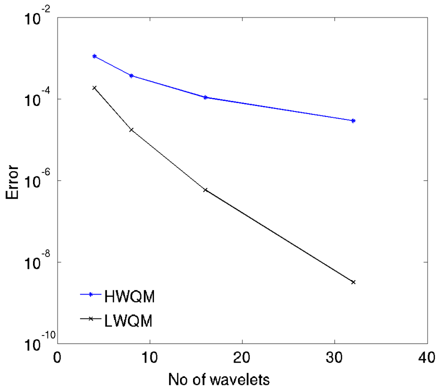

FIGURE 2.3. Comparison of errors for HWQM and LWQM for Example 2.4.3

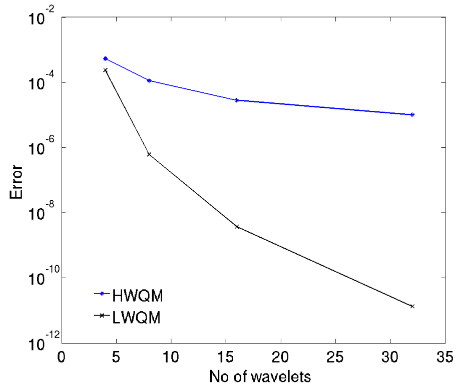

FIGURE 2.4. Comparison of errors for HWQM and LWQM for Example 2.4.4

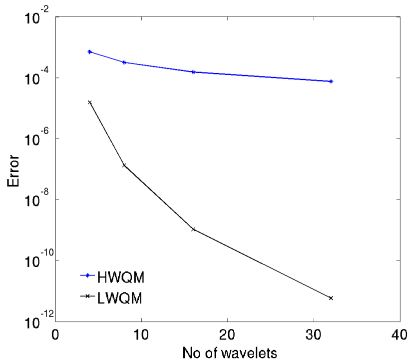

FIGURE 2.5. Comparison of errors for HWQM and LWQM for Example 2.4.5

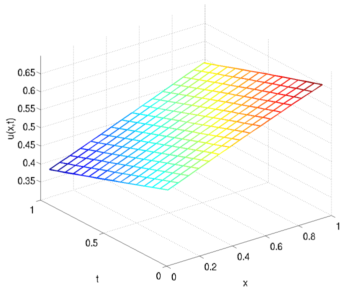

FIGURE 2.6. Numerical solution of $u(x,t)$ of Example 2.4.1 for $J = 3$

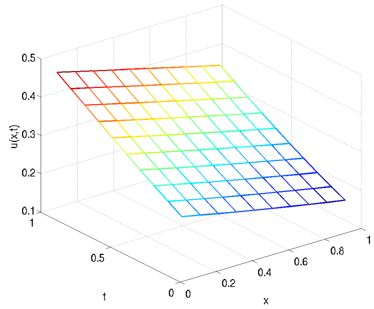

FIGURE 2.7. Numerical solution of $u(x,t)$ of Example 2.4.2 for $N = 10$

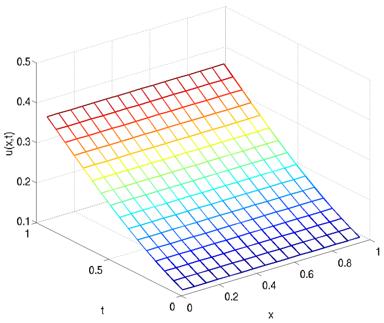

FIGURE 2.8. Numerical solution of $u(x,t)$ of Example 2.4.3 for $J = 3$

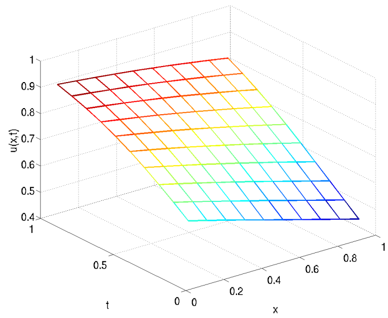

FIGURE 2.9. Numerical solution of $u(x,t)$ of Example 2.4.4 for $N = 10$

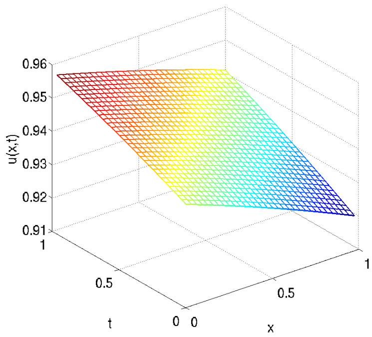

FIGURE 2.10. Numerical solution of $u(x,t)$ of Example 2.4.5 for $J = 5$,$a = 0.5$

CHAPTER 3

CLASS OF PARTIAL INTEGRO DIFFERENTIAL EQUATIONS

This chapter[1] discusses the numerical method based on wavelets for a class of partial integro differential equations.

3.1. Introduction

It is evident from the literature that differential equations with nonlocal integral terms can model certain physical situations more accurately than classical differential equation [**109, 110, 112, 113, 114, 153, 157**]. Recently, finite difference based numerical methods [**20, 21, 155**] were studied for a two dimensional parabolic integro differential equation (TDPIDE). In this paper, efficient wavelet based numerical methods for the following parabolic type TDPIDE is proposed.

$$\frac{\partial u}{\partial t} = \frac{\partial^2 u}{\partial x^2} + \frac{\partial^2 u}{\partial y^2} + au - bu^2 - cu^\gamma \int_0^t u(x, y, s)\mathrm{d}s + g(x, y, t) \tag{3.1}$$

where a, b and c are non-negative constants. If the effect of temperature feedback is taken into consideration, Equation (3.1) represents the neutron flux in the nuclear reactor dynamics [**112, 113, 114, 146, 147, 156**] for the choice of $b = 0$ and $\gamma = 1$. For the choice $c = 0$, equation (3.1) reduces to the well known Fisher's equation. Equation (3.1) is also considered as the partial differential equation version of the well known Volterra population model.

$$u'(t) = au(t) - bu^2(t) - cu(t) \int_0^t u(s)\mathrm{d}s \tag{3.2}$$

[1]This chapter forms the paper by K.H. Kumar and V.A. Vijesh in Journal Computers and Mathematics with Applications, Article in press.

where a, b and c are non-negative constants and represents the coefficient of birth rate, intra-species competition and the toxicity respectively. The term $cu(t)\int_0^t u(s)\mathrm{d}s$ denotes the influence of toxin accumulation on the species [**157**].

Developing numerical methods for two dimensional partial integro differential equation (TDPIDE) is a tedious job as one has to handle the integral terms together with two dimensional partial derivatives simultaneously. It is interesting to note that a large collection of numerical methods, including wavelet methods, are available in the literature for the ordinary integro-differential equation (3.2) (see [**29, 69, 117, 118, 119, 120**] and the reference therein). However, the techniques for handling the TDPIDE numerically are very limited. Though the operational matrix methods with various type of wavelets developed extensively to solve different type of partial differential equation, methods for the two dimensional partial integro differential equation are not much available in the literature. The present work attempts to develop a new numerical technique for solving TDPIDE (3.1) based on wavelets. In this chapter an iterative method coupled with two type of wavelets is presented to solve TDPIDE with Dirichlet boundary condition numerically. In the first approach, a finite difference wavelet method is proposed, in which time domain is approximated by forward finite difference approach and space variables are approximated by wavelets. Though the accuracy obtained by this method is decent, for obtaining better accuracy one has to go for small time step. Consequently, this method requires more grid points too. To avoid this issue, similar to other published studies [**10, 49, 59, 75, 149, 151, 169**] both time as well as space domains are approximated by wavelets. The full utilization of wavelets ensures that, it produces better accuracy with less number of grid points. Though this generalization may seem to be simple, the effectiveness of the proposed scheme involves effective numerical implementation. In case of one dimension, after approximating time and space domain by wavelets one need to deal with a system of matrix equations. However, direct extension to the two dimensional case will produce an equation involving multidimensional matrix equations. This complex implementation issue is successfully and efficiently handled by using tensor [**13**] and vectorization. Moreover, the extension of the proposed approach to higher dimension is straight forward. For the future reference, this approach will be termed as fully wavelet method. Though this approach produces a higher order accuracy with a coarser grid, it suffers from either memory issue or ill-conditioning problems as the grid becomes finer. Consequently, implementation of the algorithm demands a sophisticated system with a large memory.

The organization of this chapter is as follows. Section 3.2 provides a detailed explanation of numerical implementations of the proposed schemes. The proposed iterative methods based on wavelets is illustrated in Section 3.3 by applying it to various examples. The numerical results thus obtained are compared with other numerical methods using finite difference approach [**21, 123**]. We conclude the discussion in Section 3.4 by stating the merits of the proposed methods.

3.2. Wavelet Method

This section describes the numerical algorithms for the problem 3.1. More specifically, both of these approaches are explained using Haar wavelet for two dimensional partial integro differential equation. It is straightforward to replace Haar wavelet with Legendre wavelet in these methods.

3.2.1. Finite Difference based wavelet method

The following scheme of linear two dimensional partial differential equation is obtained after applying classical quasilinearization to the two dimensional partial differential equation (3.1).

$$
\begin{aligned}
\frac{\partial u_{n+1}}{\partial t} &= \frac{\partial^2 u_{n+1}}{\partial x^2} + \frac{\partial^2 u_{n+1}}{\partial y^2} + f(u_n) + g(x,y,t) + \frac{df(u_n)}{du}(u_{n+1} - u_n) \\
&\quad - c u_n^{\gamma} \int_0^t u_n(x,y,s)\mathrm{d}s - c\gamma u_n^{\gamma-1} \int_0^t u_n(x,y,s)\mathrm{d}s (u_{n+1} - u_n) \\
&\quad - c u_n^{\gamma} \Big(\int_0^t u_{n+1}(x,y,s)\mathrm{d}s - \int_0^t u_n(x,y,s)\mathrm{d}s\Big) \; n = 0,1,2,\cdots
\end{aligned} \tag{3.3}
$$

where $f(u) = au - bu^2$. In this approach, to solve the linear differential equation in the iterative procedure (3.3), finite difference technique and wavelets are used to approximate the time and space derivatives respectively. First, the time derivative of the problem is discretized as follows

$$
\frac{\partial u}{\partial t} \approx \frac{u(x,y,t+h) - u(x,y,t)}{h} \tag{3.4}
$$

where h is the step size. After time discretization the linear partial differential equation in (3.3) becomes

$$\begin{aligned}\frac{u_{n+1}(x,y,t+h)}{h} &= \frac{\partial^2 u_{n+1}}{\partial x^2}(x,y,t+h)+\frac{\partial^2 u_{n+1}}{\partial y^2}(x,y,t+h)+f(u_n(x,y,t+h))\\ &\quad +g(x,y,t+h)+f'(u_n(x,y,t+h)(u_{n+1}(x,y,t+h)-u_n(x,y,t+h))\\ &\quad +\frac{u_{n+1}(x,y,t)}{h}+\gamma c u_n^{\gamma}(x,y,t+h)\int_0^{t+h}u_n(x,y,s)\mathrm{d}s\\ &\quad -u_{n+1}(x,y,t+h)c\gamma u_n^{\gamma-1}(x,y,t+h)\int_0^{t+h}u_n(x,y,s)\mathrm{d}s\\ &\quad -c u_n^{\gamma}(x,y,t+h)\int_0^{t+h}u_{n+1}(x,y,s)\mathrm{d}s \qquad (3.5)\end{aligned}$$

where $n = 0, 1, 2\cdots$. Clearly (3.5) is a partial differential equation in two variable x and y. In this section, the method discussed in [**10, 49, 59, 75, 149, 151, 169**] for partial differential equation is extended for partial integro differential equation. At time step $t+h$, other than the term $\frac{u_{n+1}(x,y,t)}{h}$ rest of the terms are evaluated at the same time step $t+h$. This approach can be explained by assuming that the partial derivatives as well as other functions arising in the linear partial differential equation (3.5) are square integrable functions. Thus

$$\frac{\partial^2 u(x,y,t+h)}{\partial x^2} = \sum_{i=1}^{2M}\sum_{j=1}^{2M} a_{i,j}h_i(x)h_j(y) = H^T(x)AH(y) \qquad (3.6)$$

$$\frac{\partial^2 u(x,y,t+h)}{\partial y^2} = \sum_{i=1}^{2M}\sum_{j=1}^{2M} b_{i,j}h_i(x)h_j(y) = H^T(x)BH(y). \qquad (3.7)$$

where $A = [a_{i,j}], B = [b_{i,j}], H(\zeta) = [h_i(\zeta)]$. The following equations are obtained by integration from (3.6) and (3.7).

$$\begin{aligned}u(x,y,t+h) &= P_2^T(x)AH(y)-D_1xAH(y)+u(0,y,t+h)\\ &\quad +(u(1,y,t+h)-u(0,y,t+h))x, \qquad (3.8)\\ u(x,y,t+h) &= H^T(x)BP_2^T(y)-H^T(x)BD_1y+u(x,0,t+h)\\ &\quad +(u(x,1,t+h)-u(x,0,t+h))y \qquad (3.9)\end{aligned}$$

The integral term in the equation (3.5) is approximated by

$$\int_0^{t+h} u(x,y,s)\mathrm{d}s = \int_0^{t+h} \Big(P_2^T(x)AH(y) - D_1 xAH(y) + u(0,y,s)$$

$$+(u(1,y,s) - u(0,y,s))x\Big)\mathrm{d}s, \tag{3.10}$$

$P_1(\zeta) = [p_{i,1}(\zeta)]$, $P_2(\zeta) = [p_{i,2}(\zeta)]$ and $D_1 = \int_0^1 p_{i,1}(\zeta)\mathrm{d}\zeta$ for $1 \le i \le 2M$. For collocation, the points in the set $\{(x_i, y_j) : x_i = y_i = \frac{i-0.5}{2M}, 1 \le i, j \le 2M\}$ are considered.

By equating (3.8) and (3.9) one can get $4M^2$ equations. Another $4M^2$ equations can be obtained by substituting the expressions (3.6)−(3.10) of u_{xx}, u_{yy}, u and $\int_0^{t+h} u(x,y,s)\,\mathrm{d}s$ in the given linear partial integro differential equation (3.5). The resulting system needs to be solved for Haar coefficients $a_{i,j}$'s and $b_{i,j}$'s. Then the solution $u(x,y,t+h)$ can be obtained from (3.8) or (3.9).

3.2.1.1. **Numerical Implementation.** Using the collocation points in equations (3.6)−(3.10) we obtain,

$$\frac{\partial^2 u_{n+1}(x,y,t+h)}{\partial x^2} = \phi^T A_{n+1}\phi \tag{3.11}$$

$$\frac{\partial^2 u_{n+1}(x,y,t+h)}{\partial y^2} = \phi^T B_{n+1}\phi \tag{3.12}$$

$$u_{n+1}(x,y,t+h) = P_2^T A_{n+1}\phi - F_2^T A_{n+1}\phi + G_1 \tag{3.13}$$

$$u_{n+1}(x,y,t+h) = \phi^T B_{n+1}P_2 - \phi^T B_{n+1}F_2 + G_2 \tag{3.14}$$

$$\int_0^{t+h} u(x,y,s)\mathrm{d}s = (t+h)\big(P_2^T A_{n+1}\phi - F_2^T A_{n+1}\phi\big) + G_3 \tag{3.15}$$

where $A_{n+1} = [a_{i,j}]$, $B_{n+1} = [b_{i,j}]$, $\phi = [H(x_i)] = [H(t_j)]$, $F_2 = D_1 X, F_2 = C_1 X$, $X = [x_i]$, $G_1 = x_i u(1,y_j,t+h) - x_i u(0,y_j,t+h) + u(0,y_j,t+h)$, $G_2 = y_j u(x_i,1,t+h) - y_j u(x_i,0,t+h) + u(x_i,0,t+h)$, $G_3 = \int_0^{t+h}\big(x_i u(1,y_j,s) - x_i u(0,y_j,s) + u(0,y_j,s)\big)\mathrm{d}s$, $P_2 = [P_2(x_i)] = [P_2(y_j)]$ and $\{(x_i,y_j) : x_i = y_i = \frac{i-0.5}{2M}, 1 \le i,j \le 2M\}$. Here A_0, B_0 are obtained from the initial approximation u_0.

The following is obtained by equating (3.13) and (3.14).

$$P_2^T A_{n+1}\phi - F_2^T A_{n+1}\phi - \phi^T B_{n+1}P_2 + \phi^T B_{n+1}F_2 = G_4 \tag{3.16}$$

where $G_4 = G_2 - G_1$. Using collocation points the discretized version of equations (3.5) can be written as

$$\begin{aligned}\frac{P_2^T A_{n+1}\phi}{h} - \frac{F_2^T A_{n+1}\phi}{h} &= \phi^T A_{n+1}\phi + \phi^T B_{n+1}\phi + G_{12} + G_{13} \\ &+(G_8 - G_{10} - (t+h)G_{11}) \circ \big(P_2^T A_{n+1}\phi - F_2^T A_{n+1}\phi\big) \\ &+\frac{G_5 - G_1}{h} + G_1 \circ \big(G_8 - G_{10}\big) - G_3 \circ G_{11} - G_5 \circ G_8 + G_{11} \circ G_7\end{aligned} \tag{3.17}$$

$G_5 = u_n(x_i, y_j, t)$, $G_6 = u_n(x_i, y_j, t+h)$, $G_7 = \int_0^{t+h} u_n(x_i, y_j, s)\mathrm{d}s$, $G_8 = f'(u_n(x_i, y_j, t+h))$, $G_9 = c\gamma u_n^{\gamma-1}(x_i, y_j, t+h)$, $G_{10} = G_9 \circ G_7$, $G_{11} = \gamma c u_n^{\gamma}(x_i, y_j, t+h)$, $G_{12} = g(x_i, y_j, t+h)$, $G_{13} = f(x_i, y_j, t+h)$ and '$\circ$' denotes the Hadamard product. This results in two equations (3.16) and (3.17) in two unknown matrices A_{n+1} and B_{n+1}. By using vectorization the above equations can be brought into the form $L_1\theta_1 = b_1$ with θ_1 having the entries A_{n+1} and B_{n+1}. Finally, the solution for the two dimensional partial integro differential equation is obtained by using one of the equations (3.8) or (3.9).

3.2.2. Fully wavelet method

In this section we propose a method for solving the linear two dimensional partial integro differential equation at each step of the iteration (3.3). Though few authors studied operational matrix method for two dimensional partial differential equation [**58, 149, 170**] the proposed approach is different from all of these. In this approach, we approximate both time and space derivatives using wavelets to solve the linear integro differential equation (3.3) in the iterative procedure. Assume that the partial derivatives as well as other functions arising in (3.3) are square integrable functions in their respective domain. Thus

$$\frac{\partial^2 u(x,y,t)}{\partial x^2} = \sum_{i=1}^{2M}\sum_{j=1}^{2M}\sum_{k=1}^{2M} a_{i,j,k} h_i(x) h_j(y) h_k(t) \tag{3.18}$$

$$\frac{\partial^2 u(x,y,t)}{\partial y^2} = \sum_{i=1}^{2M}\sum_{j=1}^{2M}\sum_{k=1}^{2M} b_{i,j,k} h_i(x) h_j(y) h_k(t) \tag{3.19}$$

$$\frac{\partial u(x,y,t)}{\partial t} = \sum_{i=1}^{2M}\sum_{j=1}^{2M}\sum_{k=1}^{2M} c_{i,j,k} h_i(x) h_j(y) h_k(t). \tag{3.20}$$

We define $d_{i,1} = \int_0^1 h_i(\zeta)\mathrm{d}\zeta$, $p_{i,1} = \int_0^t h_i(\zeta)\mathrm{d}\zeta$ and $p_{i,2} = \int_0^t p_{i,1}(\zeta)\mathrm{d}\zeta$. Integrating (3.18) and (3.19) with respect to x and y leads to

$$\frac{\partial u(x,y,t)}{\partial x} = \sum_{i=1}^{2M}\sum_{j=1}^{2M}\sum_{k=1}^{2M} a_{i,j,k}(p_{i,1}(x) - d_{i,1})h_j(y)h_k(t) + u(1,y,t) - u(0,y,t) \tag{3.21}$$

$$\frac{\partial u(x,y,t)}{\partial y} = \sum_{i=1}^{2M}\sum_{j=1}^{2M}\sum_{k=1}^{2M} b_{i,j,k}h_i(x)(p_{j,1}(y) - d_{j,1})h_k(t) + u(x,1,t) - u(x,0,t) \tag{3.22}$$

respectively. Further integrating (3.21),(3.22) and (3.20) with respect to x, y and t leads to

$$\begin{aligned} u(x,y,t) &= \sum_{i=1}^{2M}\sum_{j=1}^{2M}\sum_{k=1}^{2M} a_{i,j,k}(p_{i,2}(x) - d_{i,1}x)h_j(y)h_k(t) \\ &\quad +(u(1,y,t) - u(0,y,t))x + u(0,y,t) \\ u(x,y,t) &= \sum_{i=1}^{2M}\sum_{j=1}^{2M}\sum_{k=1}^{2M} b_{i,j,k}h_i(x)(p_{j,2}(y) - yd_{j,1})h_k(t) \\ &\quad +(u(x,1,t) - u(x,0,t))y + u(x,0,t) \\ u(x,y,t) &= \sum_{i=1}^{2M}\sum_{j=1}^{2M}\sum_{k=1}^{2M} c_{i,j,k}h_i(x)h_j(y)p_{k,1}(t) + u(x,y,0) \end{aligned} \tag{3.23}$$

Using (3.23), the integral term in the governing equation is approximated by

$$\begin{aligned} \int_0^t u(x,y,s)\mathrm{d}s &= \sum_{i=1}^{2M}\sum_{j=1}^{2M}\sum_{k=1}^{2M} a_{i,j,k}(p_{i,2}(x) - d_{i,1}x)h_j(y)p_{k,1}(t) \\ &\quad + \int_0^t (u(1,y,s) - u(0,y,s))x\mathrm{d}s + \int_0^t u(0,y,s)\mathrm{d}s \end{aligned} \tag{3.24}$$

After collocation, from (3.23) one gets $8M^3$ equations by equating any of the two expression of $u's$. Another set of $8M^3$ equations can be obtained by substituting the expressions of u_{xx}, u_{yy}, u_t, u given in equations (3.18)$-$(3.20), (3.22) and (3.24) respectively in the corresponding linear TDPIDE. This system needs to be solved for Haar coefficients $a_{i,j,k}$'s, $b_{i,j,k}$'s and $c_{i,j,k}$'s. Then the solution $u(x,y,t)$ can be obtained from any of the u's from (3.23).

3.2.2.1. **Numerical Implementation.** Tensor is an efficient tool to handle multi index data. In fully wavelet method, a third order tensor is used to represent the unknowns as well as the knowns. All the tensors are brought to matrix representation using a third order frontal slice [**13**] as shown in Figure 3.1.

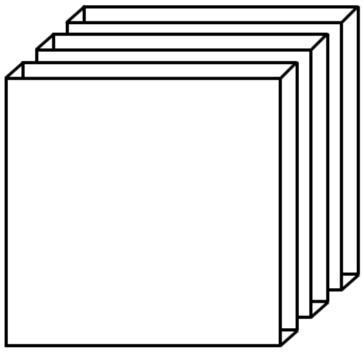

FIGURE 3.1. Frontal slice $A(:,:,k)$

Hence the equation (3.18) can be represented as

$$\begin{aligned}\frac{\partial^2 u_{n+1}}{\partial x^2} &= \sum_{i=1}^{2M}\sum_{j=1}^{2M}(a_{i,j,1}h_i(x)h_j(y)h_1(t) + a_{i,j,2}h_i(x)h_j(y)h_2(t) \\ &\quad + a_{i,j,3}h_i(x)h_j(y)h_3(t) + \cdots + a_{i,j,2M}h_i(x)h_j(y)h_{2M}(t))\end{aligned} \tag{3.25}$$

Equation (3.25) can be written as

$$\frac{\partial^2 u_{n+1}}{\partial x^2}(:,:,k) = \sum_{k_1=1}^{2M}(\phi^T A_{n+1}^{k_1}\phi)\phi(k_1,k) \tag{3.26}$$

after using the collocation points. Similarly,

$$\frac{\partial^2 u_{n+1}}{\partial y^2}(:,:,k) = \sum_{k_1=1}^{2M}(\phi^T B_{n+1}^{k_1}\phi)\phi(k_1,k) \tag{3.27}$$

$$\frac{\partial u_{n+1}}{\partial t}(:,:,k) = \sum_{k_1=1}^{2M}(\phi^T C_{n+1}^{k_1}\phi)\phi(k_1,k) \tag{3.28}$$

Hence (3.26), (3.27) and (3.28) leads to

$$
\begin{aligned}
(3.29) u_{n+1}(:,:,k) &= \sum_{k_1=1}^{2M} \big((P_2^T A_{n+1}^{k_1}\phi)\phi(k_1,k) - (F_2^T A_{n+1}^{k_1}\phi)\phi(k_1,k)\big) + H_1(:,:,k) \\
(3.30) u_{n+1}(:,:,k) &= \sum_{k_1=1}^{2M} \big((\phi^T B_{n+1}^{k_1} P_2)\phi(k_1,k) - (\phi^T B_{n+1}^{k_1} F_2)\phi(k_1,k)\big) + H_2(:,:,k) \\
(3.31) u_{n+1}(:,:,k) &= \sum_{k_1=1}^{2M} (\phi^T C_{n+1}^{k_1}\phi) P_1(k_1,k) + H_3(:,:,k).
\end{aligned}
$$

Let $v_{n+1} = \displaystyle\int_0^t u_{n+1}(x,y,s)ds$. Thus $V_{n+1}(:,:,k) = \displaystyle\int_0^{t_k} u_{n+1}(x,y,s)\mathrm{d}s$.

$$
\begin{aligned}
(3.32) \qquad V_{n+1}(:,:,k) &= \sum_{k_1=1}^{2M} \big((P_2^T A_{n+1}^{k_1}\phi) P_1(k_1,k) - (F_2^T A_{n+1}^{k_1}\phi) P_1(k_1,k)\big) \\
&\quad + H_4(:,:,k)
\end{aligned}
$$

where ϕ denotes the Haar matrix [**86**], P_1 denotes the first order integral of Haar matrix and P_2 denotes the second order integral of Haar matrix, $F_2 = D_1 X,\ F_2 = C_1 X,\ X = [x_i],\ H_1(:,:,k) = x_i u(1,y_j,t_k) - x_i u(0,y_j,t_k) + u(0,y_j,t_k),\ H_2(:,:,k) = y_j u(x_i,1,t_k) - y_j u(x_i,0,t_k) + u(x_i,0,t_k)$, $H_3(:,:,k) = u(x_i,y_j,0)$, $H_4(:,:,k) = \int_0^{t_k} (x_i u(1,y_j,s) - x_i u(0,y_j,s) + u(0,y_j,s))\mathrm{d}s$. $A_{n+1}^{k_1} = [a_{i,j,k_1}],\ B_{n+1}^{k_1} = [b_{i,j,k_1}],\ C_{n+1}^{k_1} = [c_{i,j,k_1}]$ and $\{(x_i,y_j,t_k) : x_i = y_i = t_i = \frac{i-0.5}{2M}, 1 \le i,j,k \le 2M\}$ represents the set of collocation points. Here $A_0^{k_1}, B_0^{k_1}, C_0^{k_1}$ are obtained from the initial approximation u_0. Equating (3.29) and (3.31) one can get

$$
\begin{aligned}
(3.33) \qquad & \sum_{k_1=1}^{2M} \big((P_2^T A_{n+1}^{k_1}\phi)\phi(k_1,k) - (F_2^T A_{n+1}^{k_1}\phi)\phi(k_1,k) \\
&\qquad - (\phi^T C_{n+1}^{k_1}\phi) P_1(k_1,k)\big) = H_5(:,:,k)
\end{aligned}
$$

Similarly equating (3.30) and (3.31) one can get

$$
\begin{aligned}
(3.34) \qquad & \sum_{k_1=1}^{2M} \big((\phi^T B_{n+1}^{k_1} P_2)\phi(k_1,k) - (\phi^T B_{n+1}^{k_1} F_2)\phi(k_1,k) \\
&\qquad - (\phi^T C_{n+1}^{k_1}\phi) P_1(k_1,k)\big) = H_6(:,:,k)
\end{aligned}
$$

where $H_5(:,:,k) = H_3(:,:,k) - H_1(:,:,k)$, $H_6(:,:,k) = H_3(:,:,k) - H_2(:,:,k)$. Using collocation points, the discretized version of (3.3) can be written as for $k = 1, 2, \cdots 2M$.

$$
\begin{aligned}
(3.35) \qquad & (\sum_{k_1=1}^{2M}(\phi^T C_{n+1}^{k_1}\phi)\phi(k_1,k)) - \sum_{k_1=1}^{2M}(\phi^T A_{n+1}^{k_1}\phi)\phi(k_1,k) - \sum_{k_1=1}^{2M}(\phi^T B_{n+1}^{k_1}\phi)\phi(k_1,k) \\
& -H_7(:,:,k)\circ H_{11}(:,:,k) + (H_7(:,:,k))\circ(H_{13}(:,:,k)) \\
& +(H_8(:,:,k))\circ(H_{14}(:,:,k)) = H_{17}(:,:,k)
\end{aligned}
$$

where $H_7(:,:,k) = \sum_{k_1=1}^{2M}\big((P_2^T A_{n+1}^{k_1}\phi)\phi(k_1,k) - (F_2^T A_{n+1}^{k_1}\phi)\phi(k_1,k)\big)$, $H_8(:,:,k) = \sum_{k_1=1}^{2M}\big((P_2^T B_{n+1}^{k_1}\phi)P_1(k_1,k) - (F_2^T B_{n+1}^{k_1}\phi)P_1(k_1,k)\big)$, $H_9(:,:,k) = u_n(x_i,y_j,t_k)$, $H_{10}(:,:,k) = \int_0^{t_k} u_n(x_i,y_j,s)\mathrm{d}s$, $H_{11} = f'(u_n(x_i,y_j,t_k))$, $H_{12}(:,:,k) = c\gamma u_n^{\gamma-1}(x_i,y_j,t_k)$, $H_{13}(:,:,k) = H_{12}(:,:,k)\circ H_{10}(:,:,k)$, $H_{14}(:,:,k) = \gamma c u_n^{\gamma}(x_i,y_j,t_k)$, $H_{15}(:,:,k) = g(x_i,y_j,t_k)$, $H_{16}(:,:,k) = f(u_n(x_i,y_j,t_k))$ and $H_{17}(:,:,k) = H_{15}(:,:,k) + H_{16}(:,:,k) + (H_{10}(:,:,k)\circ H_{14}(:,:,k)) + H_1(:,:,k)\circ\big(H_{11}(:,:,k) - H_{13}(:,:,k)\big) - H_4(:,:,k)\circ H_{14}(:,:,k) - (H_9(:,:,k)\circ H_{11}(:,:,k))$. Hence from equations (3.33), (3.34) and (3.35), one can obtain $8M^3$ equations with $8M^3$ unknown matrices A_{n+1}^1, $A_{n+1}^2, \ldots A_{n+1}^{2M}$, B_{n+1}^1, $B_{n+1}^2, \ldots B_{n+1}^{2M}$, C_{n+1}^1, $C_{n+1}^2, \ldots C_{n+1}^{2M}$. Using vectorization, these equations are written in the form $L_2\theta_2 = b_2$, where the unknown θ_2 contains the matrix entries in the order $A_{n+1}^1, \ldots, A_{n+1}^{2M}$, $B_{n+1}^1, \ldots, B_{n+1}^{2M}$ and C_{n+1}^1, $C_{n+1}^2, \ldots C_{n+1}^{2M}$. Finally, the numerical solution of the two dimensional partial integro differential equation can be obtained by substituting the unknowns in (3.29) or (3.30) or (3.31).

3.3. Numerical Experiments

In this section, the proposed quasilinearization based wavelet method for two dimensional integro differential equation are tested with appropriate examples. Throughout this section the following abbreviations and notations are used.

1. FHWM- Fully Haar wavelet method.
2. HWFDM- Haar wavelet finite difference method.
3. FLWM- Fully Legendre wavelet method.
4. LWFDM- Legendre wavelet finite difference method.
5. J denotes the resolution of Haar wavelet and N denotes number of Legendre wavelets.

Example 3.3.1.

For the choice of $a = b = 1,\ c = 0$ and $g(x,y,t) = 0$, consider the two dimensional Fisher's equation 3.1. The initial and boundary conditions are taken from the exact solution

$$u(x,y,t) = \frac{1}{2}\tanh\left(\left(\frac{y-x+3t}{4}\right) - \log\sqrt{2}\right) + \frac{1}{2}.$$

Hence

$$\begin{aligned}
u(x,y,0) &= \frac{1}{2}\tanh\left(\left(\frac{y-x}{4}\right) - \log\sqrt{2}\right) + \frac{1}{2} \\
u(-20,y,t) &= \frac{1}{2}\tanh\left(\left(\frac{20+y+3t}{4}\right) - \log\sqrt{2}\right) + \frac{1}{2} \\
u(20,y,t) &= \frac{1}{2}\tanh\left(\left(\frac{y-20+3t}{4}\right) - \log\sqrt{2}\right) + \frac{1}{2} \\
u(x,-20,t) &= \frac{1}{2}\tanh\left(\left(\frac{3t-x-20}{4}\right) - \log\sqrt{2}\right) + \frac{1}{2} \\
u(x,20,t) &= \frac{1}{2}\tanh\left(\left(\frac{20-x+3t}{4}\right) - \log\sqrt{2}\right) + \frac{1}{2}.
\end{aligned}$$

Using explicit finite difference method (FDE) and implicit finite difference method (FDI), two dimensional Fisher equation is solved numerically in [**123**]. Table 3.1 and 3.2 provide the comparison between all the proposed methods and methods discussed in [**123**] for different grid points at time $t = 1$. Table 3.1 and 3.2 show that the proposed FHWM, HWFDM and LWFDM perform better than the methods studied in [**123**]. The highest accuracy obtained by FDI [**123**] is 6.5993×10^{-4} for the grid size $80 \times 80 \times 10^3$, where as the LWFDM produces better accuracy of 8.7785×10^{-5} using a grid of size $40 \times 40 \times 100$. Among the proposed methods, Haar wavelet based method performs better than Legendre wavelet based method in terms of accuracy as well as grid size. Moreover, in case of methods based on Legendre wavelet, the finite difference approach LWFDM gives better accuracy than the fully wavelet approach FLWM. Between Haar wavelet based methods, both FHWM and HWFDM produce same accuracy. However HWFDM requires more grid points. As grid size increases, the condition number of the linear system in the fully wavelet approach also increases. Among both the wavelet methods,the condition number of resultant matrix of FLWM increases much faster than that of FHWM. This leads to a poorer performance of methods based on Legendre wavelets. Figure 3.2 represents the HWFDM numerical solution in the interval $x, y \in [-20, 20]$ at $t = 5$.

Example 3.3.2.

For the choice of $b = 1$, $c = -1$, $a = \gamma = 0$ and $g(x, y, t) = \sin \pi x \sin \pi y + 2\pi^2 t \sin \pi x \sin \pi y + (t \sin \pi x \sin \pi y)^2 - \frac{t^2}{2}(\sin \pi x \sin \pi y)$, consider the two dimensional Volterra integro partial differential equation 3.1 with the initial and boundary conditions all are zero. It is easy to verify that $u(x, y, t) = t \sin \pi x \sin \pi y$ is the exact solution of the problem. Using implicit difference scheme two dimensional Volterra differential equation is solved numerically. Table 3.3 gives the comparison between the proposed methods (HWFDM and FLWM) and the implicit difference scheme (IDS). Accuracies for the remaining methods (LWFDM and FHWM) are not provided in the table because in the case of FHWM, for obtaining better accuracy, one needs to go for higher grid sizes leading to system memory issues. For LWFDM, the condition number of the final system increases rapidly for each iteration due to initial and boundary conditions due to which the coefficient matrix becomes ill conditioned. One can easily observe that our proposed methods (HWFDM and FLWM) able to achieve the better results than the method discussed in [**21**] with lesser grid points. The highest accuracy obtained by IDS [**21**] is $8.265e^{-05}$ for the grid size $512 \times 512 \times 512$, where as one of the proposed method FLWM produces better accuracy of $2.0044e^{-05}$ using grid of size $7 \times 7 \times 7$. Unlike in Example 3.3.1, in this example Legendre wavelet methods performs better than Haar wavelet due to smooth initial and boundary conditions.

Example 3.3.3.

For the choice of $a = b = c = \gamma = 1$ and $c = 1$, consider the two dimensional population model (3.1) with initial and boundary conditions as follows, $u(x, y, 0) = \dfrac{1}{1 + e^{x+y}}$, $u(x, 0, t) = \dfrac{1}{1 + e^{x+t}}$, $u(x, 1, t) = \dfrac{1}{1 + e^{1+y+t}}$, $u(0, y, t) = \dfrac{1}{1 + e^{y+t}}$, $u(1, y, t) = \dfrac{1}{1 + e^{1+y+t}}$, and $g(x, y, t)$ is adjusted such that exact solution is $u(x, y, t) = \dfrac{1}{1 + e^{x+y+t}}$. From Table 3.4 one can easily observe that methods based on Legendre wavelets (FLWM and LWFDM) performs better than the methods based on Haar wavelets (FHWM and HWFDM). Another observation is that out of all the proposed methods, FLWM outperforms in terms of grid size and accuracy due to smooth initial and boundary conditions. Figure 3.3 represents the numerical solution (FLWM) for a fixed values x and y with $t \in [0, 20]$.

Remark 3.3.1.

1. In all the examples, the condition $\|u_{n+1} - u_n\| \leq 10^{-6}$ is used as stooping criteria and initial guess $u_0 = 0$ is used for the proposed wavelet based iterative scheme.
2. All the numerical examples are tested with Chebyshev wavelet also, the order of the error is same as Legendre wavelet.
3. All the numerical experiments are carried out using MATLAB R2010b.

3.4. Conclusion

In this work, numerical methods based on wavelets are combined with an iterative method for solving two dimensional partial integro differential equation. While approximating the derivatives, two different approaches are proposed for two dimensional problems. In the first approach, finite difference scheme and wavelets are used for approximating the time and space domains respectively. In second approach, both time as well as space domains are approximated using wavelets. The advantage of fully wavelet method is that it requires very less number of grid points to produce higher accuracy. The advantage of finite difference based wavelet approach is that it is more stable as well as it requires less memory than the fully wavelet method. It is seen through the examples that the proposed methods are efficient than the ones in the recent literature [**21, 123**] and are in good agreement with the exact solutions as discussed. Furthermore, extensions of the proposed schemes to higher dimensions is possible.

TABLE 3.1. L_∞ errors for Example 3.3.1 at $t = 1$.

Grid	FDE[**123**]	FDI[**123**]	Grid	LWFDM	Grid	FLWM
$8 \times 8 \times 2$	$1.4384e^{-01}$	$1.4336e^{-01}$	$5 \times 5 \times 2$	$1.1696e^{-01}$	$5 \times 5 \times 5$	$1.0406e^{-01}$
$20 \times 20 \times 10$	$4.8655e^{-02}$	$4.8591e^{-02}$	$10 \times 10 \times 10$	$2.4131e^{-02}$	$8 \times 8 \times 8$	$6.7239e^{-02}$
$40 \times 40 \times 2$	$2.4212e^{-02}$	$1.6159e^{-02}$	$12 \times 12 \times 50$	$8.8108e^{-03}$	$14 \times 14 \times 14$	$2.9488e^{-02}$

TABLE 3.2. L_∞ errors for Example 3.3.1 at $t = 1$.

Grid	FDE[**123**]	FDI[**123**]	Grid	HWFDM	Grid	FHWM
$8 \times 8 \times 2$	$1.4384e^{-01}$	$1.4336e^{-01}$	$2 \times 2 \times 10$	$6.075e^{-03}$	$2 \times 2 \times 2$	$8.7724e^{-02}$
$20 \times 20 \times 10$	$4.8655e^{-02}$	$4.8591e^{-02}$	$4 \times 4 \times 20$	$1.7134e^{-02}$	$4 \times 4 \times 4$	$4.3108e^{-02}$
$40 \times 40 \times 2$	$2.4212e^{-02}$	$1.6159e^{-02}$	$16 \times 16 \times 20$	$7.7795e^{-03}$	$16 \times 16 \times 16$	1.0049^{-02}

TABLE 3.3. L_∞ errors for Example 3.3.2 at $t = 1$.

Grid	IDS[**21**]	Grid	HWFDM	Grid	FLWM
$4 \times 4 \times 16$	$4.751e^{-02}$	$4 \times 4 \times 1$	$1.916e^{-02}$	$4 \times 4 \times 4$	$1.353e^{-02}$
$8 \times 8 \times 64$	$1.149e^{-02}$	$8 \times 8 \times 1$	$5.648e^{-03}$	$8 \times 8 \times 8$	$8.153e^{-06}$
$32 \times 32 \times 32$	$2.104e^{-02}$	$16 \times 16 \times 1$	$1.469e^{-03}$	$9 \times 9 \times 9$	$1.404e^{-07}$
$64 \times 64 \times 64$	$8.069e^{-04}$	$32 \times 32 \times 1$	$3.709e^{-04}$	$10 \times 10 \times 10$	$5.896e^{-08}$

TABLE 3.4. L_∞ errors for Example 3.3.3 at $t = 1$.

Grid	HWFDM	Grid	FHWM	Grid	LWFDM	Grid	FLWM
$4 \times 4 \times 10^2$	$4.8012e^{-04}$	$2 \times 2 \times 2$	$2.0723e^{-04}$	$3 \times 3 \times 10^2$	$1.1563e^{-04}$	$4 \times 4 \times 4$	$3.2791e^{-04}$
$8 \times 8 \times 10^2$	$4.1202e^{-05}$	$4 \times 4 \times 4$	$2.4197e^{-05}$	$3 \times 3 \times 10^3$	$9.9001e^{-05}$	$6 \times 6 \times 6$	$4.2918e^{-07}$
$4 \times 4 \times 10^3$	$2.0666e^{-05}$	$8 \times 8 \times 8$	$4.6801e^{-06}$	$5 \times 5 \times 10^3$	$9.9091e^{-06}$	$8 \times 8 \times 8$	$7.1410e^{-09}$

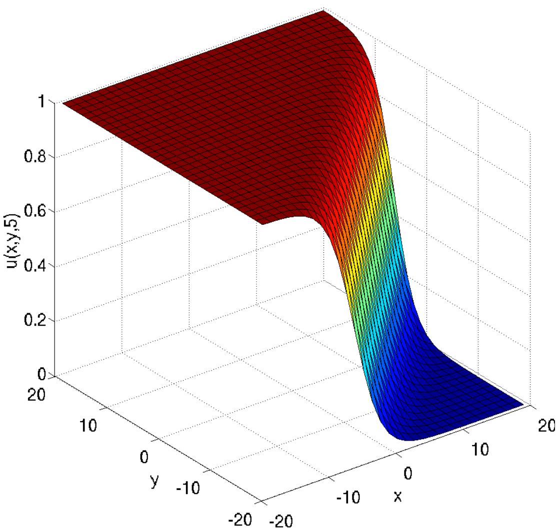

FIGURE 3.2. HWFDM for Example 3.3.1 with $J = 4$ and $h = 10^{-02}$ at $t = 5$.

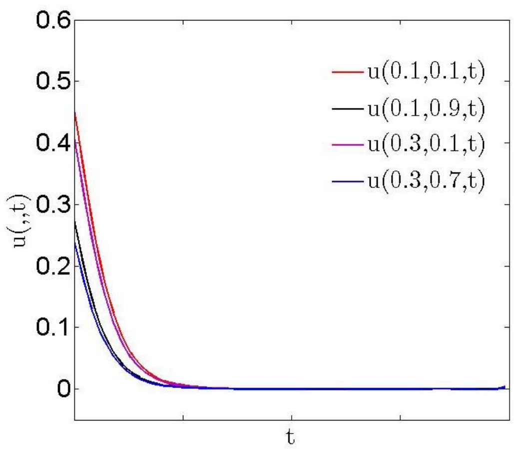

FIGURE 3.3. FLWM solution for Example 3.3.3 with $N = 10$ and $t \in [0, 20]$.

CHAPTER 4

HYPERBOLIC EQUATIONS

In this chapter[1] wavelet based numerical method is modified for two different equations namely nonlinear Klien/Sine Gordon equation and nonlinear coupled sine-Gordon equation. In the following section, wavelet based numerical method is modified for nonlinear Klien/Sine Gordon equation.

4.1. Nonlinear Klien/Sine Gordon equations

4.1.1. Introduction

This section discusses on the numerical method based on quasilinearization and wavelet for the nonlinear Klein-Gordon equation of the form

$$u_{tt}(x,t) - u_{xx}(x,t) + g(u) = f(x,t),\ 0 \leq x \leq 1,\ t \geq 0, \tag{4.1}$$

with initial conditions $u(x,0) = f_1(x)$, $u_t(x,0) = f_2(x)$, $0 \leq x \leq 1$ and boundary conditions $u(0,t) = g_1(t),\ u(1,t) = g_2(t),\ t \geq 0$. Eq (4.1) plays a key role in mathematical physics. As mentioned in [**28**], for different choices of nonlinear term $g(u)$, one can deduce important equations such as sine-Gordon, Sinh-Gordon, Liouville, Dodd-Bullough-Mikhailov and Tzitzeica-Dodd-Bullough from Eq (4.1). For example, for the choices $g(u) = u^3 - u$ and $g(u) = \sin u$, Eq (4.1) reduces to the well known generalized phi-four equation and sine-Gordon equation respectively. Eq (4.1) arises in various mathematical models such as nonlinear optics, solid state physics, propagation of fluxons in Josephson-Junctions, fluid flow, quantum field theory, quantum mechanics, condensed matter physics to name a few. Developing numerical solutions for nonlinear Klein Gordon equation has attracted much attention. Various numerical methods such as finite difference method

[1]This chapter forms the papers by V.A. Vijesh and K.H. Kumar in Journal of Combinatorics, Information and System Sciences, 40 (1) (2015), 225–244 and Journal of Computational Nonlinear Dynamics, 12(1), 011018, 05 pages.

[**128**], different types of radial basis function collocation methods [**28, 30, 56**], Jacobi collocation method [**19**], different type of Spline methods [**70, 76, 103, 127, 192**] were studied to solve Klein Gordon equation. In this direction, recently operational matrix based wavelet methods are used to solve Klein Gordon equation with initial condition in [**177**] and with initial and boundary condition in [**179**]. This approach converts the partial differential equations into system of algebraic equations using wavelet approximation and by solving the algebraic equation, one can get the numerical solution of the partial differential equation. To get a simplified algebraic system, in most of the wavelet methods [**23, 58, 62, 130, 137, 179**], wavelets were used to approximate only the spatial derivatives and these methods use finite difference approach for time derivatives. Though this approach produces a simple set of algebraic equations, it compromises on the accuracy and increases the cost of computation due to the necessity in using very small time step. It is interesting to note that by coupling Laplace transform with wavelet, for the initial value problem [**177**], time discretization using finite difference can be avoided. In this chapter an efficient wavelet based numerical schemes are proposed to solve Klein Gordon equation with initial and boundary conditions. This method produces better accuracy than the recent techniques available in the literature. More specifically, the time derivative of Klein Gordon equation is discretized using wavelets independent of Laplace transform. The resulting system of coupled matrix equations are solved using vectorization. Moreover, the iterative method used in [**177, 179**] are successive approximations and hence the order of convergence is linear. In the proposed scheme, classical quasilinearization is combined with Chebyshev and Legendre wavelets to produce two different numerical techniques. The aim of this work is to develop an efficient wavelet based quasilinearization method to solve Klein Gordon equation with initial and boundary condition which is independent of finite difference method and Laplace transform.

The organization of this section is as follows. Section 4.1.2 explains Chebyshev and Legendre wavelet collocation methods in combination with classical quasilinearization for Klein Gordon equation. Section 4.1.3 gives the details of the numerical implementations of the proposed numerical schemes. The proposed quasilinearization methods based on wavelets are illustrated in Section 4.1.4 by applying them to various examples including

Phi four equation and sine-Gordon equation. The numerical results thus obtained are compared with Jacobi collocation method(JCM) [**19**], radial basis function collocation method (RBF) [**28, 30, 56**], B-spline collocation method [**70, 76, 103, 127, 192**], finite difference method [**128**] and Legendre Wavelet [**177, 179**] . The discussion is concluded in Section 4.1.5, by stating the merits of the proposed methods.

4.1.2. Wavelets Collocation Method

This section describes the Chebyshev wavelet collocation method for solving linear hyperbolic partial differential equation. The same procedure can be followed for the Legendre wavelet collocation method also. During the discussion of collocation method, the following notations are used; $p_{i,1}(x) = \int_0^x \psi_i(t)\mathrm{d}t$, $p_{i,2}(x) = \int_0^x p_{i,1}(t)\mathrm{d}t$ and $C_{i,1} = \int_0^1 p_{i,1}(t)\mathrm{d}t$. Assume that all the partial derivatives appears in the linear partial differential equation can be expressed by Chebyshev wavelets series. Consequently,

$$\frac{\partial^2 u}{\partial x^2} = \sum_{j=1}^{N_1}\sum_{i=1}^{N_1} a_{i,j}\psi_i(x)\psi_j(t) \tag{4.2}$$

$$\frac{\partial^2 u}{\partial t^2} = \sum_{j=1}^{N_1}\sum_{i=1}^{N_1} b_{i,j}\psi_i(x)\psi_j(t). \tag{4.3}$$

Throughout this discussion, the following points in the set $\{(x_i, t_j) : x_i = t_i = \frac{i-0.5}{2M}, 1 \leq i, j \leq N\}$ are chosen for collocation. From (4.2) and (4.3), one can get $u(x,t)$ in two ways and they can be represented as follows.

$$\begin{aligned} u(x,t) &= \sum_{j=1}^{N_1}\sum_{i=1}^{N_1} a_{i,j}(p_{i,2}(x) - xC_{i,1})\psi_j(t) \\ &\qquad +(u(1,t) - u(0,t))x + u(0,t) \end{aligned} \tag{4.4}$$

$$u(x,t) = \sum_{j=1}^{N_1}\sum_{i=1}^{N_1} b_{i,j}\psi_i(x)p_{i,2}(t) + u_t(x,0)t + u(x,0) \tag{4.5}$$

Equating (4.4) and (4.5), at each collocation point, we obtain $2N_1^2$ set of equations. Similarly $2N_1^2$ set of equations are derived from the linear hyperbolic partial differential equation using the expressions of $u(x,y)$. These two sets of equations are to be solved, to obtain the unknown Chebyshev coefficients $a_{i,j}$'s and $b_{i,j}$'s. The solution can be easily obtained by substituting these coefficients in any one of the Eqns (4.4) and (4.5).

4.1.3. Numerical Implementation

The classical quasilinearization iterative procedure for the Klein Gordon equation (4.1) is given by

$$\frac{\partial^2 u_{n+1}}{\partial t^2} - \frac{\partial^2 u_{n+1}}{\partial x^2} + g(u_n) + g'(u_n)(u_{n+1} - u_n) = f(x,t) \; n = 0, 1, 2 \cdots \tag{4.6}$$

with initial conditions $u_{n+1}(x,0) = f_1(x)$, $u_{n+1_t}(x,0) = f_2(x)$, $0 \leq x \leq 1$ and boundary conditions $u_{n+1}(0,t) = g_1(t)$, $u_{n+1}(1,t) = g_2(t)$, $t \geq 0$. Some interesting convergence results can be found in the monograph [**78**]. This section provides how to implement the classical quasilinearization method to solve Klien Gordon equation. Let X^T denotes transpose of the matrix X. Using the collocation points, and the eqns (4.4) and (4.5), can be written as

$$u_{n+1}(x,t) = \Psi^T X_{n+1} P_2 - \Psi^T X_{n+1} F_1 + W_1 - W_2 + W_3 \tag{4.7}$$

$$u_{n+1}(x,t) = P_2^T Y_{n+1} \Psi + W_4 + W_5 \tag{4.8}$$

where $W_1 = x_i g_2(t_j)$, $W_2 = x_i g_1(t_j)$, $W_3 = g_1(t_j)$, $W_4 = f_2(x_i) t_j$, $W_5 = f_1(x_i)$, $X_{n+1}^T = [x_{i,j}]$, $Y_{n+1}^T = [y_{i,j}]$, $\Psi = [\psi_i(t_j)]$, $P_2 = [p_{i,2}(t_j)]$, $F_1 = x_i C_{i,1}$ and $\{(x_i, t_j) : x_i = t_i = \frac{i-0.5}{N}, 1 \leq i,j \leq 2M\}$. Here X_0 and Y_0 are obtained from the initial approximation u_0. Equating (4.7) with (4.8) we get,

$$\Psi^T X_{n+1} P_2 - \Psi^T X_{n+1} F_1 - P_2^T Y_{n+1} \Psi = -W_1 + W_2 - W_3 + W_4 + W_5. \tag{4.9}$$

After using collocation points, the equation (4.6) can be written as

$$\Psi^T Y_{n+1} \Psi - \Psi^T X_{n+1} \Psi + W_6 \circ (P_2^T Y_{n+1} \Psi) = W_7 \tag{4.10}$$

where $W_6 = g'(u_n(x_i,t_j))$, $W_7 = -W_6 \circ (W_4 + W_5) + f(x_i,t_j) - g(u_n(x_i,t_j)) - W_6 \circ u_n(x_i,t_j)$ and $\circ$ denotes the Hadamard product. To get u_{n+1} one can solve (4.9) and (4.10) with the initial guess u_0. Using vectorization, (4.9) and (4.10) can be brought into $L\theta = b$ where $\theta = \left[\mathrm{vec}(X_{n+1}) \; \mathrm{vec}(Y'_{n+1})\right]^T$ and $b = [\mathrm{vec}(W_8) \; \mathrm{vec}(W_7)]^T$,

$$L = \begin{bmatrix} P_2^T \otimes \Psi^T - F_1^T \otimes \Psi^T & -\Psi^T \otimes P_2^T \\ -\Psi^T \otimes \Psi^T & \Psi^T \otimes \Psi^T - W_9(\Psi^T \otimes P_2^T) \end{bmatrix}$$

where $W_8 = -W_1 + W_2 - W_3 + W_4 + W_5$, "vec" represents vectorization of a matrix, $\otimes$ denotes Kronecker product and W_9 is a diagonal matrix that contains elements of W_6 in it's diagonal position. Then the numerical solution of the Klein Gordon equation can be obtained by substituting these wavelet coefficients in one of the equations (4.7) and (4.8).

4.1.4. Numerical Experiments

In this section the proposed iterative based wavelet schemes for Klein Gordon equation are tested on various choices of example problems including Phi-four and sine-Gordon equations and their performance in terms of accuracy is compared. Throughout this section the following abbreviations are used.

1. CWM- Chebyshev wavelet quasilinearization method.
2. LWM- Legendre wavelet quasilinearization method.
3. N_1 denotes the number of Chebyshev wavelets and N denotes the number of Legendre wavelets.

Example 4.1.1.

Consider the nonlinear Klein-Gordon equation discussed in [**185**]

$$u_{tt} - u_{xx} + u^2 = 6xt(x^2 - t^2) + x^6t^6. \tag{4.11}$$

The initial and boundary conditions of the problem (4.1.1) are taken from [**30**]. This equation is solved numerically using different types splines in [**76, 128**] and different types of radial basis functions (RBF) in [**30, 56**]. The numerical results obtained using quasilinearization based wavelet method is compared with the numerical methods mixed finite difference and collocation method (MFDCM) [**76**], collocation method (CM) [**76**], Tension Spline [**128**], various radial basis functions thin plates splines(TPSRBF) [**30**], Gaussian (GA) [**56**] and multi quadraic (MQ) [**56**]. Table 4.1 and 4.2 show that the proposed iterative methods based on wavelets perform extremely better than all the methods in [**30, 56, 76, 128**].

Example 4.1.2.

Consider the nonlinear Klein-Gordon equation discussed in [**30, 103, 128, 179**]

$$u_{tt} - u_{xx} + u + 1.5u^3 = 0 \tag{4.12}$$

The initial and boundary conditions of the problem (4.1.2) are taken from [**103**]. This equation is solved numerically using different type of splines [**103, 128**], Finite difference based Legendre wavelet method (FLWM) [**179**] and radial basis functions (RBF) [**30**]. The numerical results obtained using the quasilinearization based wavelet method are compared with the numerical methods using finite difference based Legendre wavelet method [**179**], cubic B-splines (CBS) [**103**], tension spline [**128**], radial basis functions thin plates splines(TPSRBF) [**30**]. Table 4.3 shows that the propsed iteartive method based on wavelets performs extremely better than all the methods in [**30, 103, 127, 179**]. It is interesting to note that though the LWM takes less number of wavelets ($N = 12$) than FLWM ($N = 24$), LWM produces more accurate results than FLWM. This shows the superiority of the discretization purely based on wavelets (both time and space derivatives) which is a key benefit of the proposed scheme. More over, LWM uses only 12×12 grids whereas FLWM uses 24×10000 grids.

Example 4.1.3.

Consider the nonlinear Klein-Gordon equation discussed in [**70**]

$$u_{tt} - u_{xx} + u^2 = -x\cos t + x^2\cos^2 t \tag{4.13}$$

The initial and boundary conditions of the problem (4.1.3) are taken from [**192**]. This equation is solved numerically using various types of splines [**70, 192**], as well as various types of radial basis functions (RBFs) [**56**]. The numerical results obtained using the quasilinearization based wavelet methods are compared with the numerical methods using cubic B splines (CBS) [**70**], hybrid cubic B-spline (HCuBS) [**192**], multi-quadric radial basis functions (MQ) and Gaussian radial basis functyion [**56**]. Table 4.4 and 4.5 show that the proposed iterative method based on wavelets performs extremely better than all the methods in [**56, 70, 192**].

Example 4.1.4.

Consider the nonlinear Klein-Gordon equation discussed in [**70**]

$$u_{tt} - u_{xx} + \frac{\pi^2}{2}u + u^2 = x^2\sin^2\frac{\pi}{2}t \tag{4.14}$$

The initial and boundary conditions of the problem (4.1.4) are taken from [**70**]. In [**70**], this equation is solved numerically using cubic B-splines in (CBS) [**70**]. The solution obtained using present algorithms are compared to cubic B-splines. Table 4.6 shows that the propsed iteartive method based on wavelets performs extremely better than that obtained using CBS. Further, it is interesting to note that LWM and CWM took only 10 $\times$ 10 grids, while CBS require 5 $\times$ 100 grids.

Example 4.1.5.

Consider the non-linear Phi-four equation discussed in [**19**]

$$u_{tt} - u_{xx} + u^3 - u = 0 \tag{4.15}$$

The initial and boundary conditions of the problem (4.1.5) are taken from [**19**] This equation is solved numerically using spectral method in [**19**]. The numerical results obtained using the quasilinearization based wavelet methods are compared with the spectral method [**19**]. Table 4.7 shows that the propsed iteartive method based on wavelets performs extremely better than that in [**19**]. Moreover, it is interesting to note that LWM and CWM took same number of grids as spectral method.

We will conclude our discussion in this section by solving the following sine-Gordon equation.

Example 4.1.6.

Consider the nonlinear sine-Gordon equation discussed in [**179**]

$$u_{tt} - u_{xx} + \sin u = 0 \tag{4.16}$$

The initial and boundary conditions of the problem (4.1.6) are taken from [**179**]. The exact solution is given by $u(x,t) = 4\tan^{-1}(tsechx)$. Table 4.8 presents the comparison between the proposed schemes by varying the number of wavelets used to solve the problem.

4.1.5. Conclusion

In this chapter, numerical methods based on wavelets combined with classical quasilinearization methods for Klein-Gordon equation are proposed. To produce better accuracy, time derivatives of the Klein Gordon equation is also approximated using Chebyshev / Legendre wavelets. Comparsion of the numerical results with various schemes shows that the results obtained are better than those in some of the recent literature [**19, 30, 56, 70, 76, 103, 128, 179, 192**] and are in good agreement with the exact solution. From Figure 4.7 one can observe that Chebyshev wavelet produces better accuracy when compared to Legendre wavelet in Example 4.1.1. Legendre wavelet produces better accuracy than the Chebyshev wavelet in Example 4.1.2 which can be seen in Figure 4.8. Figures 4.8 to 4.12 assures that in the remaining Examples 4.1.3 to 4.1.6, both CWM and LWM produce almost same accuracy.

TABLE 4.1. Comparison of L_∞ errors obtained using CWM and LWM of Example 4.1.1.

t	CM [**76**] $M=4$	MFDCM[**76**] $M=4$	CWM $N_1=4$	LWM $N=4$
0.1	$5.3e^{-05}$	$5.3e^{-10}$	$4.1e^{-17}$	$4.4e^{-17}$
0.2	$5.7e^{-05}$	$9.4e^{-09}$	$4.2e^{-17}$	$6.6e^{-17}$
0.3	$4.1e^{-05}$	$5.5e^{-08}$	$5.6e^{-17}$	$7.7e^{-17}$
0.4	$5.6e^{-05}$	$3.8e^{-07}$	$7.5e^{-17}$	$1.1e^{-16}$
0.5	$4.5e^{-05}$	$5.6e^{-07}$	$6.6e^{-17}$	$1.1e^{-16}$
0.6	$5.9e^{-05}$	$7.1e^{-07}$	$5.9e^{-17}$	$9.0e^{-17}$
0.7	$5.9e^{-05}$	$7.0e^{-07}$	$9.4e^{-17}$	$1.1e^{-16}$
0.8	$4.5e^{-05}$	$8.6e^{-07}$	$1.7e^{-16}$	$1.4e^{-16}$
0.9	$6.3e^{-05}$	$7.9e^{-07}$	$3.3e^{-16}$	$2.5e^{-16}$

TABLE 4.2. Comparison of L_∞ errors obtained using CWM and LWM of Example 4.1.1 at $t = 1.0$

t	TPSRBF [**30**]	GA [**56**]	MQ [**56**]	CM [**76**]	MFDCM [**76**]	CBS [**127**]	Method-1 [**128**]	Method-2 [**128**]	CWM $N=4$	LWM $N_1=4$
1.0	$1.1e^{-05}$	$3.2e^{-04}$	$9.1e^{-04}$	$4.6e^{-05}$	$8.2e^{-07}$	$5.6e^{-14}$	$1.1e^{-08}$	$1.5e^{-09}$	$3.3e^{-16}$	$4.6e^{-16}$

TABLE 4.3. Comparison of L_∞ errors obtained using CWM and LWM of Example 4.1.2 for $N = 12, N_1 = 12$

$t=1.0$	TPSRBF [**30**]	CBS [**103**]	CBS [**127**]	Method-1 [**128**]	Method-2 [**128**]	FLWM [**179**]	CWM	LWM
$c=0.5$	$5.99e^{-06}$	$3.57e^{-05}$	$2.69e^{-08}$	$1.45e^{-07}$	$1.74e^{-10}$	$6.12e^{-06}$	$5.20e^{-12}$	$3.56e^{-12}$
$c=0.05$	$3.64e^{-07}$	$3.65e^{-06}$	$1.20e^{-08}$	$1.45e^{-07}$	$1.74e^{-10}$	$1.08e^{-07}$	$2.03e^{-12}$	$1.78e^{-12}$

TABLE 4.4. Comparison of L_∞ errors obtained using CWM and LWM of Example 4.1.3.

t	CWM $N_1 = 6$	LWM $N = 6$	CWM $N_1 = 8$	LWM $N = 8$
0.1	$6.3e^{-07}$	$4.8e^{-07}$	$2.3e^{-09}$	$2.0e^{-09}$
0.2	$8.5e^{-07}$	$6.3e^{-07}$	$1.6e^{-09}$	$1.6e^{-09}$
0.3	$7.8e^{-07}$	$7.1e^{-07}$	$1.0e^{-09}$	$8.9e^{-10}$
0.4	$6.8e^{-07}$	$4.6e^{-07}$	$1.0e^{-09}$	$9.7e^{-10}$
0.5	$6.2e^{-07}$	$4.7e^{-07}$	$1.2e^{-09}$	$1.0e^{-09}$
0.6	$4.1e^{-07}$	$4.1e^{-07}$	$1.0e^{-09}$	$9.4e^{-10}$
0.7	$8.8e^{-07}$	$6.5e^{-07}$	$8.9e^{-10}$	$8.5e^{-10}$
0.8	$5.4e^{-07}$	$4.9e^{-07}$	$1.4e^{-09}$	$1.4e^{-09}$
0.9	$1.2e^{-07}$	$9.8e^{-07}$	$1.6e^{-09}$	$1.7e^{-09}$

TABLE 4.5. Comparison of L_∞ errors obtained using CWM and LWM of Example 4.1.3 at $t = 1.0$.

$N = 41$	MQ[**56**]	$1.0e^{-04}$
$N = 41$	GA[**56**]	$2.5e^{-03}$
$h = 0.1, k = 0.005$	B-Spline [**70**]	$2.8e^{-04}$
$h = 0.04, k = 0.001$	B-Spline [**70**]	$4.6e^{-05}$
-	HCuBS[**192**]	$4.7e^{-06}$
$N = 8$	CWM	$1.7e^{-09}$
$N_1 = 8$	LWM	$2.1e^{-09}$

TABLE 4.6. Comparison of L_∞ errors obtained using CWM and LWM of Example 4.1.4.

t	x_0	x_1	x_2	x_3	x_4	x_5	Max|Error|	CWM	LWM
	0.0	0.2	0.4	0.6	0.8	1.0	[**70**]	$N_1 = 10$	$N = 10$
0.0	0.0	0.0	0.0	0.0	0.0	0.0	0.0	$6.7e^{-10}$	$9.0e^{-10}$
0.01	0.0	0.0031	0.0063	0.0094	0.0126	0.0157	$6.5e^{-07}$	$5.4e^{-10}$	$6.3e^{-10}$
0.02	0.0	0.0063	0.0126	0.0188	0.0251	0.0314	$2.7e^{-06}$	$4.2e^{-10}$	$4.2e^{-10}$
0.10	0.0	0.0313	0.0626	0.0939	0.1251	0.1564	$1.7e^{-04}$	$9.9e^{-11}$	$9.5e^{-11}$
0.50	0.0	0.1414	0.2828	0.4243	0.5657	0.7071	$2.3e^{-03}$	$3.8e^{-10}$	$3.4e^{-11}$
1.00	0.0	0.2000	0.4000	0.6000	0.8000	1.0000	$2.0e^{-03}$	$1.8e^{-09}$	$2.0e^{-09}$

TABLE 4.7. Comparison of absolute errors obtained using CWM and LWM of Example 4.1.5.

		Spectral[**19**]	CWM	LWM		Spectral[**19**]	CWM	LWM
x	t	$N = 12$	$N_1 = 12$	$N = 12$	t	$N = 12$	$N_1 = 12$	$N = 12$
0	0.1	$1.97e^{-09}$	$2.32e^{-10}$	$2.34e^{-10}$	0.2	$1.12e^{-10}$	$2.87e^{-10}$	$2.75e^{-10}$
0.1	0.1	$6.05e^{-11}$	$5.44e^{-12}$	$6.20e^{-12}$	0.2	$1.49e^{-10}$	$3.58e^{-12}$	$4.80e^{-12}$
0.2	0.1	$6.21e^{-10}$	$2.27e^{-12}$	$1.33e^{-12}$	0.2	$6.11e^{-10}$	$1.59e^{-12}$	$5.09e^{-13}$
0.3	0.1	$5.64e^{-10}$	$2.85e^{-12}$	$1.73e^{-12}$	0.2	$6.01e^{-10}$	$1.65e^{-12}$	$6.45e^{-13}$
0.4	0.1	$1.04e^{-09}$	$1.39e^{-12}$	$6.57e^{-13}$	0.2	$8.29e^{-10}$	$2.00e^{-12}$	$1.59e^{-12}$
0.5	0.1	$8.99e^{-10}$	$8.42e^{-13}$	$7.24e^{-13}$	0.2	$1.08e^{-09}$	$3.30e^{-12}$	$2.14e^{-12}$
0.6	0.1	$1.31e^{-09}$	$2.44e^{-12}$	$1.70e^{-12}$	0.2	$1.03e^{-09}$	$3.04e^{-12}$	$2.04e^{-12}$
0.7	0.1	$1.18e^{-09}$	$2.78e^{-12}$	$2.03e^{-12}$	0.2	$1.33e^{-09}$	$1.20e^{-12}$	$1.20e^{-12}$
0.8	0.1	$1.42e^{-09}$	$3.01e^{-12}$	$2.48e^{-12}$	0.2	$7.60e^{-10}$	$4.34e^{-13}$	$4.87e^{-13}$
0.9	0.1	$7.16e^{-10}$	$5.90e^{-12}$	$5.28e^{-12}$	0.2	$2.35e^{-10}$	$3.61e^{-13}$	$2.06e^{-12}$
1.0	0.1	$7.89e^{-11}$	$1.89e^{-11}$	$2.18e^{-11}$	0.2	$4.47e^{-12}$	$7.33e^{-11}$	$6.23e^{-11}$

TABLE 4.8. Comparison of L_∞ errors obtained using CWM and LWM of Example 4.1.6.

t	CWM $N_1 = 8$	LWM $N = 8$	CWM $N_1 = 12$	LWM $N = 12$
0.1	$5.3e^{-06}$	$5.8e^{-06}$	$6.5e^{-08}$	$6.3e^{-08}$
0.2	$6.5e^{-06}$	$6.7e^{-06}$	$7.8e^{-08}$	$8.1e^{-08}$
0.3	$1.0e^{-05}$	$9.8e^{-06}$	$9.8e^{-08}$	$9.7e^{-08}$
0.4	$1.0e^{-05}$	$1.0e^{-05}$	$9.9e^{-08}$	$9.8e^{-08}$
0.5	$9.0e^{-06}$	$9.1e^{-06}$	$8.9e^{-08}$	$9.0e^{-08}$
0.6	$8.4e^{-06}$	$8.7e^{-06}$	$1.0e^{-07}$	$9.8e^{-08}$
0.7	$8.7e^{-06}$	$9.0e^{-06}$	$9.9e^{-08}$	$9.7e^{-08}$
0.8	$7.8e^{-06}$	$7.9e^{-06}$	$8.5e^{-08}$	$8.5e^{-08}$
0.9	$5.4e^{-06}$	$5.2e^{-06}$	$6.3e^{-08}$	$6.2e^{-08}$
1.0	$2.2e^{-06}$	$3.1e^{-06}$	$1.1e^{-07}$	$1.3e^{-07}$

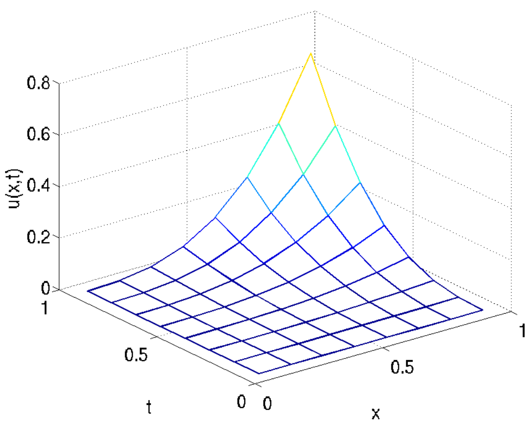

FIGURE 4.1. Numerical solution of $u(x,t)$ of Example 4.1.1 for $N_1 = 8$

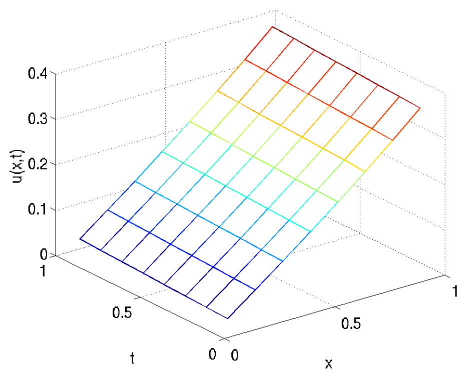

FIGURE 4.2. Numerical solution of $u(x,t)$ of Example 4.1.2 for $N = 8, c = 0.05$

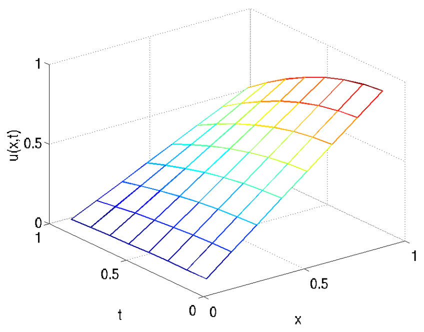

FIGURE 4.3. Numerical solution of $u(x,t)$ of Example 4.1.3 for $N_1 = 8$

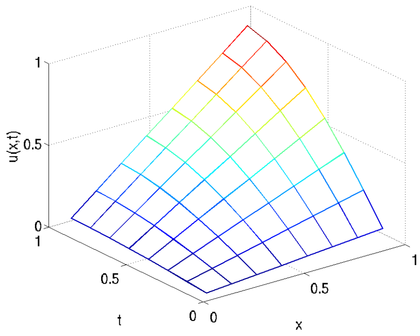

FIGURE 4.4. Numerical solution of $u(x,t)$ of Example 4.1.4 for $N = 8$

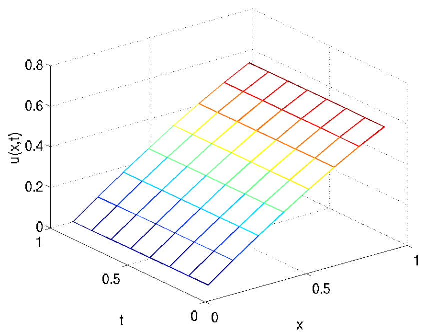

FIGURE 4.5. Numerical solution of $u(x,t)$ of Example 4.1.5 for $N_1 = 8$

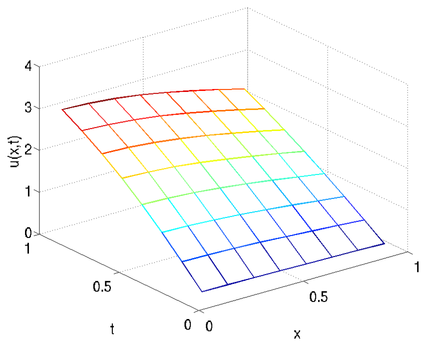

FIGURE 4.6. Numerical solution of $u(x,t)$ of Example 4.1.6 for $N = 8$

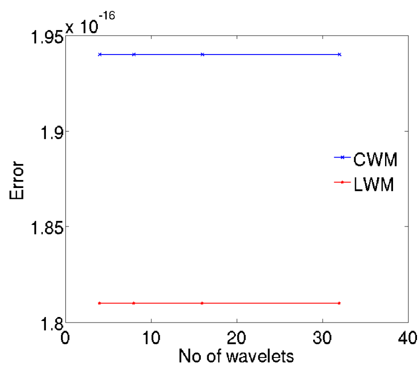

FIGURE 4.7. Comparison of errors for CWM and LWM for Example 4.1.1

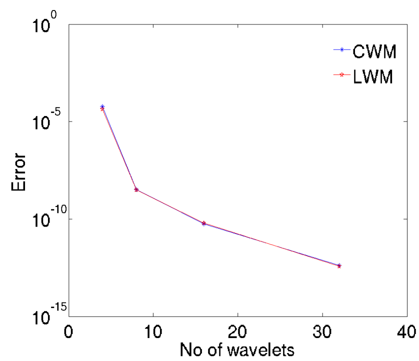

FIGURE 4.8. Comparison of errors for CWM and LWM for Example 4.1.2.

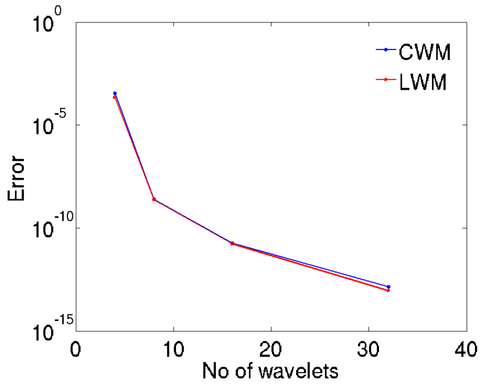

FIGURE 4.9. Comparison of errors for CWM and LWM for Example 4.1.3

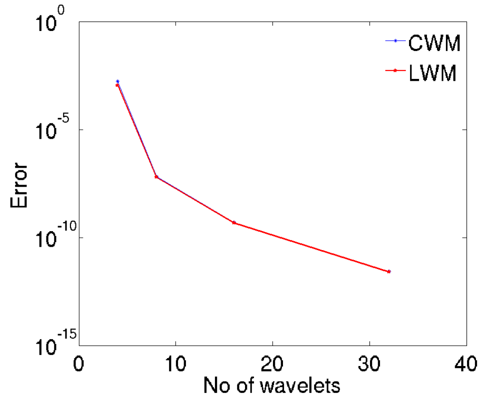

FIGURE 4.10. Comparison of errors for CWM and LWM for Example 4.1.4

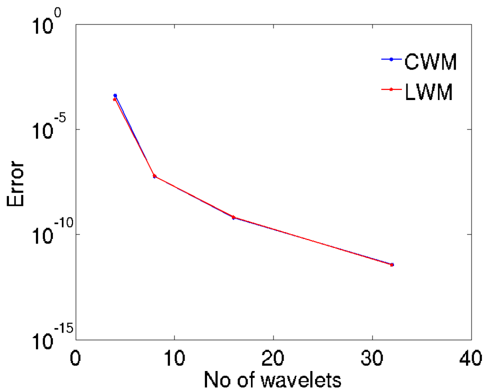

FIGURE 4.11. Comparison of errors for CWM and LWM for Example 4.1.5

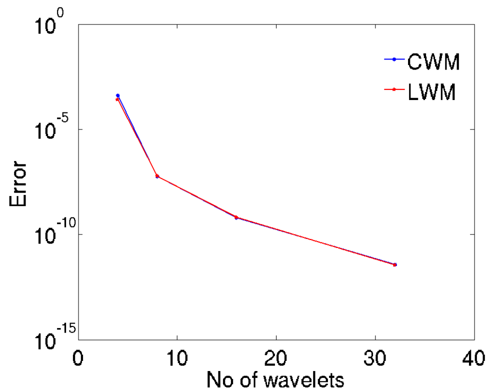

FIGURE 4.12. Comparison of errors for CWM and LWM for Example 4.1.6

The following section provides the wavelet based numerical method for coupled nonlinear sine-Gordon equation.

4.2. Coupled nonlinear sine-Gordon equations

4.2.1. Introduction

In this section, a new numerical scheme based on quasilinearization and Chebyshev wavelet is proposed for the coupled sine-Gordon equation of the form

$$\begin{aligned} u_{tt} - u_{xx} &= -\delta^2 \sin(u - w) + f(x,t) \\ w_{tt} - c^2 w_{xx} &= \sin(u - w) + g(x,t) \end{aligned} \tag{4.17}$$

with initial conditions $u(x,0) = f_1(x)$, $u_t(x,0) = f_2(x)$, $w(x,0) = f_3(x)$, $w_t(x,0) = f_4(x)$ and boundary conditions $u(0,t) = g_1(t)$, $u(1,t) = g_2(t)$, $w(0,t) = g_3(t)$, $w(1,t) = g_4(t)$. The coupled equation (4.17) was studied [**71**] to model one dimensional nonlinear wave process in two-component media as it plays a vital role in describing the open states in deoxyribonucleic acid DNA [**187**]. Many attempts were made to solve the coupled sine-Gordon equation numerically as well as analytically. For example, Adomian decomposition method [**129**], radial basis functions (RBF) [**57**], simplest equation method [**189**] and variational iteration method [**18**] have all been successfully applied to solve coupled sine-Gordon equation. Very recently, an interesting numerical technique based on radial basis function together with finite difference method was developed to handle the coupled sine-Gordon equation with initial and boundary conditions[**57**]. In this approach, the time domain was discretized using finite difference approach, while the space domain was discretized using radial basis function. The nonlinearity in the coupled sine-Gordon equation was handled by successive approximation that only gives a linear convergence. Though this approach produces decent accuracy due to the usage of finite difference, it requires more grid points. The aim of this section is to provide a new numerical technique which can produce higher accuracy with less number of grids. Due to the better approximation property of wavelets, wavelet based techniques were widely used now a days for solving different types of differential equations [**23, 37, 38, 39, 58, 62, 65, 74, 130, 137**]. It is interesting to observe that as in the RBF method discussed, most of the wavelet methods for partial differential equations are based on finite difference method [**23, 58, 62, 74, 130**] for time domain discretization. A finite difference free method based on wavelets was studied for nonlinear Klein Gordon equation [**168**]. As this approach discretizes both the domains using wavelets, it produces higher accuracy with less number of grid points. This approach is extended to coupled sine-Gordon equation in this chapter and is compared with RBF based scheme. More specifically, a wavelet method is proposed in which both time and space domain are discretized using wavelets. Consequently, the present approach produces better accuracy than the RBF based scheme [**57**] with almost one third of total grid points. Moreover, the nonlinearity in the coupled sine-Gordon equation is handled by the quasilinearization method, which has quadratic convergence in contrast to the linearly convergent successive approximation used [**57**].

The organization of this section is as follows. Section 4.2.2 explains the Chebyshev wavelet collocation methods in combination with quasilinearization for coupled sine-Gordon equation. The details of the numerical implementations procedure for the proposed numerical method is presented in Section 4.2.3. The proposed quasilinearization method based on wavelets is illustrated in Section 4.2.4 by applying it to various examples as described by Ilati et.al. [**57**]. Concluding remarks on the proposed scheme is made in Section 4.2.5.

4.2.2. Wavelet Collocation Method

After applying quasilinearization to the given nonlinear coupled equations, one has to solve a linear partial differential equation at each iteration. This section provides the collocation method for linear coupled partial differential equations using Chebyshev wavelets. With the assumption that the partial derivatives as well as other functions arising in the linear coupled partial differential equations are members of $L^2((0,1)\times(0,1))$. Therefore,

$$\frac{\partial^2 u}{\partial x^2} = \sum_{j=1}^{N_1}\sum_{i=1}^{N_1} a_{j,i}\psi_i(x)\psi_j(t) = \Psi^T(t)A\Psi(x) \tag{4.18}$$

$$\frac{\partial^2 u}{\partial t^2} = \sum_{j=1}^{N_1}\sum_{i=1}^{N_1} b_{j,i}\psi_i(x)\psi_j(t) = \Psi^T(t)B\Psi(x) \tag{4.19}$$

$$\frac{\partial^2 w}{\partial x^2} = \sum_{j=1}^{N_1}\sum_{i=1}^{N_1} c_{j,i}\psi_i(x)\psi_j(t) = \Psi^T(t)C\Psi(x) \tag{4.20}$$

$$\frac{\partial^2 w}{\partial t^2} = \sum_{j=1}^{N_1}\sum_{i=1}^{N_1} d_{j,i}\psi_i(x)\psi_j(t) = \Psi^T(t)D\Psi(x) \tag{4.21}$$

where $A^T = [a_{i,j}], B^T = [b_{i,j}], C^T = [c_{i,j}], D^T = [d_{i,j}]$, $\Psi(x) = [\psi_i(x)]^T$ and $\Psi(t) = [\psi_j(t)]^T$ for $1 \leq i, j \leq N_1$. For collocation, the points in the set $\{(x_i, t_j) : x_i = t_i = \frac{i-0.5}{N_1}, 1 \leq i, j \leq N_1\}$ are chosen. Using (4.18) and (4.19) one can obtain $u(x,t)$ in two different representations as shown below.

$$u(x,t) = \Psi^T(t)AP^2\Psi(x) - \Psi^T(t)AC_1x + (u(1,t) - u(0,t))x + u(0,t) \tag{4.22}$$

$$u(x,t) = \Psi^T(t)(P^T)^2B\Psi(x) + tu_t(x,0) + u(x,0), \tag{4.23}$$

Similarly, using (4.20) and (4.21), $w(x,t)$ can be represented in two different ways as follows.

$$w(x,t) = \Psi^T(t)CP^2\Psi(x) - \Psi^T(t)CC_1x + (w(1,t) - w(0,t))x + w(0,t) \tag{4.24}$$

$$w(x,t) = \Psi^T(t)(P^T)^2D\Psi(x) + tw_t(x,0) + w(x,0) \tag{4.25}$$

where P is the operational matrix for integration [**11, 12**] and $C_1 = P\int_0^1 \Psi(t)\mathrm{d}t$. From (4.22) - (4.25) we get $4N_1^2$ equations. Another $4N_1^2$ can be obtained by substituting the expressions of u_{tt}, w_{tt}, u, w, u_{xx} and w_{xx} given by (4.19) ,(4.21), (4.22), (4.24), (4.18) and (4.20) respectively in the corresponding linear PDE. This system needs to be solved for Chebyshev coefficients $a_{i,j}$'s, $b_{i,j}$'s, $c_{i,j}$'s and $d_{i,j}$'s. Then the solutions $u(x,t)$ and $w(x,t)$ can be obtained from (4.22) or (4.23) and (4.24) or (4.25) respectively.

4.2.3. Numerical Implementation

The following scheme of linear coupled partial differential equations are obtained after applying classical quasilinearization to the coupled sine-Gordon equation (4.17).

$$\begin{aligned}\frac{\partial^2 u_{n+1}}{\partial t^2} - \frac{\partial^2 u_{n+1}}{\partial x^2} &= \delta^2(w_{n+1} - w_n)\cos(u_n - w_n) + \delta^2(u_n - u_{n+1})\cos(u_n - w_n)\\ &\quad -\delta^2\sin(u_n - w_n) + f(x,t), \quad n = 0, 1, 2\cdots\end{aligned} \tag{4.26}$$

$$\begin{aligned}\frac{\partial^2 w_{n+1}}{\partial t^2} - c^2\frac{\partial^2 w_{n+1}}{\partial x^2} &= (w_n - w_{n+1})\cos(u_n - w_n) + (u_{n+1} - u_n)\cos(u_n - w_n)\\ &\quad +\sin(u_n - w_n) + g(x,t), \quad n = 0, 1, 2\cdots\end{aligned} \tag{4.27}$$

with initial conditions $u_{n+1}(x,0) = f_1(x)$, $u_{n+1_t}(x,0) = f_2(x)$, $w_{n+1}(x,0) = f_3(x)$, $w_{n+1_t}(x,0) = f_4(x)$ and boundary conditions $u_{n+1}(0,t) = g_1(t)$, $u_{n+1}(1,t) = g_2(t)$,

$w_{n+1}(0,t) = g_3(t)$, $w_{n+1}(1,t) = g_4(t)$. This section explains how to couple the classical quasilinearization method with Chebyshev wavelet collocation method to solve coupled sine-Gordon equations. Let us assume that B' denotes transpose of the matrix B. Using the collocation points, the equations (4.22) - (4.25) can be rewritten as

$$u_{n+1}(x,t) = \phi^T A_{n+1} P_2 - \phi^T A_{n+1} F_1 + K_1 - K_2 + K_3 \tag{4.28}$$

$$u_{n+1}(x,t) = P_2^T B_{n+1}\phi + K_4 + K_5 \tag{4.29}$$

$$w_{n+1}(x,t) = \phi^T C_{n+1} P_2 - \phi^T C_{n+1} F_1 + K_6 - K_7 + K_8 \tag{4.30}$$

$$w_{n+1}(x,t) = P_2^T D_{n+1}\phi + K_9 + K_{10} \tag{4.31}$$

where $A_{n+1}^T = [a_{i,j}]$, $B_{n+1}^T = [b_{i,j}]$, $C_{n+1}^T = [c_{i,j}]$, $D_{n+1} = [d_{i,j}]$, $\phi = [\Psi(x_i)] = [\Psi(t_j)]$, $P_2 = P^2\Psi(x_i) = P^2\Psi(t_j)$, $F_1 = C_1 X$, $X = [x_i]$, , $K_1 = x_i g_2(t_j)$, $K_2 = x_i g_1(t_j)$, $K_3 = g_1(t_j)$, $K_4 = t_j f_2(x_i)$, $K_5 = f_1(x_i)$, $K_6 = x_i g_4(t_j)$, $K_7 = x_i g_3(t_j)$, $K_8 = g_3(t_j)$, $K_9 = t_j f_4(x_i)$, $K_{10} = f_3(x_i)$ and $\{(x_i,t_j) : x_i = t_i = \frac{i-0.5}{N_1}, 1 \le i,j \le N_1\}$. Here A_0, B_0, C_0, D_0 are obtained from the initial approximations u_0 and w_0. Equating (4.28),(4.29) and (4.30),(4.31) we get,

$$\phi^T A_{n+1} P_2 - \phi^T A_{n+1} F_1 - P_2^T B_{n+1}\phi = K_{11} \tag{4.32}$$

$$\phi^T C_{n+1} P_2 - \phi^T C_{n+1} F_1 - P_2^T D_{n+1}\phi = K_{12} \tag{4.33}$$

where $K_{11} = K_4 + K_5 - K_1 + K_2 - K_3$ and $K_{12} = K_9 + K_{10} - K_6 + K_7 - K_8$. After using collocation points, (4.26) and (4.27) can be rewritten as

$$\phi^T B_{n+1}\phi - \phi^T A_{n+1}\phi - \delta^2 K_{13} \circ (P_2^T D_{n+1}\phi) + \delta^2 K_{13} \circ (P_2^T B_{n+1}\phi) = K_{14} \tag{4.34}$$

$$\phi^T D_{n+1}\phi - c^2\phi^T C_{n+1}\phi + K_{13} \circ (P_2^T D_{n+1}\phi) - K_{13} \circ (P_2^T B_{n+1}\phi) = K_{15} \tag{4.35}$$

where $K_{13} = \cos(K_{16} - K_{17})$, $K_{18} = \sin(K_{16} - K_{17})$, $K_{16} = u_n(x_i,t_j)$, $K_{17} = w_n(x_i,t_j)$, $K_{14} = f(x_i,t_j) - \delta^2 K_{18} + \delta^2 K_{13} \circ (K_{16} + K_9 + K_{10} - K_{17} - K_4 - K_5)$ and $K_{15} = g(x_i,t_j) + K_{18} + K_{13} \circ (K_{17} + K_4 + K_5 - K_{16} - K_9 - K_{10})$ with '$\circ$' denoting the Hadamard product. Now, one will end up with four known equations (4.32), (4.33), (4.34), (4.35) and four unknown matrices A_{n+1}, B_{n+1}, C_{n+1}, D_{n+1}. By using vectorization the above equations can be brought into the form $L\theta = \nu$ where the entries of A_{n+1}, B_{n+1}, C_{n+1}, D_{n+1}, form the vector θ. The numerical solution of the coupled sine-Gordon equation can be obtained by using either equation (4.22) or (4.23) for u and similarly by using either equation (4.24) or (4.25) for w.

4.2.3.1. ***Convergence and error analysis***. A function $u(x,t) \in L^2((0,1)\times(0,1))$ can be expanded using Chebyshev wavelets as

$$u(x,t) = \sum_{j=1}^{\infty}\sum_{i=1}^{\infty} c_{j,i}\psi_i(x)\psi_j(t). \tag{4.36}$$

The following theorem guarantee convergence of the Chebyshev wavelet series.

Theorem 4.2.1. *If a function $u(x,t) \in C([0,1]\times[0,1])$ has a bounded second order partial derivatives, then the Chebyshev wavelet method converges uniformly to $u(x,t)$.*

Proof. The estimation follows that is similar to the proof as published previously [**2, 93**].

$$\begin{aligned}
|c_{j,i}| &\leq \frac{2\pi L}{(2n_1)^{\frac{1}{2}}(2n)^{\frac{5}{2}}(m^2-1)}; \quad m>1 \\
|c_{j,i}| &\leq \frac{2\pi^2 L_1}{(2n)^{\frac{3}{2}}(2n_1)^{\frac{1}{2}}}; \quad m=1.
\end{aligned}$$

where $|\frac{\partial^2 u}{\partial x^2}| \leq L$ and $|\frac{\partial u}{\partial x}| \leq L_1$, n, m depends on i and n_1, m_1 depends on j as mentioned in the definition. Hence (4.36) is absolutely convergent. □

Theorem 4.2.2. *If a function $u(x,t) \in C([0,1]\times[0,1])$ has a bounded second order partial derivative, then we have the following accuracy estimation.*

$$\begin{aligned}
\|u(x,t) - \sum_{i=1}^{N_1}\sum_{j=1}^{N_2} c_{ji}\psi_i(x)\psi_j(t)\| &\leq \left(\sum_{i=N_1}^{\infty}\sum_{n_1=2^{k_1}}^{\infty} \frac{4\pi^2 L^2}{(2n)^5(2n_1)(m^2-1)^2}\right)^{\frac{1}{2}}; \quad m>1 \\
\|u(x,t) - \sum_{i=1}^{N_1}\sum_{j=1}^{N_2} c_{ji}\psi_i(x)\psi_j(t)\| &\leq \left(\sum_{i=N_1}^{\infty}\sum_{n_1=2^{k_1}}^{\infty} \frac{4\pi^4 L_1^2}{(2n)^3(2n_1)}\right)^{\frac{1}{2}}; \quad m=1.
\end{aligned}$$

where $|\frac{\partial^2 u}{\partial x^2}| \leq L$ and $|\frac{\partial u}{\partial x}| \leq L_1$, n, m depends on i and n_1, m_1 depends on j as mentioned in the definition.

Proof. The proof is similar to the proof referenced in previous studies [**93**, Theorem 7]. □

4.2.4. Numerical Experiments

This section provides results of the numerical experiments done on various test problems as described by Ilati et.al.[**57**] using the proposed Chebyshev wavelet based method (CWM). The solutions, corresponding errors and the number of required grid points compared to recently published RBF based scheme [**57**] was used to prove the efficiency of the proposed scheme. N_1 indicates the number of Chebyshev wavelets.

Example 4.2.1.

Consider the coupled sine-Gordon equation

$$\begin{aligned} u_{tt} - u_{xx} &= -\sin(u-w) + f(x,t) \\ w_{tt} - w_{xx} &= \sin(u-w) + g(x,t), \quad -2 \le x \le 2,\ 0 \le t \le T \end{aligned}$$

where

$$\begin{aligned} f(x,t) &= 2\sin(x) + t^2\sin(x) - \sin(t^2\cos(x) - t^2\sin(x)) \\ g(x,t) &= 2\cos(x) + t^2\cos(x) + \sin(t^2\cos(x) - t^2\sin(x)) \end{aligned}$$

with the initial conditions $u(x,0) = w(x,0) = u_t(x,0) = w_t(x,0) = 0$ and Dirichlet boundary conditions $u(-2,t) = t^2\sin(-2),\ u(2,t) = t^2\sin(2),\ w(-2,t) = t^2\cos(-2)$ and $w(2,t) = t^2\cos(2)$. It is easy to verify that $u(x,t) = t^2\sin(x),\ w(x,t) = t^2\cos(x), \quad x \in [-2,2],\ 0 < t \le T$ are the exact solution. The numerical solutions of Example 1 in [**57**] are obtained by methods based on the radial basis functions, Gaussian (GA) and multiquadrics (MQ) coupled with QR factorization. Table 4.9 gives the comparison between the GA-RBF-QR, GA-RBF and CWM in terms of accuracy and grid points. It is interesting to note that GA-RBF-QR produces higher accuracy for the grid size 204800, where as CWM enhances accuracy just by using 128 grid points. Table 4.10 gives the comparison between the MQ-RBF-QR and CWM in terms of accuaracy and grid points. It is interesting to note that MQ-RBF-QR produces higher accuracy with a grid size of 204800, where as CWM produces better accuracy by just using 128 grid points. Figure 4.13 represent the graphs of the numerical and analytical solutions at time $t = 2$ in the interval $-6 \le x \le 6$.

Example 4.2.2.

Consider the coupled sine-Gordon equation

$$\begin{aligned} u_{tt} - u_{xx} &= -\sin(u - w) \\ w_{tt} - w_{xx} &= \sin(u - w), \quad 40 \le x \le 70,\ 0 \le t \le T \end{aligned}$$

with the initial conditions $u(x, 0) = \cos(\alpha x)$, $w(x, 0) = 0$, $u_t(x, 0) = 0$, $w_t(x, 0) = 0$ and Dirichlet boundary conditions

$$\begin{aligned} u(40, t) &= \cos(40\alpha) - \frac{1}{2}\alpha^2 t^2 \cos(40\alpha) - \frac{1}{2}t^2 \cos(40\alpha) + \frac{1}{24}\alpha^2 t^4(\alpha^2 + 1)\cos(40\alpha) \\ &+ \frac{1}{24}t^4(2 + \alpha^2)\cos(40\alpha) \\ u(70, t) &= \cos(70\alpha) - \frac{1}{2}\alpha^2 t^2 \cos(70\alpha) - \frac{1}{2}t^2 \cos(70\alpha) + \frac{1}{24}\alpha^2 t^4(\alpha^2 + 1)\cos(70\alpha) \\ &+ \frac{1}{24}t^4(2 + \alpha^2)\cos(70\alpha) \\ w(40, t) &= \frac{1}{2}t^2 \cos(40\alpha) - \frac{1}{24}\alpha^2 t^4 \cos(40\alpha) - \frac{1}{24}t^4(\alpha^2 + 2)\cos(40\alpha) \\ w(70, t) &= \frac{1}{2}t^2 \cos(70\alpha) - \frac{1}{24}\alpha^2 t^4 \cos(70\alpha) - \frac{1}{24}t^4(2 + \alpha^2)\cos(70\alpha) \end{aligned}$$

where $\alpha = 1.6$. Though the exact solutions are infinite series

$$\begin{aligned} u(x, t) &= \cos(\alpha x) - \frac{1}{2}\alpha^2 t^2 \cos(\alpha x) - \frac{1}{2}t^2 \cos(\alpha x) + \frac{1}{24}\alpha^2 t^4(\alpha^2 + 1)\cos(\alpha x) \\ &+ \frac{1}{24}t^4(\alpha^2 + 2)\cos(\alpha x) + \cdots \\ w(x, t) &= \frac{1}{2}t^2 \cos(\alpha x) - \frac{1}{24}\alpha^2 t^4 \cos(\alpha x) - \frac{1}{24}t^4(\alpha^2 + 2)\cos(\alpha x) + \cdots \end{aligned}$$

we consider the following approximate solution as exact solution for preparing the error tables.

$$\begin{aligned} u(x, t) &= \cos(\alpha x) - \frac{1}{2}\alpha^2 t^2 \cos(\alpha x) - \frac{1}{2}t^2 \cos(\alpha x) + \frac{1}{24}\alpha^2 t^4(\alpha^2 + 1)\cos(\alpha x) \\ &+ \frac{1}{24}t^4(\alpha^2 + 2)\cos(\alpha x) \\ w(x, t) &= \frac{1}{2}t^2 \cos(\alpha x) - \frac{1}{24}\alpha^2 t^4 \cos(\alpha x) - \frac{1}{24}t^4(\alpha^2 + 2)\cos(\alpha x) \end{aligned}$$

The numerical solutions of Example 2 [**57**] are obtained by methods based on the multiquadric RBF coupled with QR factorization. Table 4.11 shows the comparison between the MQ-RBF-QR and CWM in terms of accuracy and grid points. It is interesting to note that CWM produces higher accuracy for almost one third of the grid size compared to MQ-RBF-QR. Figure 6.1 represent the graphs of the numerical and analytical solution at time $t = 0.3$ in the interval $40 \leq x \leq 70$.

4.2.5. Conclusion

In this study we have discussed in detail, an efficient numerical method based on Chebyshev wavelet combined with quasilinearization method for coupled sine-Gordon equation with initial boundary conditions. The proposed wavelet based scheme produces higher accuracy with lower number of grid points than the radial basis function (RBF) based method. In order to handle the nonlinearity as seen with RBF based scheme [**57**] that uses successive approximation, our proposed wavelet based scheme incorporates quasilinearization. Consequently, the proposed wavelet based iterative scheme converges faster.

TABLE 4.9. L_∞ errors for $t = 1$ for Example 4.2.1

Grid	GA RBF-QR[**57**]		GA RBF[**57**]		Grid	CWM	
	u_{err}	w_{err}	u_{err}	w_{err}	(N_1, N_1)	u_{err}	w_{err}
(20,20)	$2.4865e^{-02}$	$2.4879e^{-02}$	$1.6141e^{19}$	$2.9515e^{20}$	(6,6)	$6.8047e^{-04}$	$2.5910e^{-03}$
(20,40)	$1.2175e^{-02}$	$1.2159e^{-02}$	$1.8609e^{37}$	$3.9877e^{36}$	(7,7)	$3.3363e^{-04}$	$1.0296e^{-04}$
(20,80)	$6.0175e^{-03}$	$6.0072e^{-03}$	$4.0760e^{156}$	$3.8883e^{156}$	(8,8)	$8.7614e^{-06}$	$4.4558e^{-05}$
(20,160)	$2.9906e^{-03}$	$2.9850e^{-02}$	$5.5694e^{188}$	$1.9918e^{183}$	(9,9)	$4.5432e^{-06}$	$1.3230e^{-06}$
(20,5120)	$9.2891e^{-05}$	$9.2712e^{-05}$	NaN	NaN	(10,10)	$8.1446e^{-08}$	$5.0900e^{-07}$

TABLE 4.10. L_∞ errors for $t = 1$ for Example 4.2.1

Grid	MQ RBF-QR[**57**]		Grid	CWM	
	u_{err}	w_{err}	(N_1, N_1)	u_{err}	w_{err}
(20,10)	$2.8620e^{-02}$	$2.4687e^{-02}$	(5,5)	$1.5923e^{-02}$	$5.3623e^{-03}$
(20,40)	$7.7483e^{-03}$	$1.1674e^{-02}$	(6,6)	$6.8047e^{-04}$	$2.5910e^{-03}$
(20,160)	$3.6067e^{-03}$	$4.4709e^{-03}$	(7,7)	$3.3363e^{-04}$	$1.0296e^{-04}$
(20,640)	$7.3924e^{-04}$	$7.4249e^{-04}$	(8,8)	$8.7614e^{-06}$	$4.4558e^{-05}$
(20,5120)	$9.2352e^{-05}$	$9.2622e^{-05}$	(9,9)	$4.5432e^{-06}$	$1.3230e^{-06}$

TABLE 4.11. L_∞ errors at different times t for Example 4.2.2

Method	MQ RBF[**57**]		CWM	
Grid	(15,1000)		(72,72)	
t	u_{err}	w_{err}	u_{err}	w_{err}
0.1	$2.8175e^{-04}$	$5.3129e^{-05}$	$3.1351e^{-04}$	$4.2048e^{-07}$
0.2	$1.1133e^{-03}$	$1.9834e^{-04}$	$1.1127e^{-03}$	$8.8512e^{-06}$
0.3	$2.4543e^{-03}$	$3.8742e^{-04}$	$9.0672e^{-04}$	$2.2674e^{-05}$
0.4	$4.2658e^{-03}$	$5.2184e^{-04}$	$5.6136e^{-04}$	$1.7233e^{-05}$
0.5	$6.5513e^{-03}$	$5.9676e^{-04}$	$6.7713e^{-04}$	$4.0033e^{-05}$
0.6	$9.4133e^{-03}$	$5.2000e^{-04}$	$1.1260e^{-03}$	$3.7948e^{-05}$

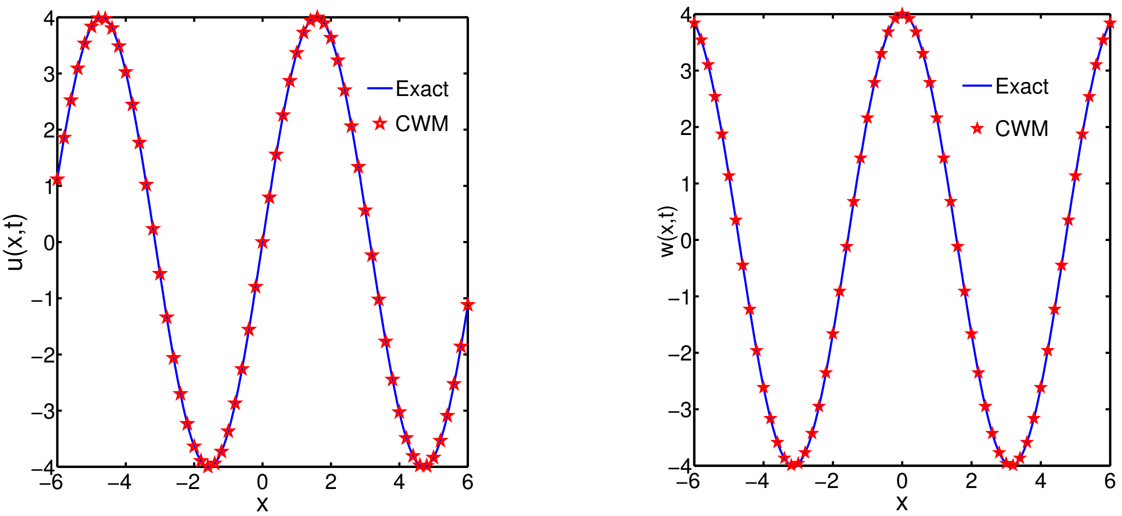

(A) (B)

FIGURE 4.13. Numerical and exact solutions of $u(x,t)$ and $w(x,t)$ at $t=2$ for Example 4.2.1

CHAPTER 5

FOURTH ORDER ELLIPTIC EQUATION WITH NONLOCAL BOUNDARY CONDITIONS

This chapter[1] discusses about wavelet methods for fourth order elliptic equations with nonlocal boundary conditions.

5.1. Introduction

Fourth order elliptic equations with various boundary conditions find relevance in the study of traveling waves in suspension bridges [**26, 80, 99**] and static deflection of a bending beam [**14, 40, 188**]. Very few works can be found in the literature that deal with fourth order elliptic equation

$$\Delta^2 u(x,y) - b_0 \Delta u(x,y) + c_0 u(x,y) = f(x,y,u(x,y)), \tag{5.1}$$

where $a \le x \le b$ and $c \le y \le d$ with nonlocal boundary conditions $u(x,i_1) = \int_c^d \int_a^b \beta(x,y)$ $u(x,y)\mathrm{d}x\mathrm{d}y + g^{(1)}(x,i_1)$, $u(i_2,y) = \int_c^d \int_a^b \beta(x,y)u(x,y)\mathrm{d}x\mathrm{d}y + g^{(1)}(i_2,y)$, $\Delta u(x,i_1) = \int_c^d \int_a^b \beta(x,y)\Delta u(x,y)\mathrm{d}x\mathrm{d}y - g^{(0)}(x,i_1)$, $\Delta u(i_2,y) = \int_c^d \int_a^b \beta(x,y)\ \Delta u(x,y)\mathrm{d}x\mathrm{d}y - g^{(0)}(i_2,y)$ where $i_1 = c,\ d$, $i_2 = a,\ b$, b_0 and c_0 are constants with $b_0 \ge 0$ and $f(x,y,u)$, $\beta(x,y)$ and $g^{(l)}(x')(l = 0,1)$ are continuous functions in their respective domains. To solve this problem numerically, interesting finite difference iterative schemes are developed in [**89, 115**].

The present article proposes numerical techniques based on two different iterative schemes using Legendre wavelets for solving (5.1). Numerical schemes based on Legendre wavelets are recently reported in the literature for solving different types of differential equations like ordinary differential equation [**108**], delay differential equation [**137**], partial differential equation [**75, 169**] and q-difference equation [**167**]. Though there are considerably many methods based on wavelet techniques for different types of differential

[1]This chapter forms the paper by K.H. Kumar and V.A. Vijesh, under review

equations, very few works are available for linear second order elliptic partial differential equations [**8, 10**] with Dirichlet, Neumann and mixed boundary conditions. In the literature, some methods are reported for integral equations and ordinary integro differential equations. [**1, 7, 17, 50**]. Recently in [**9**], Islam et al. proposed a new numerical method based on Haar wavelets for third and fourth order ordinary differential equation with nonlocal boundary conditions. In this direction, a Haar wavelet method is proposed for a second order linear elliptic partial differential equation with one nonlocal boundary condition in [**59**]. One of the drawbacks in its approach is that it demands even the fourth order derivatives to be existing and belonging to $L^2[0,1]$.

In the present article, two numerical methods based on Legendre wavelets are developed for (5.1). In the first approach, classical quasilinearization is combined with Legendre wavelets for solving the fourth order elliptic equation with nonlocal boundary conditions. Though the accuracy obtained by this method is decent enough, it is found to produce considerably insignificant accuracy for a certain class of solutions. Moreover, as the number of wavelets increases, the size of the resultant matrix increases rapidly. To overcome this issue, another iterative method is also proposed where the nonlinear fourth order elliptic equation (5.1) with nonlocal boundary conditions is transformed to a coupled second order differential equation with nonlocal boundary conditions. Later with the help of an iterative scheme discussed in [**89**], the coupled equation is linearized and solved for its numerical solution. It was observed that depending on the nature of the solutions, one of the two iterative procedures will outperform the other. The main contributions of this study are

- Two efficient iterative schemes are proposed to solve (5.1) numerically.
- The second scheme also supplies an effective method for solving second order elliptic equation with nonlocal boundary conditions.
- In contrast to [**59**], this scheme requires only the second order derivative to be existing in $L^2[0,1]$.

The organization of this chapter is as follows.Two different Legendre wavelet collocation methods in combination with iterative schemes are provided in Section 5.2 for two dimensional fourth-order nonlinear elliptic equations with nonlocal boundary conditions. The proposed methods are illustrated in Section 5.3 by applying it to different examples. The obtained numerical results are compared with an existing numerical method based on finite difference scheme (FD) [**115**]. The discussion is concluded in Section 5.4.

5.2. Wavelets collocation method

This section gives descriptions on two iterative methods based on Legendre wavelets for solving (5.1) numerically. More specifically, discussions on solving linear problems arising at each iteration of the procedures proposed are detailed. Throughout the discussion, the following most frequently used definition of Legendre wavelets is adopted [**169**].

5.2.1. Legendre Wavelet

The Legendre wavelet family on the interval $[0,1]$ is defined as

$$\psi_i(x) = \begin{cases} 2^{\frac{k}{2}}\sqrt{m+\frac{1}{2}}L_m(2^k x - \hat{n}) & \text{if } x \in [\frac{\hat{n}-1}{2^k}, \frac{\hat{n}+1}{2^k}) \\ 0 & \text{otherwise} \end{cases} \tag{5.2}$$

where $n = 1, 2, \cdots 2^{k-1}$, $m = 0, 1, 2, \cdots$, $i = n + 2^{k-1}m$ and $L_m(x)$ is the well known Legendre polynomial of degree m. To generate Legendre polynomials the following recurrence relation is used.

$$L_0(x) = 1, \quad L_1(x) = x \tag{5.3}$$

$$L_{m+1}(x) = \left(\frac{2m+1}{m+1}\right) xL_m(x) - \left(\frac{m}{m+1}\right) L_{m-1}(x) \tag{5.4}$$

for $m = 1, 2, 3\cdots$. From the orthogonal property of Legendre polynomial, it can be easily seen that Legendre wavelet is an orthonormal subset of $L^2(0,1)$. Consequently, the Legendre wavelet family forms a basis for $L^2(0,1)$. Hence, any member f of $L^2(0,1)$ can be expressed as an infinite sum of Legendre wavelets, i.e. $h(x) = \sum_{i=1}^{\infty} a_i\psi_i(x)$.

5.2.2. Method I

In the first approach, classical quasilinearization is coupled with Legendre wavelets for solving fourth order elliptic differential equation (5.1) with nonlocal boundary conditions.

With the help of classical quasilinearization, the problem is linearized first and then all the terms in the governing equation and the kernal $\beta(x,y)$ in the boundary conditions are approximated using Legendre wavelets. At each step of the iteration, one has to solve the following linear fourth order elliptic equation with nonlocal boundary conditions.

$$\Delta^2 u_{n+1}(x,y) - b_0\Delta u_{n+1}(x,y) + c_0 u_{n+1}(x,y) = f(x,y,u_n(x,y)) + f'(u_n)(u_{n+1}-u_n) \tag{5.5}$$

with the boundary conditions

$$\begin{aligned}
u_{n+1}(x,i_1) &= \int_0^1\int_0^1 \beta(x,y)u_{n+1}(x,y)\mathrm{d}x\mathrm{d}y + g^{(1)}(x,i_1),\\
u_{n+1}(i_1,y) &= \int_0^1\int_0^1 \beta(x,y)u_{n+1}(x,y)\mathrm{d}x\mathrm{d}y + g^{(1)}(i_1,y),\\
\Delta u_{n+1}(x,i_1) &= \int_0^1\int_0^1 \beta(x,y)\Delta u_{n+1}(x,y)\mathrm{d}x\mathrm{d}y - g^{(0)}(x,i_1),\\
\Delta u_{n+1}(i_1,y) &= \int_0^1\int_0^1 \beta(x,y)\Delta u_{n+1}(x,y)\mathrm{d}x\mathrm{d}y - g^{(0)}(i_1,y)
\end{aligned}$$

where $i_1 = 0$ and 1. Using the Legendre wavelets, the following approximations are made for (5.5).

$$\frac{\partial^4 u_{n+1}(x,y)}{\partial x^4} = \sum_{i=1}^{N}\sum_{j=1}^{N} a_{i,j}^{n+1}\psi(x)\psi(y) = \Psi^T(x)A_{n+1}\Psi(y) \tag{5.6}$$

$$\frac{\partial^4 u_{n+1}(x,y)}{\partial y^4} = \sum_{i=1}^{N}\sum_{j=1}^{N} b_{i,j}^{n+1}\psi(x)\psi(y) = \Psi^T(x)B_{n+1}\Psi(y). \tag{5.7}$$

$\beta(x,y) = \Psi^T(x)K\Psi(y)$, $\dfrac{\partial^2 u_{n+1}(x,y)}{\partial x^2} = \Psi^T(x)C_{n+1}\Psi(y)$, $u_{n+1}(x,y) = \Psi^T(x)D_{n+1}\Psi(y)$, $\dfrac{\partial^2 u_{n+1}(x,y)}{\partial y^2} = \Psi^T(x)E_{n+1}\Psi(y)$ where $A_{n+1} = [a_{ij}^{n+1}]_{N\times N}$, $B_{n+1} = [b_{ij}^{n+1}]_{N\times N}$, $K = [k_{ij}^{n+1}]_{N\times N}$, $C = [c_{ij}^{n+1}]_{N\times N}$, $D = [d_{ij}^{n+1}]_{N\times N}$ and $E = [e_{ij}^{n+1}]_{N\times N}$. The following is obtained by integrating (5.6)

$$\frac{\partial^3 u_{n+1}(x,y)}{\partial x^3} = \Psi^T(x)P^T A_{n+1}\Psi(y) + G_1(y) \tag{5.8}$$

$$\frac{\partial^2 u_{n+1}(x,y)}{\partial x^2} = \Psi^T(x)P^{T^2} A_{n+1}\Psi(y) + G_1(y)x + G_2(y) \tag{5.9}$$

$$\frac{\partial u_{n+1}(x,y)}{\partial x} = \Psi^T(x)P^{T^3} A_{n+1}\Psi(y) + G_1(y)\frac{x^2}{2} + G_2(y)x + G_3(y) \tag{5.10}$$

$$u_{n+1}(x,y)=\Psi^T(x)P^{T^4}A_{n+1}\Psi(y)+G_1(y)\frac{x^3}{6}+G_2(y)\frac{x^2}{2}+G_3(y)x+G_4(y) \tag{5.11}$$

Similarly after integrating (5.7), one can get the following equations

$$\frac{\partial^3 u_{n+1}(x,y)}{\partial y^3}=\Psi^T(x)B_{n+1}P\Psi(y)+G_5(x) \tag{5.12}$$

$$\frac{\partial^2 u_{n+1}(x,y)}{\partial y^2}=\Psi^T(x)B_{n+1}P^2\Psi(y)+yG_5(x)+G_6(x) \tag{5.13}$$

$$\frac{\partial u_{n+1}(x,y)}{\partial y}=\Psi^T(x)B_{n+1}P^3\Psi(y)+\frac{y^2}{2}G_5(x)+yG_6(x)+G_7(x) \tag{5.14}$$

$$u_{n+1}(x,y)=\Psi^T(x)B_{n+1}P^4\Psi(y)+\frac{y^3}{6}G_5(x)+\frac{y^2}{2}G_6(x)+yG_7(x)+G_8(x). \tag{5.15}$$

Using the given boundary conditions, the unknown G_i's$(i=1,\dots 8)$ can be obtained as follows. $G_4(y)=u_{n+1}(0,y)$, $G_8(x)=u_{n+1}(x,0)$, $G_2(y)=\dfrac{\partial^2 u_{n+1}(0,y)}{\partial x^2}$ and $G_6(x)=\dfrac{\partial^2 u_{n+1}(x,0)}{\partial y^2}$. Further integrating (5.8), (5.10),(5.12) and (5.14), one can obtain the remaining G_i's$(i=1,3,5,7)$. More specifically,

$$\begin{aligned}
G_1(y) &= \frac{\partial^2 u_{n+1}(1,y)}{\partial x^2}-\frac{\partial^2 u_{n+1}(0,y)}{\partial x^2}-I_1^TP^TA_{n+1}\Psi(y)\\
G_5(x) &= \frac{\partial^2 u_{n+1}(x,1)}{\partial y^2}-\frac{\partial^2 u_{n+1}(x,0)}{\partial y^2}-\Psi^T(x)B_{n+1}PI_1\\
G_3(y) &= u_{n+1}(1,y)-u_{n+1}(0,y)-I_1^TA_{n+1}P^3\Psi(y)-\frac{G_1(y)}{6}-\frac{G_2(y)}{2}\\
G_7(x) &= u_{n+1}(x,1)-u_{n+1}(x,0)-\Psi^T(x)B_{n+1}P^3I_1-\frac{G_5(x)}{6}-\frac{G_6(x)}{2}.
\end{aligned}$$

where $I_1=\int_0^1\Psi(\zeta)\mathrm{d}\zeta$. The simplification of one of the boundary conditions is demonstrated below.

$$\begin{aligned}
u_{n+1}(x,0) &= \int_0^1\int_0^1\beta'(x,y)u_{n+1}(x,y)\mathrm{d}x\mathrm{d}y+g^{(1)}(x,0) && (5.16)\\
&= \int_0^1\int_0^1\Psi^T(x)K\Psi(y)\Psi^T(s)D_{n+1}\Psi(s')\mathrm{d}x\mathrm{d}y+g^{(1)}(x,0)\\
&= \int_0^1\int_0^1\Psi^T(x)K^1_{n+1}\Psi(y)\mathrm{d}x\mathrm{d}y+g^{(1)}(x,0)\\
u_{n+1}(x,0) &= I_1^TK^1_{n+1}I_1+g^{(1)}(x,0) && (5.17)
\end{aligned}$$

K^1_{n+1} is obtained as follows $K^1_{n+1} = \text{inv}(\phi^T)K^2_{n+1}\text{inv}(\phi)$, $K^2_{n+1} = K^2 \circ K^3_{n+1}$, $K^2 = \phi^T K\phi$, $K^3_{n+1} = \phi^T D_{n+1}\phi$ and ϕ is Legendre matrix [**175**]. Similarly, $u_{n+1}(x,1) = I_1^T K^1_{n+1}I_1+g^{(1)}(x,1)$, $u_{n+1}(0,y) = I_1^T K^1_{n+1}I_1+g^{(1)}(0,y)$, $u_{n+1}(1,y) = I_1^T K^1_{n+1}I_1+g^{(1)}(1,y)$, $\Delta u_{n+1}(x,0) = I_1^T(K^4_{n+1}+K^5_{n+1})I_1 - g^{(0)}(x,0)$, $\Delta u_{n+1}(x,1) = I_1^T(K^4_{n+1}+K^5_{n+1})I_1 - g^{(0)}(x,1)$, $\Delta u_{n+1}(0,y) = I_1^T(K^4_{n+1}+K^5_{n+1})I_1-g^{(0)}(0,y)$, $\Delta u_{n+1}(1,y) = I_1^T(K^4_{n+1}+K^5_{n+1})I_1- g^{(0)}(1,y)$. Using $\dfrac{\partial^2 u_{n+1}(x,y)}{\partial x^2}$ and $\dfrac{\partial^2 u_{n+1}(x,y)}{\partial y^2}$, K^4_{n+1} and K^5_{n+1} can be obtained similar to that of K^1_{n+1}. Using the collocation points $\{(x_i,y_j) : x_i = y_i = \frac{i-0.5}{N}, 1 \le i,j \le N\}$ in equations 5.6−5.15 one can obtain

$$\frac{\partial^4 u_{n+1}(x,y)}{\partial x^4} = \phi^T A_{n+1}\phi \ , \ \frac{\partial^4 u_{n+1}(x,y)}{\partial y^4} = \phi^T B_{n+1}\phi \tag{5.18}$$

$$\frac{\partial^2 u_{n+1}(x,y)}{\partial x^2} = \phi^T P^{T^2} A_{n+1}\phi + H_{10}^T H_1 + H_9^T H_2 \tag{5.19}$$

$$\frac{\partial^2 u_{n+1}(x,y)}{\partial y^2} = \phi^T B_{n+1}P^2\phi + H_5^T H_{13} + H_6^T H_9 \tag{5.20}$$

$$u_{n+1}(x,y) = \phi^T P^{T^4} A_{n+1}\phi + H_{12}^T H_1 + H_{11}^T H_2 + H_{10}^T H_3 + H_9^T H_4 \tag{5.21}$$

$$u_{n+1}(x,y) = \phi^T B_{n+1}P^4\phi + H_5 H_{14}^T + H_6^T H_{15} + H_7^T H_{13} + H_8^T H_9 \tag{5.22}$$

where $H_1 = G_1(y_j)$, $H_2 = G_2(y_j)$, $H_3 = G_3(y_j)$, $H_4 = G_4(y_j)$, $H_5 = G_5(x_i)$, $H_6 = G_6(x_i)$, $H_7 = G_7(x_i)$, $H_8 = G_8(x_i)$, $H_9 = [1,1,1,\cdots]_{N\times N}$, $H_{10} = x_i$, $H_{11} = \dfrac{x_i^2}{2}$, $H_{12} = \dfrac{x_i^3}{6}$, $H_{13} = y_j$, $H_{14} = \frac{y_j^3}{6}$, $H_{15} = \frac{y_j^2}{2}$ and P is operational matrix of integration [**133**]. Finally one will end up with five unknown matrices A_{n+1}, B_{n+1}, C_{n+1}, D_{n+1} and E_{n+1} at each iteration along with five matrix equations obtained from (5.18) to (5.22) and (5.5) given by

$$\begin{aligned}
\phi^T\Big(A_{n+1}+B_{n+1}-b_0C_{n+1}-b_0E_{n+1}+c_0D_{n+1}\Big)\phi - M_1\circ\big(\phi^T D_{n+1}\phi\big) &= M\\
\phi^T P^{2^T} A_{n+1}\phi + H_{10}^T H_1 + H_9^T H_2 - \phi^T C_{n+1}\phi &= 0\\
\phi^T B_{n+1}P^2\phi + H_5^T H_{13} + H_6^T H_9 - \phi^T E_{n+1}\phi &= 0\\
\phi^T P^{T^4} A_{n+1}\phi + H_{12}^T H_1 + H_{11}^T H_2 + H_{10}^T H_3 + H_9^T H_4 - \phi^T D_{n+1}\phi &= 0\\
\phi^T B_{n+1}P^4\phi + H_5^T H_{14} + H_6^T H_{15} - H_7^T H_{13} + H_8^T H_9 - \phi^T D_{n+1}\phi &= 0
\end{aligned}$$

where $M = [f(x_i,y_j,u_n(x_i,y_j))]_{N\times N} - M_1\circ M_2$, $M_1 = [\dfrac{\partial f}{\partial u}(u_n(x_i,y_j)]_{N\times N}$,
$M_2 = [u_n(x_i,y_j)]_{N\times N}$. By using vectorization one can easily find out the unknown matrices.

5.2.3. Method II

Though the accuracy obtained by the above method is decent enough, the size of the resultant matrix gets very high as the number of wavelets increases. Consequently, to reduce the size of the resultant matrix, the fourth order elliptic equation with nonlocal boundary conditions is transformed to a coupled nonlinear second order differential equation with nonlocal boundary conditions [**89, 116**]. Later, an iterative scheme is proposed to solve the problem numerically. At each step of the iteration instead of solving a fourth order linear elliptic equation, two second order linear elliptic equations are solved one after the other. As a result, the size of the resultant matrix is reduced by half. At first, equation (5.1) can be written as [**89, 116**]

$$\begin{aligned} -\Delta u(x,y) + \mu u(x,y) = v(x,y), \\ -\Delta v(x,y) + \mu^{+} v(x,y) = \bar{c}u(x,y) + f(x,y,u(x,y)), \end{aligned} \tag{5.23}$$

$0 \le x \le 1$ and $0 \le y \le 1$ with the boundary conditions

$$\begin{aligned} u(x,i_1) &= \int_0^1\int_0^1 \beta(x,y)u(x,y)\mathrm{d}x\mathrm{d}y + g^{(1)}(x,i_1) \\ u(i_1,y) &= \int_0^1\int_0^1 \beta(x,y)u(x,y)\mathrm{d}x\mathrm{d}y + g^{(1)}(i_1,y) \\ v(x,i_1) &= \int_0^1\int_0^1 \beta(x,y)v(x,y)\mathrm{d}x\mathrm{d}y + g^{(2)}(x,i_1) \\ v(i_1,y) &= \int_0^1\int_0^1 \beta(x,y)v(x,y)\mathrm{d}x\mathrm{d}y + g^{(2)}(i_1,y) \end{aligned}$$

where $i_1 = 0,\, 1,\, \mu + \mu^{+} = b_0,\, \mu\mu^{+} = c^{*},\, c^{*} = c_0 + \bar{c},\, \bar{c} \ge max\{-\frac{\partial f(x,y,u)}{\partial u},\ \alpha^{*} \le u \le \beta^{*}\}$, $c^{*} \ge 0,\, b_0^2 - 4c^{*} \ge 0,\, g^{(2)} = g^{(0)} + \mu g^{(1)},\, (u,v) = (u, \mu u + \Delta u)$ for $x \in [a,b], y \in [c,d]$, α^{*} and β^{*} being the lower and upper solutions of (5.23) [**89, 116**]. The iterative procedure proposed to solve (5.23) is as follows [**89**]. The above problem (5.23) can be linearized[**89**] as follows

$$\begin{aligned} -\Delta u^{n+1}(x,y) + \mu u^{n+1}(x,y) &= v^{n}(x,y), \\ -\Delta v^{n+1}(x,y) + \mu^{+} v^{n+1}(x,y) &= \bar{c}u^{n+1}(x,y) + f(x,y,u^{n+1}(x,y)) \end{aligned} \tag{5.24}$$

with the boundary conditions

$$
\begin{aligned}
u^{n+1}(x,i_1) &= \int_0^1\int_0^1 \beta(x,y)u^{n+1}(x,y)\mathrm{d}x\mathrm{d}y + g^{(1)}(x,i_1)\\
u^{n+1}(i_1,y) &= \int_0^1\int_0^1 \beta(x,y)u^{n+1}(x,y)\mathrm{d}x\mathrm{d}y + g^{(1)}(i_1,y)\\
v^{n+1}(x,i_1) &= \int_0^1\int_0^1 \beta(x,y)v^{n+1}(x,y)\mathrm{d}x\mathrm{d}y + g^{(2)}(x,i_1)\\
v^{n+1}(i_1,y) &= \int_0^1\int_0^1 \beta(x,y)v^{n+1}(x,y)\mathrm{d}x\mathrm{d}y + g^{(2)}(i_1,y).
\end{aligned}
$$

All the terms in the governing equation (5.24) and the kernel function $\beta(x,y)$ in the boundary conditions can be approximated using Legendre wavelets as

$$\frac{\partial^2 u_{n+1}(x,y)}{\partial x^2} = \sum_{i=1}^{N}\sum_{j=1}^{N} q_{i,j}^{n+1}\psi_i(x)\psi_j(y) = \Psi^T(x)Q_{n+1}\Psi(y) \tag{5.25}$$

$$\frac{\partial^2 u_{n+1}(x,y)}{\partial y^2} = \sum_{i=1}^{N}\sum_{j=1}^{N} r_{i,j}^{n+1}\psi_i(x)\psi_j(y) = \Psi^T(x)R_{n+1}\Psi(y) \tag{5.26}$$

$$\frac{\partial^2 v_{n+1}(x,y)}{\partial x^2} = \sum_{i=1}^{N}\sum_{j=1}^{N} s_{i,j}^{n+1}\psi_i(x)\psi_j(y) = \Psi^T(x)S_{n+1}\Psi(y) \tag{5.27}$$

$$\frac{\partial^2 v_{n+1}(x,y)}{\partial y^2} = \sum_{i=1}^{N}\sum_{j=1}^{N} z_{i,j}^{n+1}\psi_i(x)\psi_j(y) = \Psi^T(x)Z_{n+1}\Psi(y). \tag{5.28}$$

$\beta(x,y) = \Psi^T(x)K\Psi(y)$, $u_{n+1}(x,y) = \Psi^T(x)W_{n+1}\Psi(y)$, $v_{n+1}(x,y) = \Psi^T(x)V_{n+1}\Psi(y)$, where $Q_{n+1} = [q_{ij}^{n+1}]_{N\times N}$, $R_{n+1} = [r_{ij}^{n+1}]_{N\times N}$, $S_{n+1} = [s_{ij}^{n+1}]_{N\times N}$, $Z_{n+1} = [z_{ij}^{n+1}]_{N\times N}$, $K = [k_{ij}^{n+1}]_{N\times N}$, $W = [u_{ij}^{n+1}]_{N\times N}$, $V = [v_{ij}^{n+1}]_{N\times N}$. The following are obtained by integrating $(5.25) - (5.28)$.

$$\frac{\partial u_{n+1}(x,y)}{\partial x} = \Psi^T(x)P^TQ_{n+1}\Psi(y) + F_1(y) \tag{5.29}$$

$$u_{n+1}(x,y) = \Psi^T(x)P^{T^2}Q_{n+1}\Psi(y) + F_1(y)x + F_2(y) \tag{5.30}$$

$$\frac{\partial u_{n+1}(x,y)}{\partial y} = \Psi^T(x)R_{n+1}P\Psi(y) + F_3(x) \tag{5.31}$$

$$u_{n+1}(x,y) = \Psi^T(x)R_{n+1}P^2\Psi(y) + yF_3(x) + F_4(x) \tag{5.32}$$

$$\frac{\partial v_{n+1}(x,y)}{\partial x} = \Psi^T(x)P^T S_{n+1}\Psi(y) + F_5(y) \tag{5.33}$$

$$v_{n+1}(x,y) = \Psi^T(x)P^{T^2} S_{n+1}\Psi(y) + F_5(y)x + F_6(y) \tag{5.34}$$

$$\frac{\partial v_{n+1}(x,y)}{\partial y} = \Psi^T(x)S_{n+1}P\Psi(y) + F_7(x) \tag{5.35}$$

$$v_{n+1}(x,y) = \Psi^T(x)S_{n+1}P^2\Psi(y) + yF_7(x) + F_8(x) \tag{5.36}$$

Using the given boundary conditions, the unknown F_i's$(i = 1, \ldots 8)$ can be obtained as follows. $F_2(y) = u_{n+1}(0,y)$, $F_4(x) = u_{n+1}(x,0)$, $F_6(y) = v_{n+1}(0,y)$, $F_8(x) = v_{n+1}(x,0)$,

$$\begin{aligned}
F_1(y) &= u_{n+1}(1,y) - u_{n+1}(0,y) - I_1^T P^T Q_{n+1}\Psi(y) \\
F_3(x) &= u_{n+1}(x,1) - u_{n+1}(x,0) - \Psi^T(x)R_{n+1}PI_1 \\
F_5(y) &= v_{n+1}(1,y) - v_{n+1}(0,y) - I_1^T P^T S_{n+1}\Psi(y) \\
F_7(x) &= v_{n+1}(x,1) - v_{n+1}(x,0) - \Psi^T(x)Z_{n+1}PI_1
\end{aligned}$$

The simplification of one of the boundary conditions is demonstrated below

$$u_{n+1}(x,0) = \int_0^1\int_0^1 \beta'(x,y)u_{n+1}(x,y)\mathrm{d}x\mathrm{d}y + g^{(1)}(x,0) \tag{5.37}$$

$$= \int_0^1\int_0^1 \Psi^T(x)K\Psi(y)\Psi^T(x)W_{n+1}\Psi(y)\mathrm{d}x\mathrm{d}y + g^{(1)}(x,0) \tag{5.38}$$

$$= \int_0^1\int_0^1 \Psi^T(x)L^1_{n+1}\Psi(y)\mathrm{d}x\mathrm{d}y + g^{(1)}(x,0) \tag{5.39}$$

$$u_{n+1}(x,0) = I_1^T L^1_{n+1} I_1 + g^{(1)}(x,0) \tag{5.40}$$

L^1_{n+1} is obtained from [**175**] as follows $L^1_{n+1} = \mathrm{inv}(\phi^T)L^2_{n+1}\mathrm{inv}(\phi)$, $L^2_{n+1} = L^3 \circ L^4_{n+1}$, $L^3 = \phi^T K\phi$, $L^4_{n+1} = \phi^T W_{n+1}\phi$ and ϕ is Legendre matrix. Similarly, $u_{n+1}(x,1) = I_1^T L^1_{n+1}I_1 + g^{(1)}(x,1)$, $u_{n+1}(0,y) = I_1^T L^1_{n+1}I_1 + g^{(1)}(0,y)$, $u_{n+1}(1,y) = I_1^T L^1_{n+1}I_1 + g^{(1)}(1,y)$, $v_{n+1}(x,0) = I_1^T L^1_{n+1}I_1 - g^{(0)}(x,0)$, $v_{n+1}(x,1) = I_1^T L^1_{n+1}I_1 - g^{(0)}(x,1)$, $v_{n+1}(0,y) = I_1^T L^1_{n+1}I_1 - g^{(0)}(0,y)$, $v_{n+1}(1,y) = I_1^T L^1_{n+1}I_1 - g^{(0)}(1,y)$. Using the same set of collocation points used for Method$-I$, equations (5.25)$-$(5.36) can be expressed as

$$\frac{\partial^2 u_{n+1}(x,y)}{\partial x^2} = \phi^T Q_{n+1}\phi \quad , \quad \frac{\partial^2 u_{n+1}(x,y)}{\partial y^2} = \phi^T R_{n+1}\phi \tag{5.41}$$

$$\frac{\partial^2 v_{n+1}(x,y)}{\partial x^2} = \phi^T S_{n+1}\phi \tag{5.42}$$

$$\frac{\partial^2 v_{n+1}(x,y)}{\partial y^2} = \phi^T Z_{n+1}\phi \tag{5.43}$$

$$u_{n+1}(x,y) = \phi^T {P^T}^2 Q_{n+1}\phi + J_1^T J_3 + J_2^T J_4 \tag{5.44}$$

$$u_{n+1}(x,y) = \phi^T R_{n+1} P^2\phi + J_5^T J_1 + J_6^T J_2 \tag{5.45}$$

$$v_{n+1}(x,y) = \phi^T {P^T}^2 S_{n+1}\phi + J_1^T J_7 + J_2^T J_8 \tag{5.46}$$

$$v_{n+1}(x,y) = \phi^T Z_{n+1} P^2\phi + J_9^T J_{11} + J_{10}^T J_2 \tag{5.47}$$

where $J_1 = x_i,,\ J_2 = [1,1,1\ldots]_{N\times N},\ J_3 = F_1(y_j),\ J_4 = F_2(y_j),\ J_5 = F_3(x_i),\ J_6 = F_4(x_i),$ $J_7 = F_5(y_j),\ J_8 = F_6(y_j),\ J_9 = F_7(x_i),\ J_{10} = F_8(x_i),\ J_{11} = y_j$. The following set of equations are obtained from (5.44), (5.45) and (5.24).

$$\begin{aligned}
-\phi^T Q_{n+1}\phi - \phi^T R_{n+1}\phi + \mu\phi^T W_{n+1}\phi &= M_1\\
\phi^T {P^T}^2 Q_{n+1}\phi - \phi^T W_{n+1}\phi &= -J_1^T J_3 - J_2^T J_4\\
\phi^T R_{n+1} P^2\phi - \phi^T W_{n+1}\phi &= -J_5^T J_{11} - J_6^T J_2
\end{aligned}$$

At each iteration one has to solve for the unknowns Q_{n+1}, R_{n+1} and W_{n+1} with the help of vectorization. The following set of set of equations can be obtained from (5.46), (5.47) and (5.24) by updating u_{n+1} in the second equation for v_{n+1},

$$\begin{aligned}
-\phi^T S_{n+1}\phi - \phi^T Z_{n+1}\phi + \mu^+\phi^T V_{n+1}\phi &= M_2\\
\bar{\phi}^T {P^T}^2 S_{n+1}\phi - \phi^T V_{n+1}\phi &= -J_1^T J_7 - J_2^T J_8\\
\phi^T Z_{n+1} P^2\phi - \phi^T V_{n+1}\phi &= -J_9^T J_{11} - J_{10}^T J_2
\end{aligned}$$

where $M_1 = v_n(x_i,y_j)$ and $M_2 = \bar{c}u_{n+1}(x_i,y_j) + f(x_i,y_j,u^{n+1}(x_i,y_j))$. By solving the above set of equations, v_{n+1} can also be obtained.

Remark 5.2.1. *One can easily observe that for each iteration in method–I, a set of $6N^2$ equations need to be solved simultaneously, where as in method–II, one needs to solve only $3N^2$ equations twice.*

5.3. Numerical Experiments

In this section, Legendre wavelet based methods $I\&II$ are illustrated by applying it to the two dimensional fourth order elliptic differential equation with nonlocal boundary conditions. The advantages of the proposed methods are shown by comparing it with the recent literature [**115**]. The following abbreviations and notations are used in this section.

1. "LWM$-I$" denotes Legendre wavelet classical quasilinearization method.
2. "LWM$-II$" denotes Legendre wavelet iterative scheme.
3. N denotes the number of Legendre wavelets.

Example 5.3.1.

Consider the fourth order elliptic equation (5.1) for the choice of $b_0 = 10$ and $c_0 = 1$ with the following initial and boundary conditions:

$$\begin{aligned}
u(x,0) &= \int_0^2 \int_0^1 xyu(x,y)\mathrm{d}x\mathrm{d}y + \theta_1, & u(x,2) &= \int_0^2 \int_0^1 xyu(x,y)\mathrm{d}x\mathrm{d}y + \theta_1 \\
u(0,y) &= \int_0^2 \int_0^1 xyu(x,y)\mathrm{d}x\mathrm{d}y + \theta_1, & u(1,y) &= \int_0^2 \int_0^1 xyu(x,y)\mathrm{d}x\mathrm{d}y + \theta_1 \\
\triangle u(x,0) &= \int_0^2 \int_0^1 xy\triangle u(x,y)\mathrm{d}x\mathrm{d}y - \theta_2, & \triangle u(x,2) &= \int_0^2 \int_0^1 xy\triangle u(x,y)\mathrm{d}x\mathrm{d}y - \theta_2 \\
\triangle u(0,y) &= \int_0^2 \int_0^1 xy\triangle u(x,y)\mathrm{d}x\mathrm{d}y - \theta_2, & \triangle u(1,y) &= \int_0^2 \int_0^1 xy\triangle u(x,y)\mathrm{d}x\mathrm{d}y - \theta_2
\end{aligned}$$

where $\theta_1 = \frac{4\alpha}{\pi^2}$, $\theta_2 = 5\alpha$, $\alpha = (\lambda_0^2 + b_0\lambda_0 + c_0)^{-1}$ and $\lambda_0 = \frac{5\pi^2}{4}$. The exact solution for the above problem is $u(x,t) = 1 - \alpha \sin \pi x \sin \frac{\pi y}{2}$. From Table 5.1, it is clear that the proposed methods LWM$-I$ and LWM$-II$ can achieve better results than FD [**115**] with lesser number of grid points. Both the proposed methods perform better than the scheme (FD) in [**115**] in terms of grid size and accuracy. Out of the both proposed methods, LWM$-I$ performs better that LWM$-II$. Figure 5.1 represents the plot between number of iterations and $r = \dfrac{\|u_{n+1} - u_*\|_\infty}{\|u_n - u_*\|_\infty^2}$ which shows the quadratic convergence. Figure 5.2 represents the LWM$-I$ solution for $N = 10$.

Example 5.3.2.

Consider the fourth order elliptic equation (5.1) for the choice of $b_0 = 5$ and $c_0 = 2$ with the following initial and boundary conditions:

$$u(x,0)=\int_0^2\int_0^1 x^2yu(x,y)\mathrm{d}x\mathrm{d}y,\qquad u(x,2)=\int_0^2\int_0^1 x^2yu(x,y)\mathrm{d}x\mathrm{d}y$$
$$u(0,y)=\int_0^2\int_0^1 xyu(x,y)\mathrm{d}x\mathrm{d}y,\qquad u(1,y)=\int_0^2\int_0^1 xyu(x,y)\mathrm{d}x\mathrm{d}y$$
$$\triangle u(x,0)=-2x(1-x),\qquad \triangle u(x,2)=-2x(1-x)$$
$$\triangle u(0,y)=-2y(2-y),\qquad \triangle u(1,y)=-2y(2-y)$$

The exact solution of the above problem is $u(x,t)=\frac{1}{5}+xy(1-x)(2-y)$. From Table 5.2, it is clear that the proposed method LWM$-II$ is able to achieve better results than the FD [**115**] with lesser number of grid points. From Table 5.2 it can be observed that LWM$-I$ fails to produce the desired results. The error fluctuation shown in Table 5.3 is due to the nature of the solution. Figure 5.3 represents the LWM$-II$ solution for $N=5$.

Remark 5.3.1.

1. In all the examples, the condition $\|u_{n+1}-u_n\|_\infty\le 10^{-08}$ for Method$-I$and $\|u_{n+1}-u_n\|_\infty+\|v_{n+1}-v_n\|_\infty\le 10^{-08}$ for Method$-II$ are used as stopping criteria and initial guess $(u_0,v_0)=(0,0)$ is used for the proposed wavelet based iterative scheme.
2. All the numerical examples are tested with Chebyshev wavelet method also and the order of the error is same as Legendre wavelet method.
3. All the numerical experiments are carried out on a Intel Core i7 CPU 3.4 GHz desktop with 8 GB RAM, Windows 7 professional MATLAB R2010b.

5.4. Conclusion

In this work, numerical methods based on Legendre wavelets are applied for the fourth order elliptic equation with nonlocal boundary conditions. A comparison is made between classical quasilinearization method, iterative scheme and exact solution for the three examples in Section 4 and compared with other recent method [**115**] based on finite difference approach.

Table 5.1. Results of Example (5.3.1)

	FD[**115**]	LWM-I	LWM-II
Grid / (x_i, y_j)	100×100	11×11	11×11
(0.00,0.50)	$1.694e^{-07}$	$2.343e^{-14}$	$1.182e^{-10}$
(0.25,0.50)	$3.795e^{-07}$	$1.503e^{-12}$	$1.182e^{-10}$
(0.50,0.50)	$4.634e^{-07}$	$1.893e^{-12}$	$1.182e^{-10}$
(0.75,0.50)	$3.795e^{-07}$	$1.503e^{-12}$	$1.182e^{-10}$
(1.00,0.50)	$1.694e^{-07}$	$1.821e^{-14}$	$1.182e^{-10}$

Table 5.2. Results of Example(5.3.2)

(x_i, y_j)	FD[**115**]	LWM-I	LWM-II
Grid	100×100	10×10	5×5
(0.00,0.50)	$4.700e^{-09}$	$1.2915e^{-02}$	$1.937e^{-10}$
(0.25,0.50)	$4.700e^{-09}$	$2.5748e^{-01}$	$3.345e^{-10}$
(0.50,0.50)	$4.600e^{-09}$	$3.5456e^{-01}$	$3.745e^{-10}$
(0.75,0.50)	$4.700e^{-09}$	$2.5978e^{-01}$	$3.345e^{-10}$
(1.00,0.50)	$4.700e^{-09}$	$1.2915e^{-02}$	$1.937e^{-10}$

Table 5.3. Numerical results of proposed methods for Example (5.3.2)

Grid	LWM-I ($u_{L\infty}$)	LWM-II ($u_{L\infty}$)
3×3	$1.0735e^{-01}$	$1.2637e^{-02}$
5×5	$5.5771e^{-02}$	$3.9772e^{-10}$
7×7	$3.9295e^{-02}$	$3.9537e^{-10}$
9×9	$1.2075e^{-02}$	$3.9516e^{-10}$
11×11	$4.9695e^{-02}$	$3.9514e^{-10}$
13×13	$1.1104e^{-02}$	$3.9515e^{-10}$

TABLE 5.4. Number of iterations

	LWM-I	LWM-II
Example-5.3.1	4	7
Example-5.3.2	7	9

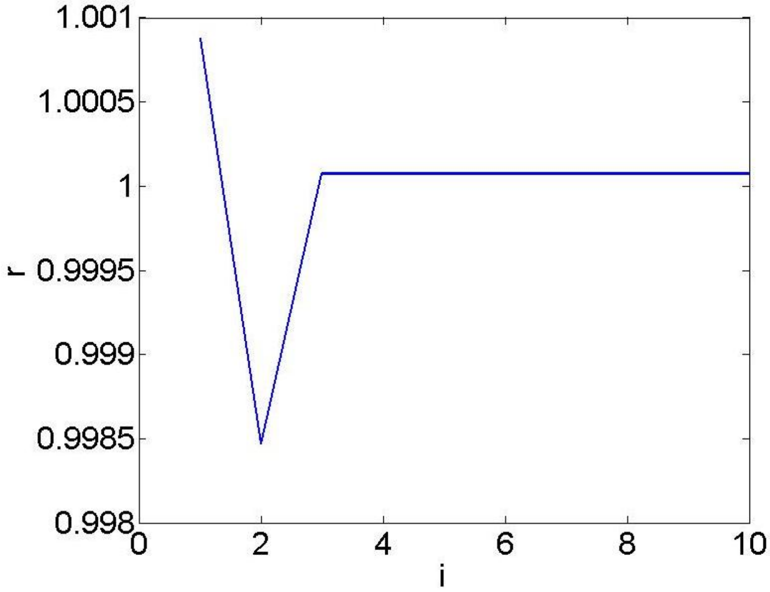

FIGURE 5.1. Plot for Example 5.3.1

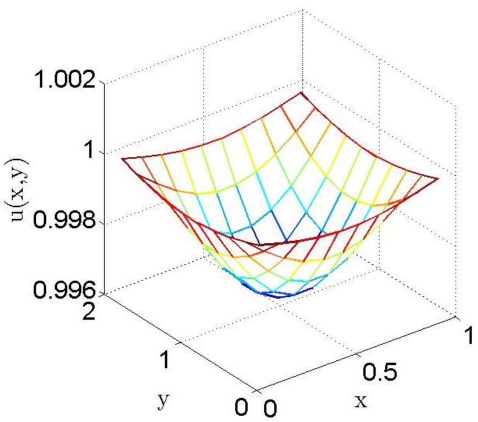

FIGURE 5.2. LWM$-I$ solution for Example 5.3.1

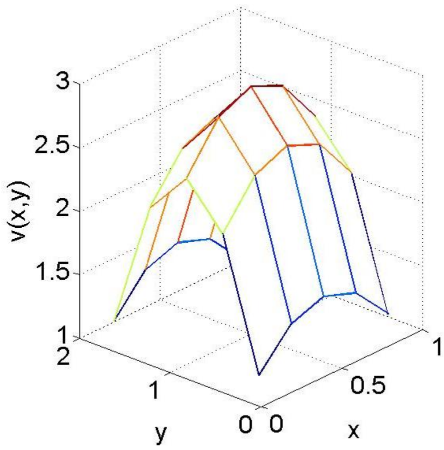

FIGURE 5.3. LWM$-II$ solution for Example 5.3.2

CHAPTER 6

q-DIFFERENCE EQUATIONS

A Legendre wavelet technique based on quasilinearization is proposed in this chapter[1] to solve q-difference equations.

6.1. Introduction

This chapter studies the existence and uniqueness, as well as develops a numerical technique to solve the following q-initial and q-boundary value problems respectively.

$$D_q[x(t)] = f(t, x(t)),\ x(0) = \alpha_0,\ t \in [0, T] \tag{6.1}$$

$$D_q^2[u(t)] = g(t, u(t)),\ u(0) = 0,\ u(1) = 0,\ t \in [0, 1] \tag{6.2}$$

where $f \in C([0, T] \times \mathbb{R}, \mathbb{R})$ and $g \in C([0, 1] \times \mathbb{R}, \mathbb{R})$. Equivalently, we are dealing with the following q-difference equations

$$x(t) - x(qt) = h_1(t, x),\ x(0) = \alpha_0$$

$$u(t) + a_1 u(qt) + a_2 u(q^2 t) = h_2(t, u),\ u(0) = 0,\ u(1) = 0$$

where $h_1(t) = (1-q)tf(t, x(t)),\ h_2(t) = (1-q)^2 t^2 g(t, u(t)),\ a_1 = -\frac{1+q}{q}$ and $a_2 = \frac{1}{q}$. The study on q-analysis started during the nineteenth century. This has been developed into a multidisciplinary subject that plays a vital role in several fields, especially in physical sciences since it provides powerful tools for studying and solving many physical problems [**32, 160**]. Further, it has a wide range of application in many mathematical areas such as basic hypergeometric functions, number theory, orthogonal polynomials and combinatorics, to name a few [**31, 61, 72, 73**].

Recently many authors [**5, 6, 148, 158**] obtained existence and uniqueness theorems for various type of q-initial and q-boundary value problems using different fixed point

[1] This chapter forms the paper by V.A. Vijesh, L.A. Sunny and K.H. Kumar in Journal of Difference Equations and Applications, 22 (4) (2016), 594–606.

theorems. Though various classical tools such as the Leray-Schauder degree theory and the Krasnoselskii's fixed point theorem were utilized to prove the existence and uniqueness theorem for problems in (6.1) and (6.2), theorems using the classical Newton's method for these problems are not much seen in the literature. The advantage of this method is that it not only guarantees the existence and uniqueness of the solution, but also produces a quadratically convergent iterative scheme to approximate the solutions. In this chapter, the idea of the classical Newton's method is used for proving the existence and uniqueness theorems for (6.1) and (6.2). Recently, the numerical solution of q-difference equations on a certain time scale has been studied using differential transformation method [**90**], variational iteration method [**91**] and series solution method [**92**]. Recently many authors developed numerical methods for various types of differential equations using wavelets [**133, 137, 169**]. For example, Razzaghi and Yousefi [**133**] developed Legendre wavelet based numerical method for ordinary differntial equations. This chapter extends the same technique [**133**] to q-initial and q-boundary value problems. More specifically, the Legendre wavelet is coupled with quasilinearization to solve the q-initial and q-boundary value problems, respectively.

This chapter is organized as follows. In Section 6.2, we provide some preliminaries and notations that are used in this chapter. Using the classical Newton's method, we prove the existence and uniqueness theorems for the q-initial and q-boundary value problems in Section 6.3. Section 6.4 introduces Legendre wavelet collocation method in combination with quasilinearization technique to solve both the problems and Section 6.5 discusses the numerical implementations of the proposed scheme. Numerical examples are given in Section 6.6 to illustrate the proposed quasilinearization method based on wavelets. The numerical results thus obtained are compared with the exact solution. We close our discussions with some concluding remarks about the proposed method in Section 6.7.

6.2. Preliminaries

In this section we recall some basic concepts of q-Calculus based on the discussions in [**63**] to make this chapter self contained.

Definition 6.2.1.

For $0 < q < 1$, we define the q-derivative of a real valued function f as

$$D_q f(t) = \frac{f(t) - f(qt)}{(1-q)t}, \;\; D_q f(0) = \lim_{t \to 0} D_q f(t).$$

Definition 6.2.2.

The higher order q-derivatives are defined inductively as

$$D_q^0 f(t) = f(t), \;\; D_q^n f(t) = D_q D_q^{n-1} f(t), \;\; n \in \mathbb{N}.$$

Definition 6.2.3.

The q-integral of a function f defined in the interval $[a, b]$ is given by

$$\int_a^x f(t) d_q t = \sum_{n=0}^{\infty} x(1-q)q^n [x f(xq^n) - a f(q^n a)], \;\; x \in [a, b],$$

and for $a = 0$, we denote

$$I_q f(x) = \int_0^x f(t) \mathrm{d}_q t = \sum_{n=0}^{\infty} x(1-q)q^n f(xq^n),$$

then

$$\int_a^b f(t) \mathrm{d}_q t = \int_0^b f(t) \mathrm{d}_q t - \int_0^a f(t) \mathrm{d}_q t.$$

As the limit $q \to 1$, the above results correspond to their counterparts in standard calculus. Throughout this chapter the following notations are used.

- $C[a, b] = \{f : [a, b] \to \mathbb{R}; f \text{ is continuous}\}$ with $\|x\| = \sup_{t \in [a,b]} |x(t)|$
- $B(x_0, r) = \{x \in C[0, T] : ||x - x_0|| < r\}$
- $\bar{B}(x_0, r) = \{x \in C[0, T] : ||x - x_0|| \leq r\}$
- $f_2(t, x)$ and $g_2(t, x)$ denote the partial derivatives of f and g with respect to the second variable, respectively.

Lemma 6.2.1. *Let $\lambda(t)$ and $f(t)$ be continuous on $[0, T]$. Then the q-difference equation*

$$D_q x(t) = \lambda(t)x(t) + f(t), \quad x(0) = \alpha_0, \quad 0 < q < 1 \tag{6.3}$$

has a unique solution in $C[0,T]$*, provided* $MT < \frac{1}{(1-q)}$*,* M *being* $\sup_{s\in[0,1]} |\lambda(s)|$.

Proof: The q- difference equation (6.3) can be written as

$$x(t) = \alpha_0 + \int_0^t \lambda(s)x(s)\mathrm{d}_q s + \int_0^t f(s)\mathrm{d}_q s$$

Define a map $T : C[0,T] \to C[0,T]$ by

$$\begin{aligned}
Tx(t) &= \alpha_0 + \int_0^t \lambda(s)x(s)\mathrm{d}_q s + \int_0^t f(s)\mathrm{d}_q s \\
|(Tx_1 - Tx_2)t| &= \left|\int_0^t \lambda(s)(x_1(s) - x_2(s))\mathrm{d}_q s\right| \\
&\leq \int_0^t |\lambda(s)||x_1(s) - x_2(s)|\mathrm{d}_q s \\
\|Tx_1 - Tx_2\| &\leq Mt\|x_1 - x_2\|
\end{aligned}$$

Assume that $\|T^k x_1 - T^k x_2\| \leq \dfrac{M^k t^k \|x_1 - x_2\|}{(1+q)(1+q+q^2)\cdots(1+q+q^2+\cdots+q^{k-1})}$, for $k = 1, 2, \cdots, n-1$. Now

$$\begin{aligned}
|(T^n x_1 - T^n x_2)t| &= \left|\int_0^t \lambda(s)(T^{n-1}x_1 - T^{n-1}x_2)(s)\mathrm{d}_q s\right| \\
&\leq \frac{M^n\|x_1 - x_2\|}{(1+q)(1+q+q^2)\cdots(1+q+q^2+\cdots+q^{n-2})} \int_0^t t^{n-1}\mathrm{d}_q s \\
&\leq \frac{M^n\|x_1 - x_2\|}{(1+q)(1+q+q^2)\cdots(1+q+q^2+\cdots+q^{n-2})} \sum_{j=0}^{\infty} t(1-q)q^j t^{n-1} q^{j(n-1)} \\
\|T^n x_1 - T^n x_2\| &\leq \frac{M^n T^n \|x_1 - x_2\|}{(1+q)(1+q+q^2)\cdots(1+q+q^2+\cdots+q^{n-1})}
\end{aligned}$$

Hence T^n is a contraction for sufficiently large n. By Contraction Principle, T has a unique fixed point. Equivalently the q-difference equation (6.3) has a unique solution.

Remark 6.2.1.

The above lemma holds for $q \geq 1$, without having any additional condition on M and T.

Lemma 6.2.2. *The boundary value problem*

$$D_q^2[u(t)] = g(t, u(t)),\ u(0) = 0,\ u(1) = 0,\ t \in [0,1] \tag{6.4}$$

where $g \in C([0,1] \times \mathbb{R}, \mathbb{R})$ *is equivalent to* $u(t) = -\int_0^1 G(t,s)g(s,u(s))\mathrm{d}_q s$ *where*

$$G(t,s) = \begin{cases} t(1-qs), & 0 \leq t \leq s \leq 1 \\ qs(1-t), & 0 \leq s \leq t \leq 1. \end{cases}$$

Lemma 6.2.3. *Let $\lambda(t)$ and $g(t)$ be continuous on $[0,1]$. Then the q-difference equation*

$$D_q^2[u(t)] = \lambda(t)u(t) + g(t), \;\; u(0) = 0, \;\; u(1) = 0 \tag{6.5}$$

has a unique solution in $C[0,1]$ provided $M < 4(1+q)$, M being $\sup_{s\in[0,T]} |\lambda(s)|$.

Proof: The q-difference equation (6.5) can be written as

$$u(t) = -\int_0^1 G(t,s)(\lambda(s)u(s) + g(s))\mathrm{d}_q s$$

Define a map $T : C[0,1] \to C[0,1]$ by

$$\begin{aligned} Tu(t) &= -\int_0^1 G(t,s)(\lambda(s)u(s) + g(s))\mathrm{d}_q s \\ |(Tu_1 - Tu_2)t| &= \left|\int_0^1 G(t,s)\lambda(s)(u_1(s) - u_2(s))\mathrm{d}_q s\right| \\ &\leq \int_0^1 |G(t,s)||\lambda(s)||u_1(s) - u_2(s)|\mathrm{d}_q s \\ \|Tu_1 - Tu_2\| &\leq \frac{1}{4(1+q)} M\|u_1 - u_2\| \end{aligned}$$

Since $M < 4(1+q)$, T is a contraction. By Contraction Principle, T has a unique fixed point. Equivalently the q-difference equation (6.5) has a unique solution.

6.3. Main Results

This section provides results for the existence and uniqueness of the solution of the nonlinear q-difference equations (6.1) and (6.2) and guarantees the convergence of the quasilinearization iterative procedure, which is an important step in the proposed numerical scheme. The proof of the main theorems are inspired by the proof of Kantorovich Theorem on classical Newton's method [**25**].

Theorem 6.3.1. *Let $x_0 \in C[0,T]$ and $B(x_0,r) \subseteq C[0,T]$. Define the constants m^* and m_* by $m^* = \max\{x(t) : t \in [0,T]; x \in B(x_0,r)\}$ and $m_* = \min\{x(t) : t \in [0,T]; x \in B(x_0,r)\}$. Assume further that*

(i) *for some $\delta > 0$, f, $f_2 \in C([0,T] \times [m_* - \delta, m^* + \delta], \mathbb{R})$;*

(ii) *there exist constants M_0, M_1 and M_2 such that $\|\alpha_0 - x_0\| \leq M_0$, $\|f(t,x_0)\| \leq M_1$ for all $t \in [0,T]$ and $|f_2(t,s)| \leq M_2$ for all $(t,s) \in [0,T] \times [m_* - \delta, m^* + \delta]$;*

(iii) *for some* $L \geq 0, |f_2(t, s_1) - f_2(t, s_2)| \leq L|s_1 - s_2|$*;*

(iv) $K = \dfrac{LT\eta}{2(1 - M_2T)^2} < 1$ *and* $r > \dfrac{\eta}{1 - M_2T} + \dfrac{4(1 - M_2T)^2}{LT(2(1 - M_2T)^2) - LT\eta}$*, where* $\eta = M_0 + TM_1$ *and* $M_2T < 1$*.*

Then the initial value problem (6.1) has a unique solution in $\overline{B}(x_0, r)$*. Moreover the quasilinearization scheme*

$$D_q x_{n+1} = f(t, x_n) + f_2(t, x_n)(x_{n+1} - x_n), \quad x_{n+1}(0) = \alpha_0 \tag{6.6}$$

is well defined, $x_n \in B(x_0, r)$ *for all* n *and the* (x_n) *converges quadratically and uniformly to the unique solution* x *of (6.1). For each* $n \in \mathbb{N}$*, the following error estimate holds* $\|x - x_{n+1}\| \leq \frac{LT}{2(1-M_2T)}\|x - x_n\|^2$*.*

Proof: Using Lemma 6.2.1, one can conclude that the linear q-difference equation

$$D_q x_1 = f(t, x_0) + f_2(t, x_0)(x_1 - x_0), \quad x_1(0) = \alpha_0$$

has a unique solution. Consequently x_1 satisfies

$$x_1(t) = \alpha_0 + \int_0^t f(s, x_0(s))\mathrm{d}_q s + \int_0^t f_2(s, x_0(s))(x_1 - x_0)\mathrm{d}_q s.$$

Note that

$$\begin{aligned}
x_1(t) - x_0(t) &= \alpha_0 - x_0 + \int_0^t f(s, x_0(s))\mathrm{d}_q s + \int_0^t f_2(s, x_0(s))(x_1 - x_0)\mathrm{d}_q s \\
|x_1(t) - x_0(t)| &\leq |\alpha_0 - x_0| + \int_0^t |f(s, x_0(s))|\mathrm{d}_q s + \int_0^t |f_2(s, x_0(s))||x_1 - x_0|\mathrm{d}_q s \\
&\leq M_0 + TM_1 + M_2T\|x_1 - x_0\| \\
\|x_1 - x_0\| &\leq \frac{\eta}{1 - M_2T} < r.
\end{aligned}$$

Hence $\|x_1 - x_0\| < r$. Consequently, $x_1 \in B(x_0, r)$. Assume that x_k exist for all $k = 1, 2, \cdots, n-1$, $x_k \in B(x_0, r)$ and

$$\|x_k - x_{k-1}\| \leq \frac{LT}{2(1 - M_2T)}\left(\frac{\eta}{1 - M_2T}\right)^2 K^{2^{k-1}-2}. \tag{6.7}$$

Using the hypothesis (iv), x_n exists and

$$\begin{aligned}
x_n(t) - x_{n-1}(t) &= \int_0^t [f(s, x_{n-1}(s)) - f(s, x_{n-2}(s))]\mathrm{d}_q s \\
&\quad + \int_0^t [f_2(s, x_{n-1}(s))(x_n - x_{n-1}) - f_2(s, x_{n-2}(s))(x_{n-1} - x_{n-2})]\mathrm{d}_q s \\
|x_n(t) - x_{n-1}(t)| &\leq \left| \int_0^t \int_0^1 f_2(s, \theta x_{n-1}(s) + (1-\theta)x_{n-2}(s))[x_{n-1} - x_{n-2}]\mathrm{d}\theta \mathrm{d}_q s \right| \\
&\quad + \left| \int_0^t [f_2(s, x_{n-1}(s))(x_n - x_{n-1}) - f_2(s, x_{n-2}(s))(x_{n-1} - x_{n-2})]\mathrm{d}_q s \right| \\
&\leq \int_0^t \int_0^1 L\theta |x_{n-1} - x_{n-2}|^2 \mathrm{d}\theta \mathrm{d}_q s + \int_0^t |f_2(s, x_{n-1}(s))|\,|x_n - x_{n-1}|\mathrm{d}_q s \\
&\leq \int_0^t \frac{L}{2}|x_{n-1} - x_{n-2}|^2 \mathrm{d}_q s + \int_0^t |f_2(s, x_{n-1}(s))|\,|x_n - x_{n-1}|\mathrm{d}_q s \\
|x_n(t) - x_{n-1}(t)| &\leq \frac{LT}{2}\|x_{n-1} - x_{n-2}\|^2 + M_2 T \|x_n - x_{n-1}\| \\
\|x_n - x_{n-1}\| &\leq \frac{LT}{2(1 - M_2 T)}\|x_{n-1} - x_{n-2}\|^2 \\
&\leq \frac{LT}{2(1 - M_2 T)} \left(\frac{LT}{2(1 - M_2 T)} \right)^2 \left(\frac{\eta}{1 - M_2 T} \right)^4 K^{2(2^{n-2} - 2)}
\end{aligned}$$

$$\|x_n - x_{n-1}\| \leq \frac{LT}{2(1 - M_2 T)} \left(\frac{\eta}{1 - M_2 T} \right)^2 K^{2^{n-1} - 2}. \tag{6.8}$$

Note that,

$$\begin{aligned}
\|x_n - x_0\| &\leq \frac{\eta}{1 - M_2 T} + \frac{LT}{2(1 - M_2 T)} \left(\frac{\eta}{1 - M_2 T} \right)^2 \sum_{j=1}^{n-1} \left[\frac{LT\eta}{2(1 - M_2 T)^2} \right]^{2^j - 2} \\
&= \frac{\eta}{1 - M_2 T} + \frac{LT}{2(1 - M_2 T)} \left(\frac{\eta}{1 - M_2 T} \right)^2 \left[\frac{LT\eta}{2(1 - M_2 T)^2} \right]^{-2} \sum_{j=1}^{n-1} \left[\frac{LT\eta}{2(1 - M_2 T)^2} \right]^{2^j} \\
&\leq \frac{\eta}{1 - M_2 T} + \frac{2}{LT} \sum_{j=0}^{\infty} \left[\frac{LT\eta}{2(1 - M_2 T)^2} \right]^j \\
\|x_n - x_0\| &\leq \frac{\eta}{1 - M_2 T} + \frac{4(1 - M_2 T)^2}{LT(2(1 - M_2 T)^2) - LT\eta}.
\end{aligned}$$

Thus $x_n \in B(x_0, r)$ for all n. Now consider

$$\begin{aligned}
\|x_{k+m} - x_k\| &\leq \|x_k - x_{k+1}\| + \|x_{k+1} - x_{k+2}\| + \cdots + \|x_{k+m-1} - x_{k+m}\| \\
&\leq \frac{LT}{2(1-M_2T)}\left(\frac{\eta}{1-M_2T}\right)^2 \left[K^{2^k-2} + K^{2^{k+1}-2} + \cdots + K^{2^{k+m-1}-2}\right] \\
&\leq \frac{LT}{2(1-M_2T)}\left(\frac{\eta}{1-M_2T}\right)^2 \sum_{j=0}^{\infty} K^{2^k j} \\
\|x_{k+m} - x_k\| &\leq \frac{LT}{2(1-M_2T)}\left(\frac{\eta}{1-M_2T}\right)^2 \frac{K^{2^k}}{1-K^{2^k}}
\end{aligned}$$

Since $K < 1$, $\|x_{k+m} - x_k\| \to 0$ as $k \to \infty$. Thus the (x_n) is a Cauchy sequence and converges to $x \in B(x_0, r)$. Using uniform convergence we can conclude that x is the solution of (6.1). Now to obtain the rate of convergence consider,

$$\begin{aligned}
x(t) - x_n(t) &= \textstyle\int_0^t f(s, x(s))\mathrm{d}_q s - \int_0^t f(s, x_{n-1}(s))\mathrm{d}_q s - \int_0^t f_2(s, x_{n-1}(s))(x_n - x_{n-1})\mathrm{d}_q s \\
&\leq \textstyle\int_0^t \int_0^1 f_2(s, \theta x(s) + (1-\theta)x_{n-1}(s))(x(s) - x_{n-1}(s))\mathrm{d}\theta \mathrm{d}_q s \\
&\quad - \textstyle\int_0^t f_2(s, x_{n-1}(s))(x_n - x_{n-1})\mathrm{d}_q s \\
&\leq \textstyle\int_0^t \int_0^1 L\theta |x(s) - x_{n-1}(s)|^2 \mathrm{d}\theta \mathrm{d}_q s + \left|\int_0^t f_2(s, x_{n-1}(s))(x(s) - x_n(s))\mathrm{d}_q s\right| \\
&\leq \textstyle\int_0^t \frac{L}{2}|x(s) - x_{n-1}(s)|^2 \mathrm{d}_q s + \left|\int_0^t f_2(s, x_{n-1}(s))(x(s) - x_n(s))\mathrm{d}_q s\right|
\end{aligned}$$

$$|x(t) - x_n(t)| \leq \tfrac{LT}{2}\|x - x_{n-1}\|^2 + M_2T\|x - x_n\|$$

$$\|x - x_n\| \leq \tfrac{LT}{2(1-M_2T)}\|x - x_{n-1}\|^2$$

Hence the convergence is quadratic.

Theorem 6.3.2. *Let $u_0 \in C[0,1]$ and $B(u_0, r) \subseteq C[0,1]$. Define the constants m^* and m_* by $m^* = \max\{u(t) : t \in [0,1]; u \in B(u_0, r)\}$ and $m_* = \min\{u(t) : t \in [0,1]; u \in B(u_0, r)\}$. Assume further that*

(i) *for some $\delta > 0$, $g,\ g_2 \in C([0,1] \times [m_* - \delta, m^* + \delta], \mathbb{R})$;*

(ii) *there exist constants $M_0,\ M_1$ and M_2 such that $\|u_0\| = M_0,\ \|g(t, u_0(t))\| \leq M_1$ for all $t \in [0,1]$ and $|g_2(t,s)| \leq M_2$ for all $(t,s) \in [0,1] \times [m_* - \delta, m^* + \delta]$;*

(iii) *for some $L \geq 0, |g_2(t, s_1) - g_2(t, s_2)| \leq L|s_1 - s_2|$;*

(iv) $K = \dfrac{L\eta}{8K_1^2(1+q)} < 1$ *and* $r > \dfrac{\eta}{K_1} + \dfrac{8LK_1(1+q)\eta^2}{64K_1^4(1+q)^2 - L^2\eta^2}$, *where* $\eta = M_0 + \frac{M_1}{4(1+q)}$, $K_1 = 1 - \frac{M_2}{4(1+q)}$ *and* $M_2 < 4(1+q)$.

Then the boundary value problem (6.2) *has a unique solution in* $\overline{B}(u_0, r)$*. Moreover the quasilinearization scheme*

$$D_q^2 u_{n+1} = g(t, u_n) + g_2(t, u_n)(u_{n+1} - u_n), \quad u_{n+1}(0) = u_{n+1}(1) = 0$$

is well defined, $u_n \in B(u_0, r)$ *for all* n *and the* (u_n) *converges quadratically and uniformly to the unique solution of* (6.2)*. For each* $n \in \mathbb{N}$*, the following error estimate holds* $\|u - u_n\| \leq \left(\frac{L}{8(1+q)-2M_2}\right) \|u - u_{n-1}\|^2$.

Proof: Using Lemma 6.2.3, one can conclude that the linear q-differnce equation

$$D_q^2 u_1 = g(t, u_0) + g_2(t, u_0)(u_1 - u_0), \; u_1(0) = 0, u_1(1) = 1$$

has a unique solution u_1. Consequently u_1 satisfies

$$u_1 = -\int_0^1 G(t,s)g(s, u_0(s))\mathrm{d}_q s - \int_0^1 G(t,s)g_2(s, u_0(s))(u_1 - u_0)\mathrm{d}_q s$$

Note that

$$\begin{aligned}
u_1(t) - u_0(t) &= -u_0(t) + \int_0^1 G(t,s)g(s, u_0(s))\mathrm{d}_q s + \int_0^1 G(t,s)g_2(s, u_0(s))(u_1 - u_0)\mathrm{d}_q s \\
|u_1(t) - u_0(t)| &\leq M_0 + \frac{M_1}{4(1+q)} + \frac{M_2}{4(1+q)}\|u_1 - u_0\| \\
\|u_1 - u_0\| &\leq \frac{1}{1 - \frac{M_2}{4(1+q)}}\left[M_0 + \frac{M_1}{4(1+q)}\right] = \frac{\eta}{K_1}
\end{aligned}$$

Hence $\|u_1 - u_0\| < r$ and $u_1 \in B(u_0, r)$. Assume that u_k exist for all $k = 1, 2, \cdots, n-1$ and $u_k \in B(u_0, r)$. Also

$$\|u_k - u_{k-1}\| \leq \frac{L}{8K_1(1+q)}\left(\frac{\eta}{K_1}\right)^2 K^{2^{k-1}-2} \tag{6.9}$$

Using the hypothesis (iv), u_n exists and proceeding like the previous proof, one can conclude that

$$|u_n(t) - u_{n-1}(t)| \;\leq\; \frac{L}{8(1+q)}\|u_{n-1} - u_{n-2}\|^2 + \frac{M_2}{4(1+q)}\|u_n - u_{n-1}\|$$

$$\begin{aligned}
\|u_n - u_{n-1}\| &\leq \frac{L}{8K_1(1+q)}\|u_{n-1} - u_{n-2}\|^2 \\
&\leq \frac{L}{8K_1(1+q)}\left(\frac{L}{8K_1(1+q)}\right)^2\left(\frac{\eta}{K_1}\right)^4\left[\frac{L\eta}{8K_1^2(1+q)}\right]^{2(2^{n-2}-2)} \\
(6.10)\ \|u_n - u_{n-1}\| &\leq \frac{L}{8K_1(1+q)}\left(\frac{\eta}{K_1}\right)^2 K^{2^{n-1}-2}
\end{aligned}$$

Hence

$$\begin{aligned}
\|u_n - u_0\| &\leq \frac{\eta}{K_1} + \frac{L}{8K_1(1+q)}\left(\frac{\eta}{K_1}\right)^2\sum_{j=1}^{n-1}\left[\frac{L\eta}{8K_1^2(1+q)}\right]^{2^j-2} \\
&= \frac{\eta}{K_1} + \frac{L}{8K_1(1+q)}\left(\frac{\eta}{K_1}\right)^2\left[\frac{L\eta}{8K_1^2(1+q)}\right]^{-2}\sum_{j=1}^{n-1}\left[\frac{L\eta}{8K_1^2(1+q)}\right]^{2^j} \\
\|u_n - u_0\| &\leq \frac{\eta}{K_1} + \frac{8LK_1(1+q)\eta^2}{64K_1^4(1+q)^2 - L^2\eta^2}
\end{aligned}$$

Thus $u_n \in B(u_o, r)$ for all n. Similar to the previous proof using (6.9) for any $k \in \mathbb{N}$,

$$\begin{aligned}
\|u_{k+m} - u_k\| &\leq \|u_k - u_{k+1}\| + \|u_{k+1} - u_{k+2}\| + \cdots + \|u_{k+m-1} - u_{k+m}\| \\
\|u_{k+m} - u_k\| &\leq \frac{L}{8K_1(1+q)}\left(\frac{\eta}{K_1}\right)^2\frac{K^{2^k}}{1-K^{2^k}}
\end{aligned}$$

Since $K < 1$, $\|u_{k+m} - u_k\| \to 0$ as $k \to \infty$. Thus the (u_n) is a Cauchy sequence and converges to the unique solution $u \in B(u_0, r)$. Using uniform convergence we can conclude that u is the solution of (6.2). Note that,

$$\begin{aligned}
|u_n(t) - u(t)| &\leq \left|\int_0^1\int_0^1 G(t,s)g_2(s,\theta u(s) + (1-\theta)u_{n-1}(s))(u(s) - u_{n-1}(s))\mathrm{d}\theta\mathrm{d}_qs\right| \\
&\quad + \left|\int_0^1 G(t,s)g_2(s,u_{n-1}(s))(u_n - u_{n-1})\mathrm{d}_qs\right| \\
&\leq \int_0^1\int_0^1 L\theta\ G(t,s)|u(s) - u_{n-1}(s)|^2\mathrm{d}\theta\mathrm{d}_qs \\
&\quad + \left|\int_0^1 G(t,s)g_2(s,u_{n-1}(s))(u(s) - u_n(s))\mathrm{d}_qs\right| \\
|u_n(t) - u(t)| &\leq \int_0^1 \frac{L}{2}G(t,s)|u(s) - u_{n-1}(s)|^2\mathrm{d}_qs \\
&\quad + \left|\int_0^1 G(t,s)g_2(s,u_{n-1}(s))(u(s) - u_n(s))\mathrm{d}_qs\right|
\end{aligned}$$

$$\begin{aligned}
|u_n(t)-u(t)| &\le \frac{L}{8(1+q)}|u(t)-u_{n-1}(t)|^2+\frac{M_2}{4(1+q)}\|u-u_n\| \\
\|u-u_n\| &\le \left(\frac{L}{8(1+q)-2M_2}\right)\|u-u_{n-1}\|^2
\end{aligned}$$

Hence the convergence is quadratic.

6.4. Wavelet based collocation methods

In this section, the work of Razzaghi and Yousefi [**133**] on Legendre wavelet method for ordinary differential equation has been suitably extended for solving the q-difference equations numerically. From Theorem 6.3.1 and 6.3.2, q-derivatives of the solution of the linear equations in the iterative methods can be expressed by Legendre wavelets series. Consequently

$$D_q x(t)=\sum_{i=1}^{N} b_i\psi_i(t)=B\Psi(t) \tag{6.11}$$

$$D_q^2 u(t)=\sum_{i=1}^{N} d_i\psi_i(t)=D\Psi(t) \tag{6.12}$$

where $B=[b_i]$, $D=[d_i]$ and $\Psi(t)=[\psi(t)]^T$. Throughout this study, the points in the set $\{t_i : t_i=\frac{i-0.5}{N}, 1\le i\le N\}$ are chosen for collocation to obtain the matrix representation. From (6.11), the solution of the linear equations in the iterative methods can be represented as follows.

$$x(t) = \sum_{i=1}^{N} b_i p_{i,1}(t)+x(0) \tag{6.13}$$

$$u(t) = \sum_{i=1}^{N} d_i p_{i,2}(t)-t\sum_{i=1}^{N} d_i C_{i,1}+[u(1)-u(0)]t+u(0) \tag{6.14}$$

From (6.13) or (6.14), at each collocation point, we obtain N^2 set of equations. Similarly another N^2 set of equations are derived from the given q-initial or q-boundary value problems using the expressions of $x(t)$ or $u(t)$. Solving these two sets of equations, we obtain the unknown Legendre coefficients b_i's or d_i's respectively. The solution can be easily obtained by substituting these coefficients in (6.13) or (6.14).

6.5. Numerical Implementation

This section provides the numerical implementation procedure for the iterative method to solve the q-initial value problem. The procedure is similar for the q-boundary value problem as well. We choose $M = 3$ and $k = 2$. i.e., $N = 6$. Thus we have from [**133**],

$$\left.\begin{cases} \psi_1(t) = \sqrt{2} \\ \psi_2(t) = \sqrt{6}(4t-1) \\ \psi_3(t) = \sqrt{10}(\frac{3}{2}(4t-1)^2 - \frac{1}{2}) \end{cases}\right\}, 0 \le t < \frac{1}{2} \tag{6.15}$$

$$\left.\begin{cases} \psi_4(t) = \sqrt{2} \\ \psi_5(t) = \sqrt{6}(4t-3) \\ \psi_6(t) = \sqrt{10}(\frac{3}{2}(4t-3)^2 - \frac{1}{2}) \end{cases}\right\}, \frac{1}{2} \le t < 1 \tag{6.16}$$

On q-integrating, we obtain the following functions, respectively, for ψ_1,ψ_2,ψ_3,ψ_4,ψ_5,ψ_6,

$$I_q\psi_1(t) = \begin{cases} \sqrt{2}t & , 0 \le t < \frac{1}{2} \\ \frac{1}{\sqrt{2}} & , \frac{1}{2} \le t < 1. \end{cases}$$

$$I_q\psi_2(t) = \begin{cases} \sqrt{6}t\left(\frac{4t}{1+q} - 1\right) & , 0 \le t < \frac{1}{2} \\ \sqrt{6}\left(\frac{1}{1+q} - \frac{1}{2}\right) & , \frac{1}{2} \le t < 1. \end{cases}$$

$$I_q\psi_3(t) = \begin{cases} \sqrt{10}t\left(\frac{24t^3}{1+q+q^2} - \frac{12t^2}{1+q} + t\right) & , 0 \le t < \frac{1}{2} \\ \sqrt{10}\left(\frac{3}{1+q+q^2} - \frac{3}{1+q} + \frac{1}{2}\right) & , \frac{1}{2} \le t < 1. \end{cases}$$

$$I_q\psi_4(t) = \begin{cases} 0 & , 0 \le t < \frac{1}{2} \\ \sqrt{2}\left(t - \frac{1}{2}\right) & , \frac{1}{2} \le t < 1. \end{cases}$$

$$I_q\psi_5(t) = \begin{cases} 0 & , 0 \le t < \frac{1}{2} \\ \sqrt{6}\left(\frac{4t^2}{1+q} - 3t + \frac{1+3q}{2(1+q)}\right) & , \frac{1}{2} \le t < 1. \end{cases}$$

$$I_q\psi_6(t) = \begin{cases} 0 & , 0 \le t < \frac{1}{2} \\ \sqrt{10}\left(\frac{24t^3}{1+q+q^2} - \frac{36t^2}{1+q} + 13t - \frac{3}{1+q+q^2} + \frac{9}{1+q} - \frac{13}{2}\right) & , \frac{1}{2} \le t < 1. \end{cases}$$

After using collocation points the equation (6.6) can be written as

$$\Phi^T B_{n+1} = (P_1^T C_{n+1}) \circ G + H \tag{6.17}$$

where $\Phi = [\Psi(t_j)], P_1 = [p_{i,1}(t_j)], G = f_2(t_j, x_n(t_j)), H = f(t_j, x_n(t_j)) - (f_2(t_j, x_n(t_j))) \circ (x_n(t_j) - x(0))$, where $\circ$ denotes the Hadamard product and T denotes the transpose of the matrix. We used the well known function *fsolve* in matlab to solve above equation with initial guess. The stopping condition is $||x_{n+1} - x_n|| < 10^{-04}$. By substituting the c_{n+1} in (6.13), we obtain the approximate numerical solution of $x(t)$. The same procedure can be followed for q-boundary value problem also.

6.6. Examples

In this section the proposed quasilinearization method is demonstrated by solving Riccati type q-difference equation numerically. Throughout this section the following abbreviations have been used.

1. LWM- Legendre wavelet quasilinearization method.
2. N_1 denotes the number of Legendre wavelets.

Example 6.6.1.

Consider the following Ricatti type q- initial value problem

$$x(t) = x(qt) + (1-q)t\left(x^2 + \frac{2t^2}{15} - \frac{t^4}{9} - \frac{1}{25} - \frac{t}{2}\right),\ x(0) = \frac{1}{5}. \tag{6.18}$$

When $q = 0.5, M_0 = 0, M_1 = \frac{2}{15}, M_2 = \frac{2}{5}$, all the conditions of the Theorem 6.3.1 are satisfied and thus 6.18 has a unique solution $x(t) = \frac{1}{5} - \frac{t^2}{3}$ in $\overline{B}(x_0, r)$ where $x_0 = \frac{1}{5}$ and $r > 1.5$. Table 6.1 provides the comparison between exact solution and the numerical solution using LWM. The solutions obtained for various values of q has also been provided in the table. Figure 6.2 shows the plot of the exact solution, LWM solution for various values of q and $x(t)$ at different values of q.

Example 6.6.2.

Consider the following Ricatti type q-boundary value problem

$$\begin{aligned} qu(t) = (1+q)u(qt) - u(q^2t) &+ q(1-q)^2t^2\left(u^2 - 4t^4 + 8t^3 - 4t^2 - 3\right) \\ u(0) &= 0,\ u(1) = 0. \end{aligned} \tag{6.19}$$

When $M_0 = 0, M_1 = 2q+2, M_2 = 1$, all the conditions of the Theorem 6.3.2 are satisfied and thus (6.19) has a unique solution in $\overline{B}(u_0, r)$ where $u_0 = 0$ and $r > \frac{2(1+q)}{3+4q} + \frac{4(3+4q)(1+q)^2}{(3+4q)^4 - 4(1+q)^2}$. When $q = 0.5$, the exact solution of (6.19) is $u(t) = 2t - 2t^2$ where $M_0 = 0, M_1 = 3, M_2 = 1$ and $r > 0.67$. Table 6.2 provides the comparison between exact solution and the numerical solution using LWM. The solutions obtained for various values of q has also been provided in the table. Figure 6.3 shows the plot of the exact solution, LWM solution for various values of q and $x(t)$ at different values of q.

6.7. Conclusion

In this chapter, by utilizing the classical Newton's method, existence and uniqueness theorems for q-difference equations with initial and boundary conditions have been studied. Consequently, a set of sufficient conditions to ensure the quadratic convergence of quasilinearization scheme to approximate the solutions of q-difference equations have been proved. Another important contribution of this work is the development of a wavelet based numerical method to solve the q-difference equations numerically.

TABLE 6.1. Solution of Example (6.6.1) for various values of q.

	Exact($q = 0.5$)	LWM($N = 6$)	LWM($N = 6$)	LWM($N = 6$)	LWM($N = 6$)
t	$x(t)$	$x(t)$	$q = 0.3$	$q = 0.7$	$q = 0.9$
0	0.2000	0.2000	0.2000	0.2000	0.2000
0.1	0.1967	0.1967	0.1961	0.1971	0.1974
0.2	0.1867	0.1867	0.1845	0.1883	0.1896
0.3	0.1700	0.1700	0.1650	0.1737	0.1766
0.4	0.1467	0.1467	0.1377	0.1533	0.1585
0.5	0.1167	0.1167	0.1026	0.1272	0.1353
0.6	0.0800	0.0800	0.0601	0.0951	0.1068
0.7	0.0367	0.0367	0.0108	0.0570	0.0730
0.8	-0.0133	-0.0133	-0.0453	0.0126	0.0337
0.9	-0.0700	-0.0700	-0.1076	-0.0382	-0.0115

TABLE 6.2. Solution of Example (6.6.2) for various values of q.

	Exact($q = 0.5$)	LWM($N = 6$)	LWM($N = 6$)	LWM($N = 6$)	LWM($N = 6$)
t	$u(t)$	$u(t)$	$q = 0.3$	$q = 0.7$	$q = 0.9$
0	0.0	0.0	0.0	0.0	0.0
0.1	0.1800	0.1800	0.2072	0.1603	0.1446
0.2	0.3200	0.3200	0.3688	0.2851	0.2574
0.3	0.4200	0.4200	0.4856	0.3743	0.3382
0.4	0.4800	0.4800	0.5583	0.4276	0.3867
0.5	0.5000	0.5000	0.5877	0.4449	0.4027
0.6	0.4800	0.4800	0.5696	0.4264	0.3862
0.7	0.4200	0.4200	0.5040	0.3724	0.3374
0.8	0.3200	0.3200	0.3889	0.2832	0.2566
0.9	0.1800	0.1800	0.2218	0.1589	0.1440

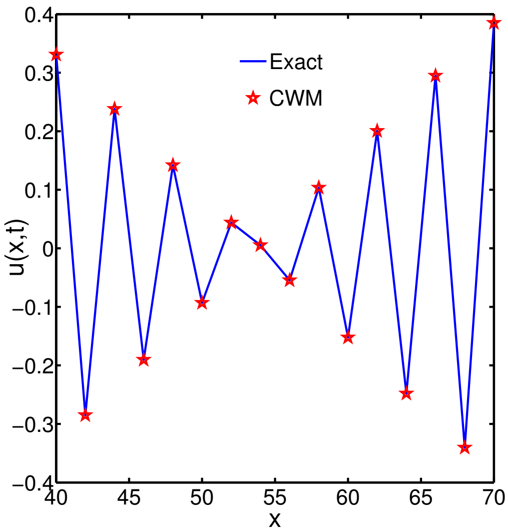

(A)

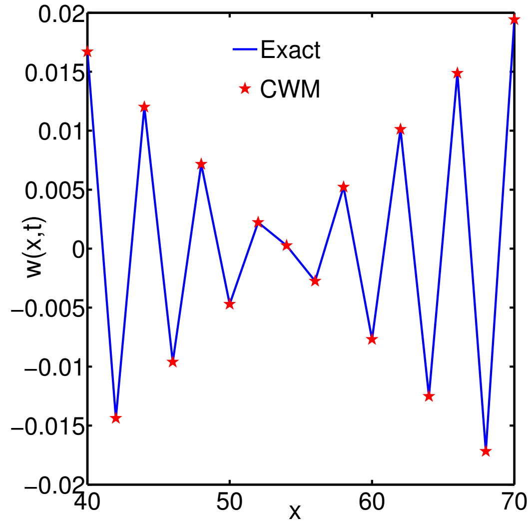

(B)

FIGURE 6.1. Numerical and exact solutions of $u(x,t)$ and $w(x,t)$ at $t = 0.3$ for Example 4.2.2

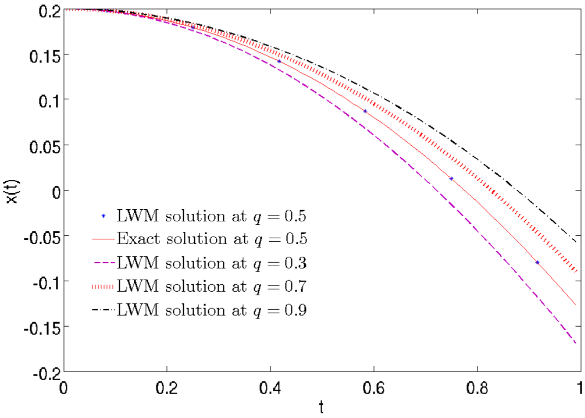

FIGURE 6.2. Exact solution at $q = 0.5$ and LWM solution at $q = 0.3, 0.5, 0.7, 0.9$ for Example (6.6.1).

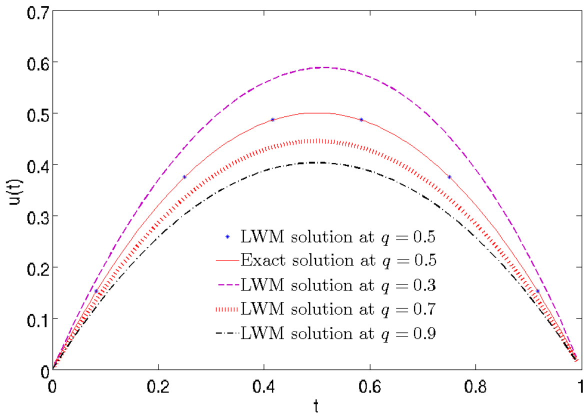

FIGURE 6.3. Exact solution at $q = 0.5$ and LWM solution at $q = 0.3, 0.5, 0.7, 0.9$ for Example (6.6.2).

BIBLIOGRAPHY

[1] Adibi H., Assari P. (2011), *On the numerical solution of weakly singular Fredholm integral equations of the second kind using Legendre wavelets*, J. Vib. Control, 17 (5), 689-698.

[2] Adibi H., Assari P. (2010), *Chebyshev wavelet method for numerical solution of fredholm integral equations of the first kind*, Math. Probl. Eng., Article ID 138408, 17 pages.

[3] Adibi H., Assari P. (2009), *Using CAS wavelets for numerical solution of Volterra integral equations of the second kind*, Dyn. Contin. Discrete Impuls. Syst. Ser. A Math. Anal., 16(5), 673-685 .

[4] Abualrub T., Sadek I. (2014), *Legendre wavelet operational matrix of derivative for optimal control in a convective–diffusive fluid problem*, J. Franklin Inst., 351, 682–693.

[5] Ahmad B. (2011), *Boundary value problems for nonlinear third order q-difference equations*, Elec. J Diff. Eqns., 94, 1–7.

[6] Ahmad B., Ntouyas S.K. (2011), *Boundary value problems for q-difference inclusions*, Abst. Appl. Anal., Article ID 292860, 15 pages.

[7] Avaji M., Dehcheshmeh S.S., Hafshejani J.S., Ghahfarokhi D.F. (2013), *On the solution of linear and nonlinear fractional integro-differential equations in nano-transistors* , J. Comput. Theor. Nanosci., 10, 510–513.

[8] Aziz I., Islam S. (2015), *An efficient modified Haar wavelet collocation method for numerical solution of two-dimensional elliptic PDEs*, Differ. Equ. Dyn. Syst., 25 (2), 347–360.

[9] Aziz I., Islam S., Nisar M. (2016), *An efficient numerical algorithm based on Haar wavelet for solving a class of linear and nonlinear nonlocal boundary-value problems*, Calcolo, 53, 621–633.

[10] Aziz I., Islam S., Sarler B. (2013), *Wavelets collocation methods for the numerical solution of elliptic BV problems*, Appl. Math. Model., 37, 676–694.

[11] Babolian E., Fattahzadeh F. (2007), *Numerical computation method in solving integral equations by using Chebyshev wavelet operational matrix of integration*, Appl. Math. Comput., 188, 1016–1022.

[12] Babolian E., Fattahzadeh F. (2007), *Numerical solution of differential equations by using Chebyshev wavelet operational matrix of integration*, Appl. Math. Comput., 188, 417–426.

[13] Bader B.W., Kolda T.G. (2006), *Algorithm 862: MATLAB tensor classes for fast algorithm prototyping*, ACM Transactions on Mathematical Software, 32, 635–653.

[14] Bai A., Wang H. (2002), *On positive solutions of some nonlinear fourth-order beam equations*, J. Math. Anal. Appl., 270, 357–368.

[15] Balaji S. (2016), *A new Bernoulli wavelet operational matrix of derivative method for the solution of nonlinear singular Lane-Emden type equations arising in Astrophysics.*, J. Comput. Nonlinear Dynam., 11(5), 051013.

[16] Balaji S. (2014), *A new approach for solving Duffing equations involving both integral and non-integral forcing terms*, Ain Shams Eng. J., 5, 985–990.

[17] Banifatemi E., Razzaghi M., Yousefi S. (2007), *Two-dimensional Legendre wavelets method for the mixed Volterra-Fredholm integral equations*, J. Vib. Control, 13(11) (2007), 1667–1675.

[18] Batiha B., Noorani M.S.M., Hashim I. (2007), *Approximate analytical solution of the coupled sine-Gordon equation using the variational iteration method*, Phys. Scr., 76, 445–448.

[19] Bhrawy A.H, Assas L.M., Alghamdi M.A. (2013), *An efficient spectral collocation algorithm for nonlinear Phi-four equations,* Bound. Value Probl., article 87, 16 pages.

[20] Boglaev I. (2016), *Numerical solving nonlinear integro-parabolic equations by the monotone weighted average method*, Appl. Math. Comp., 274, 152–162.

[21] Boglaev I. (2015), *Monotone iterates for solving nonlinear integro-parabolic equations of Volterra type*, J. Appl. Comput. Math., 290, 224–238.

[22] Buică A., Precup R. (2002), *Abstract generalized quasilinearization method for coincidences*, Nonlinear Stud., 9, 371–386.

[23] Celik I. (2012), *Haar wavelet method for solving generalized Burgers–Huxley equation*, Arab J. Math. Sci., 18, 25–37.

[24] Chen C.F., Hsiao C.H. (1997) , *Haar wavelet method for solving lumped and distributed-parameter systems.*, IEEE Proc. Part D, 144 (1), 87-94.

[25] Cheney W., (2001), *Analysis for applied mathematics*, Springer, New York.

[26] Chen Y., McKenna P.J. (1997), *Traveling waves in a nonlinear suspension beam: theoretical results and numerical observations*, J. Differential Equations, 135, 325–355.

[27] Danfu H., Xufeng S. (2007), *Numerical solution of integro-differential equations by using CAS wavelet operational matrix of integration*, Appl. Math. Comput., 194 , 460–466.

[28] Dehghan M., Ghesmati A. (2010), *Application of the dual reciprocity boundary integral equation technique to solve the nonlinear Klein–Gordon equation,* Comp. Phys. Comm., 181, 1410-1418.

[29] Dehghan M., Shahini M. (2015), *Rational pseudospectral approximation to the solution of a nonlinear integro-differential equation arising in modeling of the population growth*, Appl. Math. Model., 39 (18), 5521–5530.

[30] Dehghan M., Shokri A. (2009), *Numerical solution of nonlinear Klein-Gordon equation using radial basis functions,* J. Comp. App. Math., 230, 400-410.

[31] Ernst T. (1999), *The history of q calculus and a new method*, Department of Mathematics, Uppsala University, U.U.D.M. Report, 25, 1101–3591.

[32] Finkelstein R., Marcus E. (1995), *Transformation theory of the q-oscillator*, J. Math. Phys., 36, 2652–2672.

[33] Fischer B., Prestin J. (1997), *Wavelets based on orthogonal polynomials*, Math. Comp., 66 , 1593–1618.

[34] Ghasemi M., Kajani M T. (2011), *Numerical solution of time-varying delay systems by Chebyshev wavelets*, Appl. Math. Model., 35, 5235–5244.

[35] Goghary H.S., Goghary M.S. (2006), *Two computational methods for solving linear Fredholm fuzzy integral equation of the second kind*, Appl. Math.Comput., 182, 791–796.

[36] Guf J.S., Jiang W.S. (1996), *The Haar wavelets operational matrix of integration*,Internat. J. Systems Sci., 27 (7), 623–628 .

[37] Gupta A.K., Ray S.S. (2016), *A novel attempt for finding comparatively accurate solution for sine-Gordon equation comprising Riesz space fractional derivative*, Math. Methods. Appl. Science, 39, Issue 11, 2871–2882 .

[38] Gupta A.K., Ray S.S . (2015), *Numerical treatment for the solution of fractional fifth-order Sawada–Kotera equation using second kind Chebyshev wavelet method*, Appl. Math. Model., 39, 5121–5130.

[39] Gupta A.K., Ray S.S . (2015), *Numerical treatment for investigation of squeezing unsteady nanofluid flow between two parallel plates*, Powder Technology, 279, 282–289.

[40] Gupta C.P. (1988) , *Existence and uniqueness theorem for the bending of an elastic beam equation*, Appl. Anal., 26, 289–304.

[41] Hariharan G. (2014), *An efficient Wavelet analysis method to film–pore diffusion model arising in mathematical chemistry*, J. Membrane Biol., 247, 339–343.

[42] Hariharan G. (2014), *An efficient Legendre wavelet-based approximation method for a few Newell–Whitehead and Allen–Cahn Equations*, J. Membrane Biol., 247, 371–380.

[43] Hariharan G., Kannan K. (2014), *Review of wavelet methods for the solution of reaction–diffusion problems in science and engineering*, App. Math. Model., 38, 799–813.

[44] Hariharan G., Kannan K. (2013), *An Overview of Haar Wavelet Method for Solving Differential and Integral Equations*, World Applied Sciences Journal, 23 (12), 1-14.

[45] Hariharan G., Kannan K., Sharma K.R. (2009), *Haar wavelet method for solving Fisher's equation*, Appl. Math. Comp., 211, 284–292.

[46] Hariharan G., Rajaraman R. (2013), *A new coupled wavelet-based method applied to the nonlinear reaction–diffusion equation arising in mathematical chemistry*, J. Math. Chem., 51, 2386–2400.

[47] Hariharan G., Rajaraman R. (2013), *Two reliable wavelet methods to Fitzhugh–Nagumo (FN) and fractional FN equations*, J. Math. Chem., 51, 2432–2454.

[48] Hariharan G., Kannan K. (2010), *Haar wavelet method for solving some nonlinear parabolic equations*, J. Math. Chem., 48, 1044–1061.

[49] Heydari M.H., Ghaini F.M.M., Hooshmandasl M.R. (2014), *Legendre wavelets method for numerical solution of time-fractional heat equation*, Wavelets and Linear Algebra, 1, 15–24.

[50] Heydari M.H., Hooshmandasl M.R, Cattani C., Li M. (2013), *Legendre wavelets method for solving fractional population growth model in a closed system*, Math. Probl. Eng., Article ID 161030, 8 pages.

[51] Heydari M.H., Hooshmandasl M.R., Ghaini F.M.M., Cattani C. (2015), *Wavelets method for the time fractional diffusion-wave equation*, Phys. Lett. A , 379, 71–76.

[52] Heydari M.H., Hooshmandasl M.R., Ghaini F.M.M., Marji F.M., Dehghan R., Memarian M.H. (2016) , *A new wavelet method for solving the Helmholtz equation with complex solution*, Numer. Methods Partial Differential Equations, 32 (3), 741–756.

[53] Heydari M.H, Hooshmandasl M.R., Mohammadi F. (2014), *Legendre wavelets method for solving fractional partial differential equations with Dirichlet boundary conditions*, Appl. Math. Comput., 234, 267–276.

[54] Heydari M.H, Hooshmandasl M.R, Shakiba A., Cattani C. (2016), *Legendre wavelets Galerkin method for solving nonlinear stochastic integral equations*, Nonlinear Dynam., 85 (2), 1185–1202.

[55] Hsiao C.H., Wu S.P. (2007) *Numerical solution of time-varying functional differential equations via Haar wavelets*, Appl. Math. Comp. 188., 1049-1058.

[56] Hussain A., Haq S., Uddin M. (2013), *Numerical solution of Klein-Gordon and sine-Gordon equations by meshless method of lines,* Engg. Anal. Bound. Elements, 37, 1351–1366.

[57] Ilati M., Dehghan M. (2015), *The use of radial basis functions (RBFs) collocation and RBF-QR methods for solving the coupled nonlinear sine-Gordon equations,* Engg. Anal. Boun. Ele., 52, 99-109.

[58] Islam S., Aziz I., Al-Fhaid A.S., Shah A. (2013), *A numerical assessment of parabolic partial differential equations using Haar and Legendre wavelets*, Appl. Math. Model., 37, 9455–9481.

[59] Islam S., Aziz I., Ahmad M. (2015), *Numerical soution of two–dimensional elliptic PDEs with nonlocal boundary conditions*, Comput. Math. Appl., 69 (3), 180–205.

[60] Jameson L. (1994), *On the wavelet optimized finite difference method*, ICASE CR-191601.

[61] Jing S.C., Fan H Y. (1995), *q-Taylor's formula with its q-remainder*, Comm. Theor. Phy., 23, 117–20.

[62] Jiwari R. (2012), *A Haar wavelet quasilinearization approach for numerical simulation of Burgers' equation*, Comp. Phy. Comm. 183, 2413–2423.

[63] Kac V., Cheung P. (2002), *Quantum Calculus*, Springer, New York.

[64] Kajani M. T., Vencheh A H. (2004), *Solving linear integro-differential equation with Legendre wavelets*, Int. J. Comput. Math., Vol. 81 (6), 719–726.

[65] Kaur H., Mittal R.C., Mishra V. (2014), *Haar wavelet solutions of nonlinear oscillator equations*, Appl. Math. Model., (38), 4958–4971.

[66] Kaur H., Mittal R.C., Mishra V. (2013), *Haar wavelet approximate solutions for the generalized Lane–Emden equations arising in astrophysics*, Comp. Phy. Comm.,184, 2169–2177.

[67] Kaur H., Mishra V., Mittal R.C. (2013), *Numerical solution of a laminar viscous flow boundary layer equation using uniform Haar Wavelet quasi-linearization method*, World Academy of Science, Engineering and Technology, 7, 1387–1392.

[68] Keshavarz E., Ordokhani Y., Razzaghi M. (2014), *Bernoulli wavelet operational matrix of fractional order integration and its application in solving the fractional order differential equations*, Appl. Math. Model. 38 (24), 6038–6051.

[69] Khan N.A., Ara A., Jamil M. (2011), *Approximations of the nonlinear Volterra's population model by an efficient numerical method*, Math. Meth. Appl. Sci., 34, 1733–1738.

[70] Khuri S.A., Sayfy A. (2010), *A spline collocation approach for the numerical solution of a generalized nonlinear Klein-Gordon equation,* Appl. Math. Comp. 216., 1047-1056.

[71] Khusnutdinova K.R., Pelinovsky D.E. (2003), *On the exchange of energy in coupled Klein–Gordon equations*, Wave Motion 38, 1–10.

[72] Koekoek E., Swarttow R.F. (1998), *Askey-Scheme of hypergeometric orthogonal polynomials and its q-analogue*, Report No. 98–17, Delft University of Technology.

[73] Koomwinder T.H., Swarttow R.F. (1992), *On q-analogues of the Fourier and Hankel transforms*, Trans. Amer. Math. Soc., 333, 445–461.

[74] Kumar M., Pandit S. (2014), *A composite numerical scheme for the numerical simulation of coupled Burgers' equation*, Comp. Phy. Comm., 185, 809–817.

[75] Kumar K.H., Vijesh V.A.(2016), *Chebyshev wavelet quasilinearization scheme for coupled nonlinear sine-Gordon equations*, J. Comput. Nonlinear Dynam., 12(1),011018, 05 pages.

[76] Lakestani M., Dehghan M (2010), *Collocation and finite difference-collocation methods for solution of nonlinear Klein-Gordon equation,* Comp. Phys. Comm., 181, 1392-1401.

[77] Lakshmikantham V., Carl S., Heikkila S. (2009), *Fixed point theorems in ordered Banach spaces via quasilinearization*, Nonlinear Anal., 71, 3448–3458.

[78] Lakshmikantham V., Koksal S. (2003), *Monotone flows and rapid convergence for nonlinear partial differential equations*, CRC Press, London.

[79] Latto A., Tenenbaum E. (1990), *Compactly supported wavelets and the numerical solution of Burgers' equation*, C. R. Acad. Sci. Paris, Series I, 903–909.

[80] Lazer A.C., McKenna P.J. (1990), *Large-amplitude periodic oscillations in suspension bridges:some new connections with nonlinear analysis*, SIAM Rev., 32, 537–578.

[81] Lepik U. (2005), *Numerical solution of differential equations using Haar wavelets*, Math. Comput. Simulation, 68, 127–143.

[82] Lepik U. (2006), *Haar wavelet method for nonlinear integro-differential equations*, Appl. Math. Comput. 176, 324-333.

[83] Lepik U. (2007), *Numerical solution of evolution equations by the Haar wavelet method*, Appl. Math. Comput. 185, 695704.

[84] Lepik U. (2007), *Application of the Haar wavelet transform to solving integral and differential equations*, Proc. Estonian Acad. Sci. Phys. Math. 56 (1), 2846.

[85] Lepik U. (2011), *Solving PDEs with the aid of two-dimensional Haar wavelets*, Comp. Math. Appl., 61, 1873–1879.

[86] Lepik U., Hein H. (2014), *Haar wavelets with applications*, Springer International Publishing, New York.

[87] Liandrat J., Tchamitchian P. (1990), *Resolution of the 1 regularized burgers equation using a spatial wavelet approximation*, NASA Contractor Report 187480: ICASE report No. 90–83.

[88] Li B., Chen X. (2014), *Wavelet-based numerical analysis: A review and classification*, Finite Elem. Anal. Des., 81, 14–31.

[89] Sunny L.A., Vijesh V.A. , *A monotone iterative technique for nonlinear fourth order elliptic equations with nonlocal boundary conditions*, Under review.

[90] Liu H.K.(2011), *Application of a differential transformation method to strongly nonlinear damped q-difference equations*, Comp. Math. Appl., 61, 2555–2561.

[91] Liu H.K.(2012), *Application of the variational iteration method to strongly nonlinear q-difference equations*, J. Appl. Math., Article ID 704138, 12 pages.

[92] Liu H.K. (2013), *Developing a series solution method of q-difference equations*, J. Appl. Math., Article ID 743973, 4 pages.

[93] Liu N., Lin E.B.(2009), *Legendre wavelet method for numerical solutions of partial differential equations*, Numer. Methods Partial Differential Equations, 26 (1), 81–94.

[94] Lu Y. (2010), *Numerical solution of Volterra integral equations by using CAS wavelets*, Far East J. Math. Sci., 42(2), 265-274.

[95] Mahalakshmi M., Hariharan G., Kannan K. (2013), *The wavelet methods to linear and nonlinear reaction–diffusion model arising in mathematical chemistry*, J. Math. Chem., 51, 2361–2385.

[96] Maleknejad K., Sohrabi S.(2007), *Numerical solution of Fredholm integral equations of the first kind by using Legendre wavelets*, Appl. Math. Comput., 186, 836–843.

[97] Maleknejad M., Kajani M.T., Mahmoudi Y. (2003), *Numerical solution of linear Fredholm and volterra integral equation of the second kind by using Legendre wavelets*, Kybernetes, 32, 1530–1539.

[98] Mahmoudi Y. (2005), *Wavelet Galerkin method for numerical solution of nonlinear integral equation*, Appl. Math. Comput., 167 (2005), 1119–1129.

[99] McKenna P.J., Walter W. (1990), *Traveling waves in a suspension bridge*, SIAM J. Appl. Math., 50, 703–715.

[100] Mehra M. (2009), *Wavelets and differential equations - A short review*, AIP Conference Proceedings, 146, 241–252.

[101] Meng A., Wang L., Li H., Zhang W. (2015), *Legendre wavelets method for solving fractional integro-differential equations*,Int. J. Comput. Math., 2 (6), 1275–1291.

[102] Meyer, Y.(1993), *Wavelets: Algorithms and Applications*, SIAM, Philadelphia.

[103] Mittal R.C., Bhatia R.(2015) *Numerical solution of nonlinear system of Klein-Gordon equations by cubic B-spline collocation method*, Int. J. of Comp. Phys., 92(10), 2139–2159.

[104] Mittal R.C., Kaur H., Mishra V. (2015), *Haar wavelet-based numerical investigation of coupled viscous Burgers' equation*, Int. J. Comput. Math., 92 (8), 1643–1659.

[105] Mohammadi M. (2016), *Numerical Solution of Stochastic Ito-Volterra Integral Equations using Haar Wavelets*, Numer. Math. Theory Methods Appl., 9(3), 416–431.

[106] Mohammadi F., Hosseini M.M. (2011), *A new Legendre wavelet operational matrix of derivative and its applications in solving the singular ordinary differential equations*, J. Franklin Inst., 348, 1787–1796.

[107] Mohammadi F.,, Hosseini M.M., Mohyud-Din S.T. (2011), *A new operational matrix for Legendre wavelets and its applications for solving fractional order boundary values problems*, Int. J. Phys. Sci., 6 (32), 7371–7378.

[108] Mohammadi F., Hosseini M.M. (2011), *A comparative study of numerical methods for solving quadratic Riccati differential equations*, J. Franklin Inst., 348 , 156–164.

[109] Murthy A.S.V. (1992), *Solving parabolic integro-differential equations by an explicit integration method*, J. Comp. Appl. Math., 39, 121–132.

[110] Narasimha R. (1968), *Non-linear vibration of an elastic string*, J. Sound and Vibration, 8, 134–146.

[111] Oruc O., Bulut B., Esen A., (2015), *A Haar wavelet-finite difference hybrid method for the numerical solution of the modified Burgers equation*, J. Math. Chem., 53, 1592–1607.

[112] Pachpatte B.G. (1983), *On a nonlinear diffusion system arising in reactor dynamics*, J. Math. Anal. Appl. 94, 501–508.

[113] Pao C.V. (1992), *Nonlinear parabolic and elliptic equations*, Plenum Press, New York, 1992.

[114] Pao C.V. (1979), *Bifurcation analysis on a nonlinear diffusion system in reactor dynamics*, Appl. Anal., 9, 107–119.

[115] Pao C.V., Wang Y.M. (2016), *Numerical methods for fourth-order elliptic equations with nonlocal boundary conditions*, J. Comput. Appl. Math., 292, 447–468.

[116] Pao C.V., Wang Y.M. (2010), *Nonlinear fourth-order elliptic equations with nonlocal boundary conditions*, J. Math. Anal. Appl. 372, 351–365.

[117] Parand K., Abbasbandy S., Kazem S., Rad J.A. (2011), *A novel application of radial basis functions for solving a model of first-order integro-ordinary differential equation*, Commun. Nonli. Sci. Numer. Simul., 16, 4250–4258.

[118] Parand K., Delafkar Z., Pakniat N., Pirkhedri A., Haji M.K. (2011), *Collocation method using sinc and rational Legendre functions for solving Volterra's population model*, Commun. Nonli. Sci. Numer. Simul., 16, 1811-1819.

[119] Parand K., Rezaei A.R., Taghavi A. (2010), *Numerical approximations for population growth model by rational Chebyshev and Hermite functions collocation approach: A comparison*, Math. Meth. Appl. Sci., 33, 2076–2086.

[120] Parand K., Razzaghi M. (2004), *Rational Chebyshev tau method for solving Volterra's population model*, Appl. Math. Comp., 149, 893–900.

[121] Pirabaharan P., Chandrakumar R.D., Hariharan G. (2014), *An efficient wavelet based approximation method to film-pore diffusion model arising in chemical engineering*, Fractals Wavelets Appl., 92, 491-500.

[122] Pourgholi R., Esfahani A., Foadian S., Parehkar S. (2013), *Resolution of an inverse problem by Haar basis and Legendre wavelet methods*, Int. J. Wavelets Multiresolut. Inf. Process., 1350034, 21 pages.

[123] Qin W., Ding D., Ding X. (2015), *Two boundedness and monotonicity preserving methods for a generalized Fisher-KPP equation*, Appl. Math. Comput., 252, 552–567.

[124] Rajaraman R., Hariharan G. (2014), *An efficient Wavelet analysis method to film–pore diffusion model arising in mathematical chemistry*, J. Membrane Biol., 247, 561–570.

[125] Rajaraman R., Hariharan G. (2014), *A New Wavelet-based hybrid method for Fisher type equation*, Fractals Wavelets Appl., 92, 501-508.

[126] Rahimkhani P., Ordokhani Y., Babolian E. (2016), *An efficient approximate method for solving delay fractional optimal control problems*, Nonlinear Dynam., 86(3), 1649-1661

[127] Rashidinia J., Ghasemi M., Jalilian R. (2010), *Numerical solution of the nonlinear Klein-Gordon equation,* J. Comp. Appl. Math., 233(2010) 1866-1878.

[128] Rashidinia J., Mohammadi R. (2010), *Tension spline approach for the numerical solution of nonlinear Klein-Gordon equation,* Comp. Phys. Comm., 181(2010) 78-91.

[129] Ray S.S(2006), *A numerical solution of the coupled sine-Gordon equation using the modified decomposition method*, App. Math. Comp., 175, 1046–1054.

[130] Ray S.S., Gupta A.K. (2014), *Comparative analysis of variational iteration method and Haar method for the numerical solutions of Burgers-Huxley and Huxley equations*, J. Math. Chem., 52, 1066-1080.

[131] Razzaghi M., Oppenheimer S., Ahmad F. (2002), *A Legendre wavelet method for the radiative transfer equation in remote sensing*, J. Electromagn. Waves Appl., 16(12), 1681–1693.

[132] Razzaghi M., Yousefi S. (2002), *Legendre wavelets method for constrained optimal control problems*, Math. Methods Appl. Sci., 25, 529–539.

[133] Razzaghi M., Yousefi S. (2001), *The Legendre wavelets operational matrix of integration*, Internat. J. Systems Sci., 32 (4), 495–502.

[134] Razzaghi M., Yousefi S. (2001), *Legendre wavelets method for the solution of nonlinear problems in the calculus of variations*, Math. Comput. Modelling, 34, 45–54.

[135] Razzaghi M., Yousefi S. (2000), *Legendre wavelets direct method for variational problems*, Math. Comput. Simulation, 53, 185–192.

[136] Saeed U., Rehman M.U. (2014) *Wavelet-Galerkin quasilinearization method for nonlinear boundary value problems*, Abstr. Appl. Anal., Article ID 868934 (2014).

[137] Saeed U., Rehman M.U. (2013), *Haar wavelet-quasilinearization technique for fractional nonlinear differential equations*, Appl. Math. Comp., 220, 630-648.

[138] Saeed U., Rehman M.U. (2014), *Assessment of Haar wavelet-quasilinearization technique in heat convection-radiation equations*, App. Comp. Intel. and Soft Computing, Article ID 454231.

[139] Saeed U., Rehman M.U., Iqbal M.A. (2015), *Modified Chebyshev wavelet methods for fractional delay-type equations*, Appl. Math. Comp., 264(2015) 431-442.

[140] Saeedi H., Moghadam M.M., Mollahasani N., Chuev G.N. (2011), *A CAS wavelet method for solving nonlinear Fredholm integro-differential equations of fractional order*, Commun. Nonli. Sci. Numer. Simul., 16(3), pp. 1154-1163.

[141] Sahu P.K., Ray S.S. (2017), *A new Bernoulli wavelet method for numerical solutions of nonlinear weakly singular Volterra integro-differential equations*, Int. J. Comput. Math.,14(3),1750022.

[142] Sahu P.K., Ray S.S. (2017) *A new Bernoulli wavelet method for accurate solutions of nonlinear fuzzy Hammerstein–Volterra delay integral equations*, Fuzzy Sets Syst., 309, 131-144

[143] Sahu P.K., Ray S.S. (2016), *A numerical approach for solving nonlinear fractional VolterraFredholm integro-differential equations with mixed boundary conditions*, Int. J. Wavelets Multiresolut. Inf. Process., 14 (5), 15 pages.

[144] Sahu P.K., Ray S.S. (2015), *Hybrid Legendre block-pulse functions for the numerical solutions of system of nonlinear Fredholm–Hammerstein integral equations*, Appl. Math. Comput., 270, 871–878.

[145] Sahu P.K., Ray S.S. (2015), *Legendre wavelets operational method for the numerical solutions of nonlinear Volterra integro-differential equations system*, Appl. Math. Comput., 256, 715–723.

[146] Sakthivel K., Balachandran K., Park J.Y., Devipriya G. (2010), *Null controllability of a nonlinear diffusion system in reactor dynamics*, Kybernetika, 46, 890–906.

[147] Sakthivel K., Balachandran K., Nagaraj B.R. (2008), *On a class of nonlinear parabolic control systems with memory effects*, Int. J. Control, 81, 764–777.

[148] Shahed M.E., assan H.A. (2010), *Positive solutions of q-difference equation*, Proc. Amer. Math. Soc., 138, 1733–1738.

[149] Shi Z., Cao Y.Y., Chen Q.J. (2012), *Solving 2D and 3D Poisson equations and biharmonic equations by the Haar wavelet method*, Appl. Math. Model., 36 , 5143–5161.

[150] Shi P.P., LI X., LI X. (2013), *Various wavelet methods for solving fractional Fredholm-Volterra integral equations*, Integral Equations, Bound. Value Probl., Related Problems, May, 275–285.

[151] Si X., Wang C., Shen Y., Zheng L. (2016), *Numerical method to initial-boundary value problems for fractional partial differential equations with time–space variable coefficients*, Appl. Math. Model., 40, 4397–4411.

[152] Singh V.K., Postnikov E.B. (2013), *Operational matrix approach for solution of integro-differential equations arising in theory of anomalous relaxation processes in vicinity of singular point*, Appl. Math. Model. 37 , 6609–6616.

[153] Small R.D. (1983), *Population growth in a closed system*, SIAM Review, 25, 93–95.

[154] Steeb W.H., Hardy Y.,(2011), *Matrix calculus and Kronecker product*, A practical approach to linear and multilinear algebra, Second edition. World Scientific Publishing Co. Pte. Ltd., Hackensack.

[155] Sunny L.A., Vijesh V.A. , *Comments on monotone iterates for solving nonlinear integro-parabolic equations of Volterra type*, Submitted.

[156] Tao Q., Yao Z.A. (2014), *The time optimal control of parabolic integro differential equation in reactor dynamics*, Taiwanese J. Math., 18, 409–417.

[157] TeBeest K.G. (1997), *Classroom Note: Numerical and analytical solutions of Volterras population model*, SIAM Review, 39, 484–493.

[158] Thiramanus P., Tariboon J. (2014), *Nonlinear second-order q -difference equations with three-point boundary conditions*, Comp. Appl. Math., 33, 385–397.

[159] Tomas B.C., (2013), *Methods of applied Mathematics for engineers and scientists*, Cambridge University Press, New York.

[160] Tsallis C., Baldovin F., Cerbino R., Pierobon P. (2003), *Introduction to nonextensive statistical mechanics and thermodynamics*, [cond-mat/0309093].

[161] Venkatesh S.G.,. Ayyaswamy S.K., Balachandar S.R. (2013), *Legendre Wavelets based approximation method for solving advection problems*, Ain Shams Eng. J., 4, 925–932.

[162] Venkatesh S.G., Ayyaswamy S.K., Balachandar S.R. (2012), *Legendre approximation solution for a class of higher-order Volterra integro-differential equations*, Ain Shams Eng. J., 3, 417–422.

[163] Venkatesh S.G, Ayyaswamy S.K., Balachandar S.R. (2012), *Convergence analysis of Legendre wavelets method for solving Fredholm integral equations*, Appl. Math. Sci., 6, 2289–2296.

[164] Venkatesh S.G., Ayyaswamy S.K., Balachandar S.R., Kannan K. (2013), *Wavelet solution for class of nonlinear integro-differential equations*, Indian J. Sci. Technol., 6, 4670–4677.

[165] Venkatesh S.G., Ayyaswamy S.K., Balachandar S.R., Kannan K. (2012), *Legendre wavelets based approximation method for Cauchy problems*, Appl. Math. Sci., 6, 6281–6286.

[166] Verma A., Jiwari R.,Koksal M.E. (2014), *Analytic and numerical solutions of non linear diffusion equations via symmetry reductions*, Adv. in Difference Equ., 2014, 229.

[167] Vijesh V.A., Sunny L.A, Kumar K.H (2016), *Legendre wavelet–quasilinearization technique for solving q-difference equations*, J. Difference Equ. Appl., 22 (4), 594–606.

[168] Vijesh V.A., Kuma K.H. (2015), *Wavelet based numerical simulation of non linear Kilen/Sine gordon equation*, J. of Combinatorics, Information and System Sciences, 40 (1), 225–244.

[169] Vijesh V.A., Kumar K.H. (2015), *Wavelet based quasilinearization method for semi-linear parabolic initial boundary value problems*, Appl. Math. Comput., 266, 1163–1176.

[170] Wang M., Zhao F. (2012), *Haar wavelet method for solving two dimensional Burgers equation*, In: Proceedings of the 2011 2nd International congress on computer applications and computational science., Springer, 381–387.

[171] Wang L., Ma Y., Meng Z. (2014), *Haar wavelet method for solving fractional partial differential equations numerically*, Appl. Math. Comp., 227, 66–76.

[172] Wu J L. (2009), *A wavelet operational method for solving fractional partial differential equations numerically*, Appl. Math. Comp., 214, 31–40.

[173] Wu J., Chen C. (2004), *A new operational approach for solving fractional calculus and fractional differential equations numerically,* IEICE Trans. Fundam., vol. E87, 10771082.

[174] Wu Z., Yin J., Wang C.)(2006), *Elliptic and parabolic equations*, World Scientific, Singapore.

[175] Yin F., Song J. (2014), *A coupled method of Laplace transform and Legendre wavelets for nonlinear Klein-Gordon equations* , Math. Methods Appl. Sci., 37, Issue 6, 781–792.

[176] Yin F., Song J. (2012), *Solving linear PDEs with the aid of two-dimensional Legendre wavelets*, National Conference on Information Technology and Computer Science (CITCS 2012), Atlantis Press, 2012.

[177] Yin F,, Song J., Lu F. (2014) *A coupled method of Laplace transform and Legendre wavelets for nonlinear KleinGordon equations*, Math. Meth. Appl. Sci., 37, 781–792.

[178] Yin F., Song J., Cao X., Lu F. (2013), *Couple of the variational iteration method and Legendre wavelets for nonlinear partial differential equations*, J. Appl. Math., Article ID 157956, 11 pages.

[179] Yin F., Tian T.,Song J., Zhu M.(2015), *Spectral methods using Legendre wavelets for nonlinear Klein Sine-Gordon equations*, J. Comput. Appl. Math., 275, 321–334.

[180] Yousefi S.A., Razzaghi M. (2005), *Legendre wavelets method for the nonlinear Volterra-Fredholm integral equations*, Math. Comput. Simulation, 70, 1–8.

[181] Yousefi S.A., Banifatemi A. (2006), *Numerical solution of Fredholm integral equations by using CAS wavelets*, Appl. Math. Comput., 183 , 458–463.

[182] Yousefi S.A. (2006), *Numerical solution of Abel's integral equation by using Legendre wavelets*, Appl. Math. Comput., 175, 574–580.

[183] Wan Y., Zhu L.,(2017), *Solving nonlinear Volterra integro-differential equations of fractional order by using Euler wavelet method*, Adv. in Difference Equ., (27), (DOI 10.1186/s13662-017-1085-6).

[184] Wang X.T., Li Y.M. (2012), *Numerical solution of Fredholm integral equation of the second kind by general Legendre wavelets*, International J. of Innovative, 8, 1(B), 799–805.

[185] Wazwaz A.M. (2006), *The modified decomposition method for analytic treatment of differential equations,* Appl. Math. Comp. 173, 165-176.

[186] Zahra W.K., Ouf W.A., El-azab M.S. (2014), *Cubic B-spline collocation algorithm for the numerical solution of Newell Whitehead Segel type equations*, Electron. J. Math.Anal. Appl., 2, 81-100.

[187] Zhang C.T. (1987), *Soliton excitations in deoxyribonucleic acid (DNA) double helices*, Physical Review A., 35 (2), 886–891.

[188] Zhang X., Liu L. (2007),*Positive solutions of fourth-order multi-point boundary value problems with bending term*, Appl. Math. Comput., 194, 321–332.

[189] Zhao Y.M. (2014), *Exact solutions of coupled sine-Gordon equations using the simplest equation method*, J. Appl. Math., Volume 2014, Article ID 534346, 5 pages.

[190] Zheng X., Yang X. (2009), *Techniques for solving integral and differential equations by Legendre wavelets*, Internat. J. Systems Sci., 40 (11), 1127–1137.

[191] Zhi S., Yan-hua X., Jun-ping1 Z. (2016) *Haar wavelets method for solving Poisson equations with jump conditions in irregular domain*, Adv. Comput. Math., 42, 995–1012.

[192] Zin S.M., Majid A.A., Md. Ismail A.I., Abbas M.(2014), *Application of hybrid cubic B-Spline collocation approach for solving a generalized nonlinear klien-gordon equation,* Math. Problems in Engg., Article ID 108560, 10 pages.